# CHARACTERIZATION OF POTENTIAL AUTOPHAGY-RELATED THERAPEUTIC TARGETS FOR FLT3-ITD$^{+}$ AML WITH ZEBRAFISH MODELS

YI ZHENNI

PhD

The Hong Kong Polytechnic University

2023

The Hong Kong Polytechnic University

Department of Health Technology and Informatics

# Characterization of Potential Autophagy-Related Therapeutic Targets for FLT3-ITD$^{+}$ AML with Zebrafish Models

**YI Zhenni**

A thesis submitted in partial fulfillment of the requirements for the degree of Doctor of Philosophy

**June 2023**

# Certificate of Originality

I hereby declare that this thesis is my own work and that, to the best of my knowledge and belief, it reproduces no material previously published or written, nor material that has been accepted for the award of any other degree or diploma, except where due acknowledgement has been made in the text.

_____ (Signed)

YI Zhenni (Name of student)

## Abstract

Acute myeloid leukemia (AML) is a severe type of acute leukemia with a higher risk of death and relapse. Many gene mutations and altered signaling pathways have been identified which account for the mechanisms underlying the malignant proliferation of myeloid progenitor cells. Among the mutations, internal tandem duplication (ITD) found in FMS-like tyrosine kinase 3 (FLT3) is reported to be associated with elevated autophagic activity, signaling activity, and cell proliferation in AMLs that show poor prognosis. Autophagy is an important and preserved lysosomal degradation pathway responsible for breaking down cellular components to maintain cellular structure and homeostasis, thus promoting growth and development. Targeting autophagy in AML is a promising therapeutic strategy, while conventional inhibitors of autophagy induce stress on normal hematopoiesis and healthy cells. To develop more effective chemotherapy in AML treatments, novel targets in autophagy or selective autophagy pathways are worth exploring.

Zebrafish (*Danio rerio*) is an advantageous high-throughput vertebrate model for hematopoiesis studies. With primary and definitive hematopoiesis clearly mapped, the location and migration of each lineage can be easily tracked in zebrafish. Many transgenic zebrafish models of human leukemia have been created for pre-clinical studies. Besides hematopoiesis, zebrafish is also widely used to study autophagy. With well-established assays and transgenic reporter lines, zebrafish is an ideal model to study autophagy in AML *in vivo*.

In this project, potential autophagy-related targets were first identified in AML cell lines after treatment with autophagy modulators. Through mass spectrometry-mediated proteomic profiling, I found that the protein levels of the *dedicator of cytokinesis*

(*DOCK2*), *endoplasmic Reticulum Metallopeptidase 1* (*ERMP1*), and *retinoid-inducible serine carboxypeptidase* (*SCPEP1*) were substantially altered by autophagy modulations in the FLT3-ITD$^+$ AML cells. Furthermore, I also discovered another regulator, *PTEN-induced putative kinase 1* (*PINK1*), which was shown to mediate mitophagy/autophagy in hematopoietic cells. These newly discovered genes are potential autophagy-related therapeutic target candidates for FLT3-ITD$^+$ AML. Next, the roles of these genes in AML proliferation and normal hematopoiesis were further investigated in AML cell lines and zebrafish embryos, respectively, through CRISPR/cas9-mediated gene knockout.

My results demonstrate that *DOCK2* deficiency disrupted autophagy and impaired proliferation of FLT3-ITD$^+$ AML cells, while eliciting negligible effects on FLT3-WT AML cells. Loss of *dock2* in zebrafish had little effect on leukocyte development, while remarkably inhibiting the development of neutrophils and lymphocytes. *ERMP1* deficiency robustly inhibited autophagy and proliferation of AML cells. Zebrafish *ermp1* mutants showed suppressed definitive hematopoiesis (leukocyte and neutrophil development). *SCPEP1* deficiency also inhibited leukemia cell proliferation while desensitizing AML cells to the chloroquine treatment. Loss of *scpep1* in zebrafish mainly suppressed the development of neutrophils and lymphocytes. On the contrary, *PINK1* deficiency enhanced autophagy and cell proliferation of leukemia cells. *pink1* loss-of-function mutation promoted the aberrant development of hematopoietic cells through modulating autophagy in zebrafish.

In conclusion, I have provided compelling experimental evidence demonstrating the remarkable roles of a group of novel autophagy-associated genes in regulating leukemia cell proliferation and zebrafish hematopoiesis. *DOCK2*, *ERMP1*, and

*SCPEP1* can potentially be targeted for the treatment of AML, while the functional role of *PINK1* warrants further examination. My thesis work, which has generated extrapolatable data, has laid a solid foundation for the development of novel therapeutic strategies in AML. The findings of this study certainly have transitional significance and will form a basis for developing further clinical investigations by exploiting autophagy inhibitors for treating AML or other types of cancers.

# Publications

**Thesis related:**

1. **Yi ZN**, Chen XK, Ma ACH. Role of *DOCK2* in AML progression and zebrafish hematopoiesis. (Manuscript in preparation)
2. **Yi ZN**, Chen XK, Ma ACH. Loss of *PINK1* promotes the expansion of hematopoietic cells via upregulating autophagy. (Manuscript submitted under review)
3. **Yi, ZN**, Chen, XK, Ma, ACH. Modeling leukemia with zebrafish (Danio rerio): Towards precision medicine. *Exp. Cell Res*. 421, 113401 (2022).

Others:

1. Chen X, **Yi Z**, Lau JJ, Ma AC. Distinct roles of core autophagy-related genes (ATGs) in zebrafish definitive hematopoiesis. *Autophagy*; 2023. (Manuscript accepted)
2. Hasan KMM, Chen XK, **Yi ZN**, Lau JJY, Ma ACH. Genetic and chemical inhibition of autophagy in zebrafish induced myelopoiesis. *bioRxiv*; 2021. DOI: 10.1101/2021.06.14.448302.
3. Chen XK, **Yi ZN**, Wong GTC, Hasan KMM, Kwan JSK, Ma ACH, Chang RCC. Is exercise a senolytic medicine? A systematic review. *Aging cell*. 2020; e13294, PMID: 33378138.

## Conference abstracts

1. **Yi ZN**, Chen XK, Ma ACH. Loss of *PINK1* promotes the expansion of hematopoietic cells via upregulating autophagy. *12th European Zebrafish Meeting*, July 9-13, 2023. (Abstract submitted)
2. **Yi ZN**, Chen XK, Ma ACH. Role of *DOCK2* in AML progression and zebrafish hematopoiesis. *International Society for Experimental Hematology 52nd Annual Scientific Meeting*, August 17-20, 2023. (Poster submitted)
3. **Yi ZN**, Chen XK, Ma ACH. Loss of *PINK1* promotes the expansion of hematopoietic cells via upregulating autophagy. *15th Annual Swiss Zebrafish Meeting 2023*. (Abstract submitted)
4. **Yi ZN**, Chen XK, Ma ACH. Zebrafish Swim into the Cosmetic Industry. *PolyU Research Student Conference (PRSC) 2023*. (Poster)
5. **Yi ZN**, Chen XK, Ma ACH. Loss of *PINK1* promotes the expansion of hematopoietic cells via upregulating autophagy. *3rd ABCT Research Postgraduate Symposium in the Biology Discipline*, 12 August 2022. (Best poster presentation award)

## Acknowledgments

First, I would like to express my greatest gratitude to my supervisor, Dr. Alvin Chun-hang Ma, for giving me an invaluable opportunity to join his laboratory for my Ph.D. study, and for his generous patience, continuous guidance, and encouragement throughout the course of my study. Although we encountered some problematic situations during this period, we managed to get over them with his guidance and improved with valuable experiences.

I would like to thank Dr. Xiangke Chen for all the help and guidance he offered during my research study. He offered countless professional advice and academic critiques and encouraged me to carry on my research.

I would like to thank Dr. Shea-ping Yip, Dr. Zou Xiang, Dr. Kenneth Cheng, Dr. Chi Ming Wong, Dr. Gilman Siu, Dr. Huang Chien-ling, Dr. Raymond Hui, Dr. Pui-kin So, Dr. Ryan Chow, Dr. Michael Yuen, Dr. Sirui Li, and all technical staff for their professional suggestions on m research projects and academic performances.

I would like to thank Ms. Winsome Wong, Mr. David Lau, Ms. Pamela Mui, and all HTI staff for their assistance.

I would like to thank my group members Mr. Jack Lau, Mr. Chunlin He, Ms. Angela Cheung, and Mr. Zegeye Eskezia for their help and assistance.

I would like to thank Ms. Chujun Deng, Ms. Yu-wen Yeh, Ms. Yue Li, Ms. Minfeng Yang, and Ms. Xian Liu for their help and advice.

I would like to thank the Research Grant Council and the Hong Kong Polytechnic University for providing me with the opportunity to Ph.D. study.

Finally, I would like to thank my parents for their unconditional love and support during my research and study. Their understanding and encouragement are always my motivation to keep on.

# Table of Contents

# List of Figures

# List of Tables

# List of abbreviations

| | |
|---|---|
| AML | Acute myeloid leukemia |
| ALL | Acute lymphoblastic leukemia |
| MDS | Myelodysplastic syndrome |
| MPN | Myeloproliferative neoplasm |
| TET2 | Methylcytidine dioxygenase 2 |
| DNMT3A | DNA methyltransferase 3A |
| NPM1 | Nucleophosmin 1 |
| FLT3 | Fms-like tyrosine kinase 3 |
| ITD | Internal tandem duplication |
| CN-AML | Cytogenetic normal acute myeloid leukemia |
| TP53 | Tumor suppressors 53 |
| RUNX1 | Runt-related transcription factor 1 |
| IDH1 | isocitrate dehydrogenase |
| PI3K | phosphoinositide 3 kinase |
| AKT | Protein kinase B |
| STAT | signal transducer and activator of transcription/ |
| ERK | extracellular signal-regulated kinase |
| TKI | tyrosine kinase inhibitor |
| 3-MA | 3-Methyladenine |
| CQ | chloroquine |
| ATG | Autophagy-related genes |
| ULK1 | unc-51 like autophagy activating kinase 1 |
| FIP200 | FAK family kinase interacting protein of 200 kDa |
| mTOR | mammalian target of Rapamycin |
| AMPK | AMP-activated protein kinase |
| LC3 | microtubule-associated protein 1 light chain 3 |
| PINK1 | Pten-induced putative kinase 1 |
| HSC | hematopoietic stem cell |
| CMP | common myeloid progenitor cells |
| CLP | common lymphoid progenitor cell |
| NK | natural killer cell |
| ICM | intermediate cell mass |

| | |
|---|---|
| HSPC | hematopoietic stem progenitor cell |
| CHT | caudal hematopoietic tissue |
| ZFN | Zinc Finger Nucleases |
| TALEN | Transcription activator-like Effector Nuclease |
| CRISPR | Clustered Regularly Interspaced Short Palindromic Repeats |
| Cas9 | CRISPR-associated protein 9 |
| MO | morpholino |
| RAPA | rapamycin |
| RNP | ribonucleoprotein |
| RFLP | restriction fragment length polymorphism |
| pH3 | Phospho-Histone H3 |
| WT | Wild type |
| WISH | Whole-mount in situ hybridization |
| DOCK2 | Dedicator of cytokinesis 2 |
| ERMP1 | Endoplasmic Reticulum Metallopeptidase 1 |
| SCPEP1 | Retinoid-inducible serine carboxypeptidase 1 |
| CTRL | Control |
| IPA | Ingenuity pathway analysis |
| UPR | Unfolded protein response |
| MS | Mass spectrometry |
| SC | Serine carboxypeptidase |

# 1. Literature Review

## 1.1 Acute Myeloid Leukemia and Molecular Targets

Leukemia is characterized by aberrant clonal expansion and defective differentiation in myeloid or lymphoid progenitor cells. Acute leukemia is defined by a relatively rapid development of symptoms compared to the chronic type of leukemia. Acute leukemia is classified into, acute myeloid leukemia (AML), found in 80% of adult cases[1], and acute lymphoblastic leukemia (ALL), found in 90% of pediatric cases[2], by their originating cell lineages. A more detailed classification of AML subtypes is assigned by their cytogenetic phenotype ( normal and abnormal karyotype) and gene mutations[3]. Blood malignancies, for example, myeloproliferative neoplasm (MPN) and myelodysplastic syndrome (MDS) can also transform into secondary AML.

AML was found to prevail in older people (more than ¾>60 years old) of a median age of 68 years old, while aged people more frequently encounter multidrug resistance and poor response to chemotherapy[4]. The founder events of leukemogenesis begin with a number of epigenetic changes such as methylation in the chromosome, usually induced by loss-of-function mutations in *methylcytidine dioxygenase 2* (*TET2*), *DNA methyltransferase 3A* (*DNMT3A*), and other modifier genes[5]. As the disease progresses, mutations from oncogenes, *Fms-like tyrosine kinase 3* (*FLT3*), and *nucleophosmin 1* (*NPM1*) occur, while gene alterations in the transcription factors and RNA splicers appear at a later stage of leukemogenesis[6]. These combined factors induce immature myeloid cells to accumulate in the peripheral blood, bone marrow, and lymph nodes which eventually lead to hematopoietic insufficiency.

AML patients show symptoms of anemia, thrombocytopenia, or granulocytopenia because of a lack of erythrocytes, platelets, or granulocyte. The diagnosis of AML is mostly based on pathological and cytologic analysis of bone marrow and blood cells, hallmarked by the presence of over 30% myeloid blasts (immature myeloid cells)[7]. Patients of MDS and MPN also show defective hematopoiesis, while distinguished from AML by their progression stage and severity. When the number of immature cells in the bone marrow drops below 5% and the normal cells recover, it is viewed as complete remission of AML[8].

Traditional chemotherapy treatment of AML includes 3 days of daunorubicin and 7 days of cytarabine ("7+3" regimen). However, the overall 5-year survival rates of AML patients are only 25-40% in less-aged patients (<60 years old) and 5-15% in aged patients. Patients with risky genetic mutations like FLT3-ITD showed a much lower remission rate of 10-15% compared with 40-60% of the others towards general chemotherapy[7]. Clinically, a more efficient treatment is to combine chemotherapy with hematopoietic stem cell transplantation when compatible donors are available. However, aged patients are unable to undertake the stress-induced immune response from transplantation, with dismal recovery due to unfavorable cytogenetics and other age-related conditions.

Cytogenetic normal (CN)-AML represents ~ 50% of all AML cases and they are genetically heterogeneous, with fusion genes due to translocations, inversions, loss of function, and hyper-active gene mutations being found in leukemic cells[9]. Chromosomal abnormalities such as loss of the long arm of chromosome 5 (5q-), deletions of chromosome 20q, or gain of chromosome 8, are found in around 20% of AML cases[10]. From whole-genome sequencing results, the mostly found altered genes in AML fall into eight functional categories: DNA methylation, signaling and

kinase genes, tumor suppressors, chromatin modifiers, myeloid transcription factors, cohesion complex, spliceosome complex, and *nucleophosmin 1* (*NPM1*), which occupies its own category[11] and mutations in *DNMT3A*, *FLT3*, *CEBPA*, *RAS*, *IDH*, *NPM1*, *RUNX1*, *TP53*, *STAG2*, and *SF3B1* were recurrently found in patients with CN-AML (**Fig. 1.1**).

*DNMT3A* mutations occur in ~30% of cases of CN-AML, which causes hindered DNA methylation that disrupts the normal structure of chromosome[11,12]. FLT3 is a type of class III tyrosine kinase receptor that predominantly expresses in hematopoietic progenitor cells such as granulocyte progenitor cells[13]. FLT3 normally functions to promote myeloid cell proliferation and differentiation. The *internal tandem duplication* (*ITD*) mutation of *FLT3* is a gain-of-function mutation that promotes autophosphorylation and activates downstream signaling. Found in over 30% of AML cases, it is considered an unfavorable risk factor clinically[11].

CCAAT Enhancer Binding Protein Alpha (CEBPA) protein modulates the expression of genes involved in cell cycle regulation. Its mutation is highly correlated with the poor prognosis of AML[14]. *RAS* oncogenes encode a family of guanine nucleotide-binding proteins (GDP). Mutations in *NRAS*, *KRAS*, and *HRAS* are found in ~10%–15% of AML cases[15].

Isocitrate dehydrogenase (IDH) protein catalyzes the reaction of isocitrate to alpha-ketoglutarate, while converting the reaction when alpha-ketoglutarate is reduced to 2-hydroxyglutarate (2-HG)[16]. Mutations of *IDH* found in AML include point mutations of R132 and R140 from *IDH1*, or R140 from *IDH2*[17]. IDH mutation was recognized among 8-12% of AML patients[1]. Numerous inhibitors that target IDH1 were developed, such as AG221 and AG120[18].

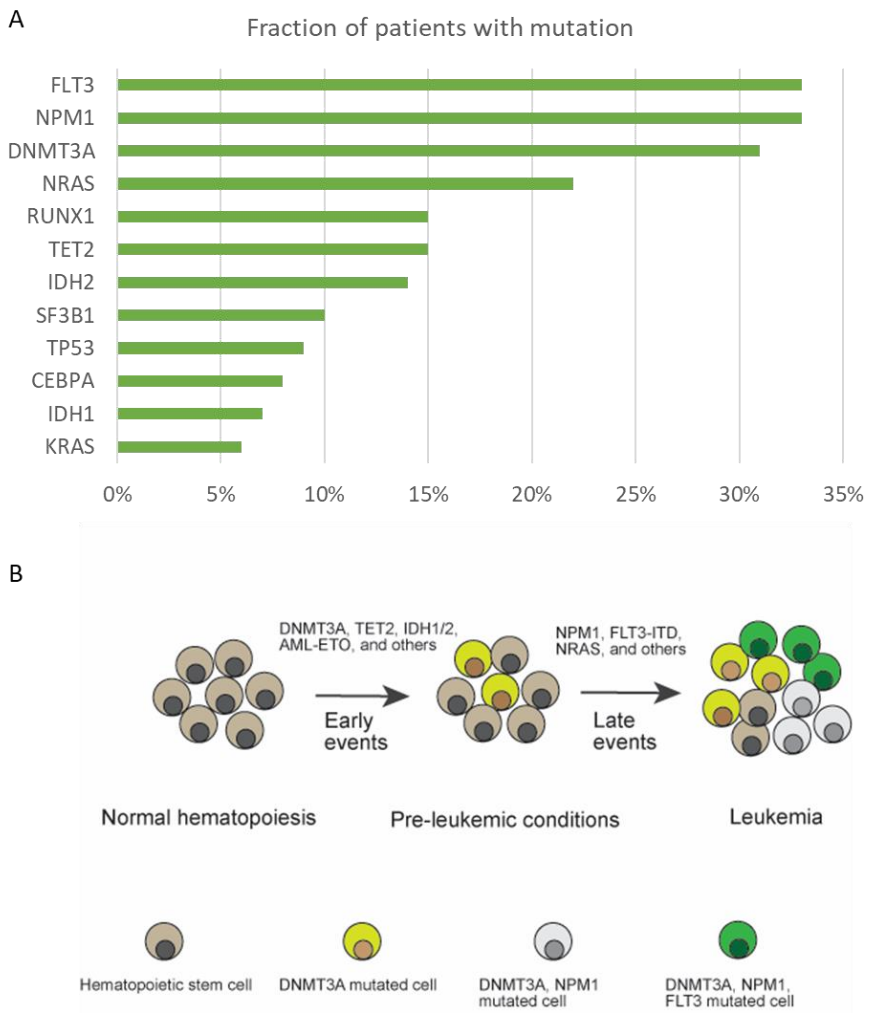


Figure 1.1 Gene mutations and leukemogenesis in AML

A, recurrent mutations found in patients of cytogenetic-normal acute myeloid leukemia. B, leukemic cell development and mutation events from early to late stage. FLT3-ITD, internal tandem duplication of FMS-like tyrosine kinase. NPM1, nucleophosmin 1. DNMT3A, DNA methyltransferase 3A. RUNX1, runt-related transcription factor 1. TET2, methylcytidine dioxygenase 2. IDH2, isocitrate dehydrogenase. SF3B1, splicing factor 3b subunit 1. TP53, tumor suppressor 53. CEBPA, CCAAT Enhancer Binding Protein Alpha.

NPM1 is a ubiquitously expressed nucleolar protein with multiple functions in chromatin remodeling and genomic stability[19]. In AML, the mutation in the nucleolar localization signal region of *NPM1* that renders it located within the cytoplasm (*NPMc*), was found in 35% of AML cases[9]. Mutations in other genes, such as transcription factors *Runt-related transcription factor 1* (*RUNX1*) and tumor suppressors *TP53*, *cohesin complex subunit 2* (*STAG2*), or missense mutations in *splicing factor 3b subunit 1* (*SF3B1*) occur at a frequency around 10%[20].

Combined effects of malignant proliferation, defective differentiation, and chromosome instability contribute to the acute development of myeloid leukemia. Since these mutations are frequently acquainted in AML patients, profiling studies of them help in the classification of leukemia types and guide in more specific treatments. In clinical practice, mutations in *FLT3*, *NPM1*, and *CEBPA* have been adopted as markers to reflect AML, whereas the prognostic practice of mutations in *RUNX1*, *TP53*, *DNMT3A*, or *IDH1* mutations is still under evaluation.

*FLT3* is specifically expressed in hematopoietic stem and progenitor cells during normal hematopoiesis. FLT3 protein consists of 2 tyrosine kinase domains (TKDs) and a juxta membrane domain (JMD)[21]. While binding with the FLT3 ligands leads to autophosphorylation and promotes the proliferation of hematopoietic progenitors via phosphoinositide 3-kinase/ protein kinase B (PI3K/AKT) and signal transducer and activator of transcription/ extracellular signal-regulated kinase (STAT/ERK) signaling pathways (**Fig. 1.2).** Internal tandem duplication of *FLT3* (*FLT3-ITD*) is a duplication within the juxta membrane domain of exons 11 and 12. Commonly found in AML patients, it causes constitutive activation of FLT3 kinase and rapid leukemic cell growth, thus patients who possess the mutation are at higher risk of relapse and inferior survival[22,23].

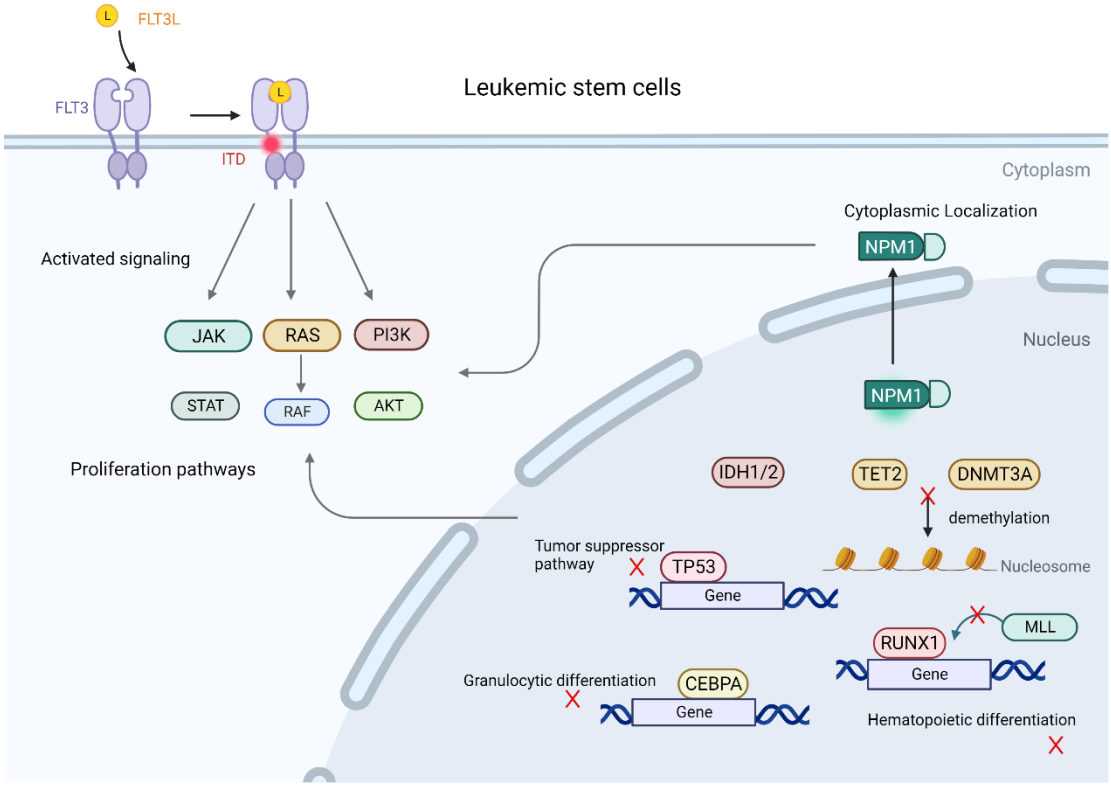


Figure 1.2 Mutations and abnormal molecular pathways involved in AML

Schematic graph of FLT3 activation, gene mutations, and signaling pathways in AML. FLT3, FMS-like tyrosine kinase-3. ITD, internal tandem duplication. FLT3L, FLT3 ligand. JAK-STAT, Janus kinase/signal transducer and activator of transcription. PI3K-AKT, phosphoinositide-3-kinase–protein kinase B. MLL, mixed-lineage leukemia. NPM1, nucleophosmin 1. DNMT3A, DNA methyltransferase 3A. RUNX1, runt-related transcription factor 1. TET2, methylcytidine dioxygenase 2. IDH2, isocitrate dehydrogenase. TP53, tumor suppressor 53. CEBPA, CCAAT Enhancer Binding Protein Alpha.

*FLT3* mutation was identified as an adverse molecular marker of AML over a decade, and it has been extensively studied to develop novel targeted therapeutics ever since[23].

In the leukemic cells, *FLT3-ITD* triggers a continuing activation of kinase activity and activates the downstream effectors AKT, STAT5, and ERK from the PI3K-AKT, JAK-STAT, and RAS/RAF/MEK/ERK pathways. *FLT3-ITD* mutation was also found to correlate with activation and phosphorylation of the forkhead transcription factor, FOXO3A, which is a known autophagy regulator, and promoted autophagy while negatively regulating the FOXO3A pathway of apoptosis[24]. This signaling crosstalk suggests a potential multi-target therapy for further investigation.

Numerous studies have been performed to develop kinase inhibitors that target FLT3 activity. Novel inhibitors such as quizartinib, midostaurin, and sorafenib showed promising for early treatment, but patients quickly grow drug tolerance within a few months with only transient or partial remission. Other multi-target inhibitors targeting VEGFR, KIT, or RAF kinases have also been tested in clinical trials and approved (**Table 1.1**).

Considering why patients develop resistance to FLT3 inhibitors, several hypotheses have been raised. First, leukemic stem cells may have acquired secondary mutations that resist drug treatments. Sequencing data of the resistant FLT3-ITD$^{+}$ leukemic cells show that drug treatment tends to induce secondary mutations, such as *FLT3-ITD (F691)*, *FLT3-ITD (D835)*, and *FLT3-ITD (Y842)* that confer resistance to many kinase inhibitors[23]. Second, leukemia cells may acquire novel mutations in other genes and complement the FLT3 activity loss in leukemia.

Table 1.1 Types of kinase inhibitors and their targets.

| | Type I | | | Type II | | |
|---|---|---|---|---|---|---|
| FLT3 inhibitors | Name | IC50 (nM) | Other targets | Name | IC50 (nM) | Other targets |
| 1st Generation | Sunitinib (SU11248) | ITD 5.4 D835Y >100 | VEGFR2, PDGFRb, KIT, RET | Sorafenib (DB00398) | ITD 18.5 D835Y >2000 | RAF, VEGFR1,2,3, PDGFRb, KIT, RET |
| | Midostaurin (PKC412) | ITD 9.3 D835Y 10 | PKC, Flk-1, Akt, PKA, KIT, Src, PDGFRb, VEGFR1, VEGFR2 | Ponatinib (AP24534) | ITD <1 D835Y 92 | LYN, ABL, PDGFRa, VEGFR2, FGFR1, SRC, KIT, TEK, RET |
| | Lestaurtinib (CEP-701) | ITD 8.6 D835Y 9.8 | JAK2,3, TrkA, B, C | Tandutinib (MLN518) | D 550 D835Y >10 K | KIT, PDGFRb |
| 2nd Generation | Crenolanib (CP-868-596) | ITD 57 D835Y 58 | PDGFRb | Quizartinib (AC220) | D 1.2 D835Y >100 | KIT, PDGFRb RET |

*Type I inhibitors bind to the ATP-binding site when the receptor is active. Type II binds to regions adjacent to the ATP-binding site when the receptor is inactive and inhibits its activation.

FLT3-ITD does not resist solely, more than 20 kinases work together to resist the inhibitors[11]. Third, activation of autophagy, PI3K-AKT, JAK-STAT, RAS/RAF, or MEK/ERK pathways promotes proliferation consistently even with the inhibitors. Others suggest that the expression of the drug-resistant gene, the *ATP Binding Cassette Subfamily B Member 1* (*ABCB1*) gene can help transport drugs from intra-cellular membrane to extra-cellular membrane and is involved in multi-inhibitor resistance[4].

To overcome drug resistance of leukemic cells, the direction for AML treatment is to combine multiple chemotherapeutics, for example, cytarabine and anthracycline, tyrosine kinase inhibitors (TKIs), decitabine, and azacitidine, that target a panel of AML according to their cytogenetic difference. Recent studies have shown that type I FLT3 kinase inhibitors, crenolanib in combination with type II TKI, sorafenib worked well in targeting drug-resistant FLT3-ITD$^+$ AML with better clinical results[25].

Nevertheless, there is still an unmet need to develop new therapeutics that improve the clinical outcomes of AML patients. Molecular profiling and targeted therapy can guide developing novel drug formulas and the characterization of the functions of multiple players from leukemic cells will provide important insights. For example, the growth of *IDH1* and *IDH2* mutant AML was shown to be dependent on *BCL2* (*B-cell CLL–lymphoma 2*) gene expression[26]. Thus, a BCL2 inhibitor like venetoclax was effective in inhibiting the proliferation of *IDH1/2*-mutated cells. As one of the most frequently mutated genes in AML, further study of FLT3-induced signaling, in particular, the autophagy pathway is warranted.

## 1.2 Autophagy in Normal and Malignant Hematopoiesis

Autophagy is an essential cellular process that helps cells to sustain under adverse conditions. External or internal stimuli such as metabolic stress, genome instability, nutrient or energy deprivation, and cancer chemotherapy can induce autophagy. The process of autophagy initiates with the enfolding of intracellular proteins or organelles by a phagophore, a *de novo* synthesized double membrane structure, then develops into an autophagosome, fuse with a lysosome, and produces an autolysosome, the enzymes within subsequently degrade the components and produce small molecule nutrients that join the metabolism in cells (**Fig. 1.3**).

Many autophagy modulators have been developed to induce or inhibit this process at different stages. 3-Methyladenine (3-MA) inhibits PI3K to inhibit the formation of phagophore[27], while bafilomycin A1 or chloroquine (CQ) inhibits autophagy by inhibiting the fusion of autophagosome and lysosome[28]. Autophagic removal of extra organelles and used components are pivotal processes for cell differentiation during hematopoiesis, immune response during infections, cancer progression, and aging[29–31]. Generally, autophagy is both a cytoprotective mechanism and a resources relocating system that helps cells to adjust to complex environments.

Classified by the targets of degradation, autophagy is divided into selective autophagy and non-selective autophagy. Selective autophagy targets organelles with specific receptors or tags, for example, mitophagy starts with tagging of damaged mitochondria with PTEN-induced putative kinase 1/Parkin E3 ubiquitin protein ligase (PINK1/PRKN) signals[32]. Non-selective autophagy removes large components tagged with ubiquitin, core machinery for cytoplasmic components recycling[33,34].

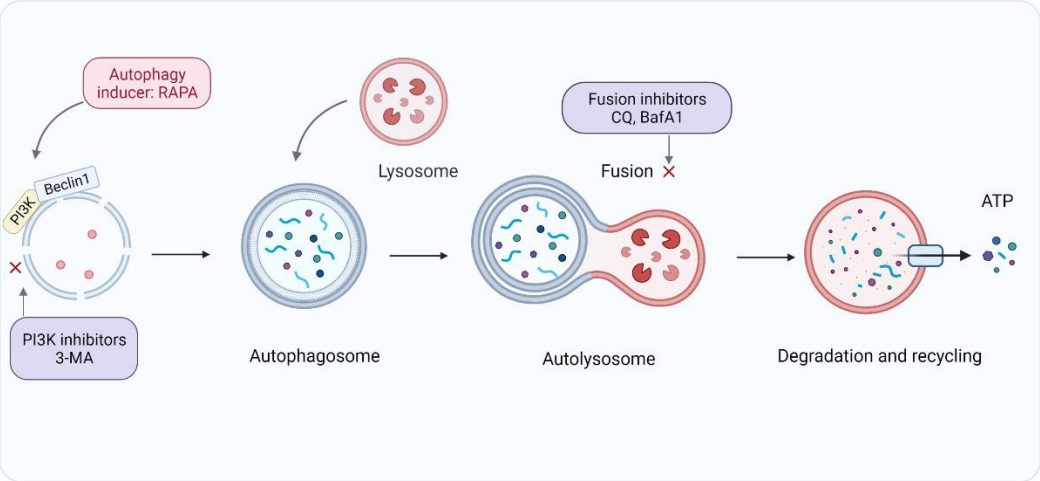


Figure 1.3 Autophagy progression and functions of autophagy modulators

Overview of autophagy process and functions of autophagy modulators in the cell. Autophagy inducers like RAPA can target mTOR to induce autophagy. The autophagy process initiates with nucleation of the PI3Kcomplex, in which Beclin 1 plays a role in forming of phagophore, here the PI3K inhibitors like 3-MA can block the formation. Then the phagophore develops into an autophagosome, which fuses with a lysosome to form the autolysosome, where CQ can function as an inhibitor to block the fusion process. The materials inside autolysosome are subsequently degraded to release energy and small molecules. PI3K, phosphoinositide-3-kinase–protein kinase B. RAPA, rapamycin. 3-MA, 3-methyladenine. CQ, chloroquine. BafA1, Bafilomycin A1. ATP, adenosine triphosphate.

Autophagy is also divided into canonical autophagy and non-canonical autophagy depending on the key gene cluster involved in the pathways. The canonical autophagy pathway involves initiator gene unc-51 like autophagy activating kinase 1 (ULK1)[35], FAK family kinase interacting protein of 200 kDa (FIP200)[36], elongation regulators ATG5/ATG7/ATG8[35,37–39], and nucleation regulators Beclin1/VPS15/VPS34[39]. Non-canonical autophagy pathways involve selective independence of key ATGs, for example, the Beclin1-independent autophagy pathway found in immune cell development[40]. Another example is PINK1-independent mitophagy[41].

Among signaling pathways that regulate autophagy, the mammalian target of Rapamycin (mTOR) is a central regulator of cell growth and an upstream regulator that controls cellular nutrient processing and adjusts metabolism. Starvation or mTOR inhibitors like rapamycin can inhibit mTOR signaling and activate the 5' AMP-activated protein kinase (AMPK) signaling pathway then trigger autophagy. Cellular autophagy initiates with the formation of the ULK1/FIP200 complex, next the ATG5-12 conjugation system regulates the elongation of the autophagosome, where microtubule-associated protein 1 light chain 3 (LC3) conjugated with the lapidated phosphatidylethanolamine (PE) to form LC3-II.

During normal hematopoiesis, the hematopoietic stem cells (HSCs) maintain their numbers between differentiation, self-renewal, and quiescence[42] (**Fig. 1.4**). Previously findings showed that mitophagy regulates mitochondrial removal in HSCs to maintain their stemness and self-renewal[43,44]. HSCs with *Atg12* deletion showed increased apoptosis in mice[34], while *Atg5* or *Atg7* deletion in HSCs induced mitochondrial damage, bone marrow failure, disrupt myelopoiesis, and eventually death[45]. Similarly, HSC-specific loss of *FIP200* in mice is embryonic lethal[46]. The

same apoptosis phenotype was found in the immunodeficient NOD scid gamma (NSG) mice transplanted with *ATG5*, *ATG7*-knockdown CD34+ HSCs[47]. In conclusion, autophagy plays a vital role in maintaining the renewal ability and differentiation of HSCs.

Differentiation of common myeloid progenitor cells (CMPs) also requires precise regulation of autophagy (**Fig. 1.4**). *FIP200* encodes a key proteins required for the formation of autophagosome[48]. Deletion of *FIP200* induced abnormal myelopoiesis, as shown by the significant increase in the number of myeloid progenitor cells in the peripheral blood of conditional knockout mice embryos[46]. The infiltrating myeloid cells present in *vav-Atg7* knockout mice resemble human acute myeloid leukemia[30]. It is known that autophagy acts as a central mechanism in phagocytotic immune responses of macrophages, granulocytes, neutrophils, and other white blood cells[49,50].

Autophagy regulates the removal of the nucleus from erythroblasts during erythropoiesis[51] and the formation of platelets during thrombocytosis[52]. Studies show that *GATA-1* (*erythroid transcription factor*) upregulates the expression of *ATG4*, *ATG8*, and *ATG12* during erythropoiesis[53]. Mice with loss of function of *Atg7*, *FIP200*, or *Ulk1* displayed a reduction in erythropoiesis and severe anemia[46,54,55]. Conditional knockout of *Nix*, a mitophagy regulator, induces reticulocyte apoptosis and anemia[56].

Autophagy also plays a role in common lymphoid progenitor cells (CLPs) differentiation(**Fig. 1.4**). For example, *Atg5* conditionally knockout mice show defective B-cell development and a loss in B lymphocytes[57]. While deletion of *Atg7* in T cells leads to impaired T cell function and development in mice[58]. Silencing of

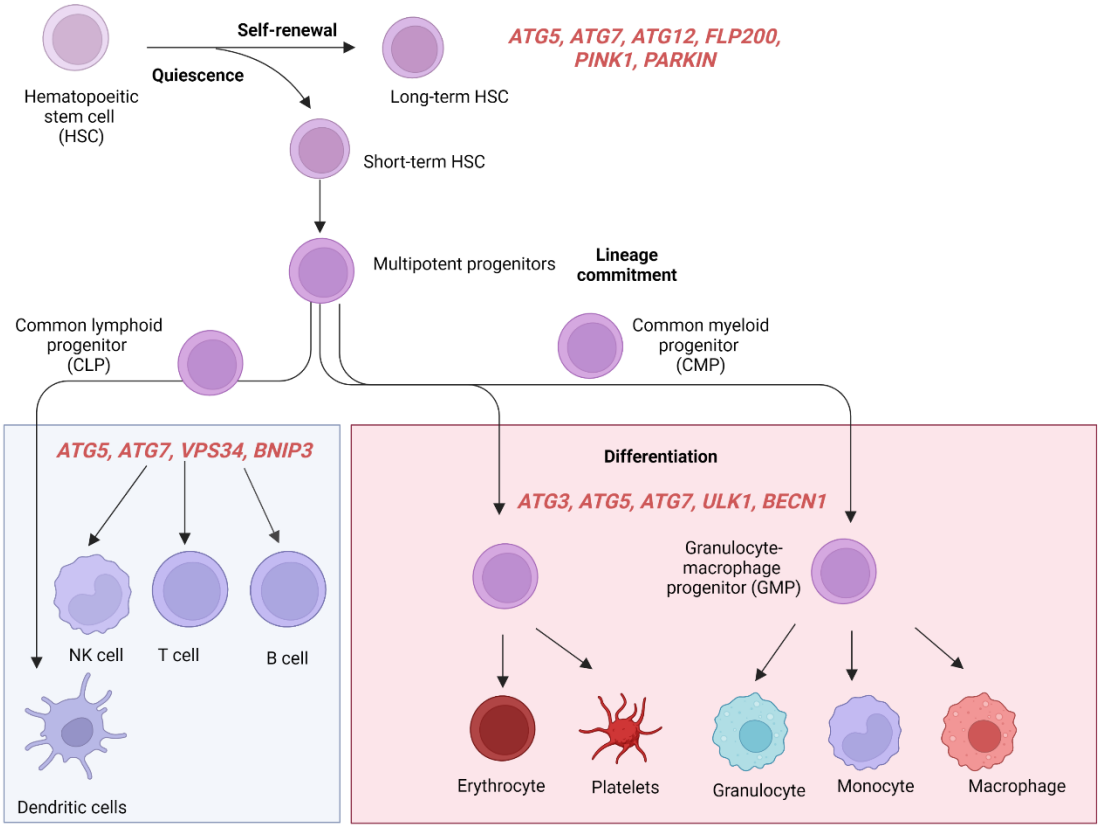


Figure 1.4 Autophagy in hematopoiesis

Overview of human hematopoiesis and key ATGs during each step. ATG, autophagy-related gene. HSC, hematopoietic stem cells. CLP, common lymphoid progenitor. CMP, common myeloid progenitor. GMP, granulocyte-macrophage progenitor. NK, natural killer. ULK1, unc-51 like kinase 1. BECN1, beclin1. PINK1, PTEN induced putative kinase 1.

*Atg3* caused ROS accumulation and mitochondria damage and cell number reduction of natural killer cells (NKs) from the bone marrow and spleen of mice[59].

Autophagy plays a dual role in cancer including AML, where it can either support cancer cell survival or induce cancer cell death (autophagy-mediated apoptosis). Studies showed that autophagy can play a tumor suppression role during the early proliferation of leukemia reacting to the stress of genomic alterations, for example, heterozygous knockout of *Atg5* results in the induction of AML in mice[60]. Conversely, more studies reported that autophagy plays a supportive role in established tumors to sustain their proliferation and survival under stress from limited space, hypoxia, nutrient, or chemotherapy. AML cells with *ATG7* knockdown showed impaired proliferation and chemoresistance, while mice leukemia models with *Atg7* deficiency have prolonged survival[61]. Deletion of *Atg3* in murine bone marrow cells prevents leukemogenesis in a transplantation model[62]. Inhibition of ULK1-mediated autophagy enhances chemotherapy-induced apoptosis in AML cells[63]. Deletion of the classic autophagy receptor *p62* jeopardizes myeloid leukemia development in the murine model[64]. Clearly, targeting autophagy exhibits harmful effects on leukemic cells at late stages of leukemia progression[65] (**Table 1.2**).

To understand the contribution of autophagy at different stages of leukemia development, more studies of the autophagy genes in AML subtypes are required. In particular, specific interactions between autophagy and frequently mutated genes such as *NPM1*, *TP53*, and *FLT3* need to be investigated.

It is reported that NPM1 mutations promote autophagy and enhance cell survival through AKT pathways[66]. Another study reported that enhanced autophagy helps resist FLT3 inhibitors in FLT3-ITD$^+$ AML[67]. Studies showed leukemia cells

displayed higher expression levels of *Atg7*, *serine/threonine kinase 11* (*STK11*), and *Beclin1* from AML patients with poor clinical outcomes[61]. Several chemotherapeutic drugs such as daunorubicin and cytarabine were identified to trigger autophagy that helps leukemic cells resist and survive[68].

Autophagy plays a pivotal role in the survival of leukemic cells; therefore, it can serve as a promising target for drug treatment against AML. It is believed that autophagy inhibitors can help sensitize leukemic cells towards drug treatments, thus overcoming drug resistance to attain a better outcome. Powerful autophagy inhibitors targeting the formation of autolysosomes such as CQ[69], bafilomycin A1[70] and Lys05[71] are introduced in combination with AC220 to treat MV4-11 and MOLM13 cells, which significantly enhanced the growth inhibitory effect and increased the apoptosis signaling pathway[72]. However, CQ usually requires a concentration of 100 uM to function efficiently *in vitro*, which is difficult to be used in patients[73]. More recently, genetic disruption of *Atg7* or *LC3* enhanced the therapeutic effect of BCR/ABL tyrosine kinase inhibitors or cytarabine[74,75] and targeting AMPK/FIS1-mediated autophagy attenuated leukemia stem cell expansion[76]. In addition, Hsp90 inhibitor 17-AAG targeting *TP53* mutation via chaperone-mediated autophagy (CMA) led to leukemia suppression[77], further indicating the potential of targeting autophagy against leukemia. Nevertheless, the lack of specificity and potential side effects hinder the clinical usage of conventional autophagy inhibitors, novel inhibitors targeting autophagy and possibly autophagy-related pathways or downstream targets specific to leukemogenesis are needed.

Table 1.2 Role of autophagy-related genes in AML progression.

| leukemic model | autophagy-modulating method | Autophagy modulation | role of autophagy in AML | Refs |
|---|---|---|---|---|
| mice with OCI-AML3 cells | shRNA against ATG7 | autophagy suppression | promoting leukemia | [59] |
| | Spautin-1 | | promoting leukemia | |
| mice with BM cells transduced with MLL-ENL | atg5 or atg7-floxed | autophagy suppression | promoting leukemia | |
| umbilical cord blood CD34+ cells | shRNA against ATG5 or ATG7 | autophagy suppression | suppressing leukemogenesis | [36] |
| MOLM-13 | shRNA against FIS1 | mitophagy suppression | promoting leukemia | [75] |
| MOLM-13 | Chloroquine, Lys05, and bafilomycin A1 | mitophagy suppression | promoting leukemia | [69] |
| NB4 cells | HSP90 inhibitor 17-AAG | autophagy improvement | suppressing leukemia | [76] |

### 1.3 Zebrafish Modelling of Normal and Malignant Hematopoiesis

Zebrafish (*Danio rerio*) is a well-established vertebrate model of human diseases[78]. Conserved gene homology, small size, high fecundity, transparency, ex-utero embryogenesis, rapid development, highly amendable to chemical and genetic manipulations, and well-characterized biological features make it an attractive model for studying developmental biology, regeneration, and cancer, including normal and malignant hematopoiesis (**Fig. 1.5**).

Similar to mammalians, zebrafish hematopoiesis is divided into two waves, primitive and definitive hematopoiesis[79]. Primitive hematopoiesis starts with the appearance of primitive erythrocytes and macrophages starting at 11 hours post-fertilization (hpf) in the cell cluster named intermediate cell mass (ICM)[80]. Definitive hematopoiesis starts at 30 hpf in the ventral wall of the dorsal aorta, characterized by the presence of hematopoietic stem progenitor cells (HSPCs), which give rise to erythroid, myeloid, and lymphoid lineages that migrate to the caudal hematopoietic tissue (CHT) (corresponds to the mammalian fetal liver) and later the kidney marrow (corresponds to mammalian bone marrow), where the life-long hematopoiesis happens[81,82].

Gene regulations in normal hematopoiesis are highly conserved between humans and zebrafish. Various lineage-specific hematopoietic regulators including hematopoietic stem and progenitor marker, *runx1*, erythroid progenitor marker, *gata1*, myeloid progenitor marker *spi1*, macrophage marker, *mpeg1*, neutrophil marker, *mpx*, as well as pan-leukocyte marker *l-plastin* are well characterized in zebrafish. Hematopoietic lineage-specific transgenic fluorescent reporter zebrafish lines are well established, which allows live monitoring of different hematopoietic lineages *in vivo*.

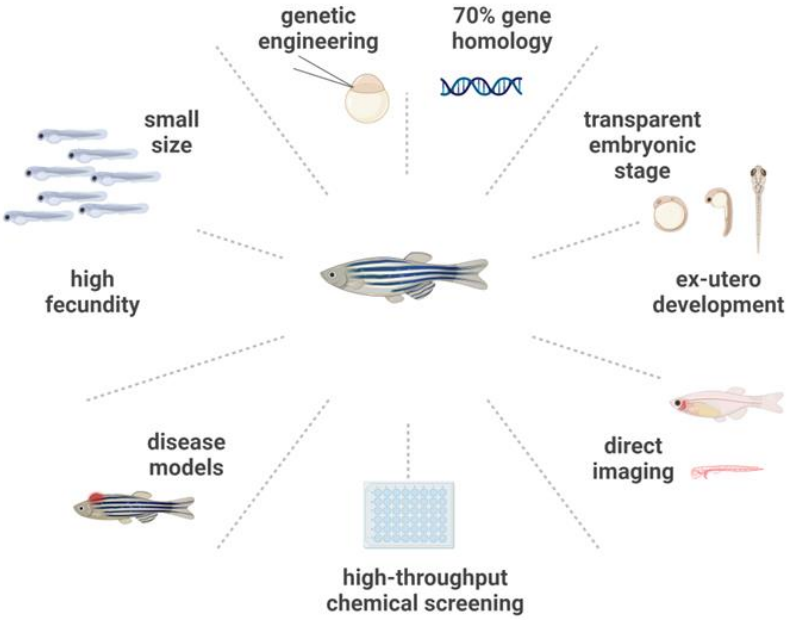


Figure 1.5 Advantages of zebrafish models in modeling leukemia.

A wide range of cancers such as leukemia, melanoma, glioblastoma, and pancreatic cancer has been modeled using zebrafish[83], partly because zebrafish is highly amendable to genetic manipulations. Zebrafish genetic models of recurrent mutations in AML were well established[84]. For instance, transgenic zebrafish lines expressing both *FLT3-ITD* and *IDH2* mutations exhibited leukemia phenotypes, which highly resemble human AML in cellular pathology, gene expression profiles as well as drug-treatment responses[85].

Animal models of leukemia aid in functional studies of driver gene mutations and the evaluation of pharmaceuticals. Although many leukemia cell lines harboring variable mutations have been used in testing potential drugs, they are inadequate in explaining the leukemogenesis and effects of the drug at the whole-organism level. Zebrafish models of leukemia provide *in vivo* platforms better than cell lines and less complicated than mice, facilitating the discovery of new molecular targets and novel drugs.

Zebrafish leukemia models can be classified by their creating techniques, as transgenic or transient, knockout or overexpression, and by the leukemia types, myeloid or lymphoid leukemia. With different creating approaches, many faithful zebrafish leukemia models were established. Zebrafish models are classified as follows: 1) chemical-induced mutagenesis models. 2) genetic models created by transgenic overexpression or knock-out by the nucleases system. 3) Transient models by mRNA expression or morpholino knockdown. 4) Xenograft models by xenotransplantation of human cell lines or primary cells (**Fig. 1.6**).

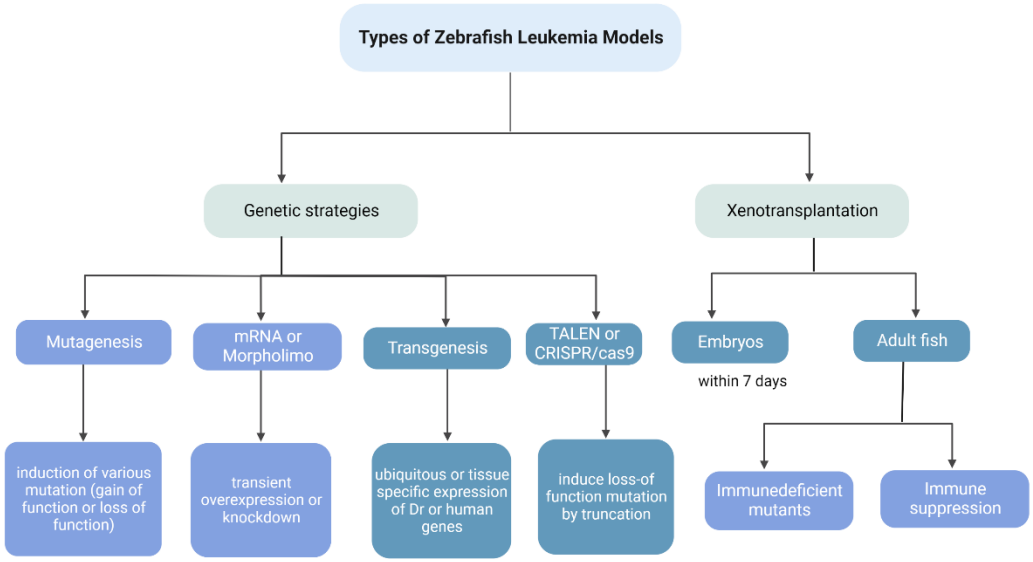


Figure 1.6 Types of zebrafish models of leukemia.

TALENs, Transcription Activator-like Effector Nucleases. CRISPR, Clustered Regularly Interspaced Short Palindromic Repeats. Cas9, CRISPR-associated protein 9.

Forward genetics, such as N-ethyl-N-nitrosourea (ENU) induced mutagenesis screens using zebrafish help identify previously unknown gene mutations that drive leukemogenesis. A previous study performed a phenotype-driven forward genetic screening by ENU-induced mutagenesis and identified a gene named *hsp9* that potentially drives MDS[86,87].

Transgenic zebrafish lines expressing human genes or loss of function mutants of zebrafish orthologs have been established. The Tol2 transposon system help facilitate the stable integration of human DNA into the zebrafish genome at high efficiency[88,89]. With this system, the human oncogenes can be expressed under the control of a ubiquitous (e.g., *cmv*, *u6*, and *b-actin*), or tissue-specific promoter (*spi1*, *fli1*, and *runx1*) to allow constitutive or conditional expression. For example, the first zebrafish transgenic model of leukemia is a zebrafish model of ALL that expresses the mouse *c-Myc* under the control of the zebrafish lymphoid tissue-specific promoter *recombination-activating gene-2* (*rag2*)[90,91]. Later, zebrafish AML models carrying *AML1- ETO*[92], *MOZ-TIF2*[93], *TEL-JAK2A*[94], and *NUP98-HOXA9*[95] fusion genes were generated respectively.

Zebrafish model of AML has been generated with *FLT3-ITD* specifically expressing in myeloid progenitor cells[96]. Zebrafish expressing myeloid progenitor-specific *spi-1 proto-oncogene* (*spi1*) promoter-driven *ETV6*-jak2a transgene showed T-ALL and CML phenotypes[94]. Crossing Tg(spi1:loxP-EGFP-loxP: *NUP98-HOXA9*) with Tg (*hsp70*:Cre) created a heat-shock inducible transgenic line that expresses human *NUP98-HOXA9* under the control of *pu.1* promoter[95].

Nuclease systems that induce gene knockouts include zinc finger nucleases (ZFN)[97], transcription activator-like effector nucleases (TALENs)[98], and the clustered regularly interspaced short palindromic repeats (CRISPR)/CRISPR

associated protein 9 (Cas9) system[99,100]. After delivery of the system at the one-cell stage, the mosaic F0 embryos are raised to maturity and outcrossed with wild-type zebrafish to generate F1. At 3 months of age, F1 is genotyped to confirm mutation and later incross to create Mendelian randomized F2 for phenotypic evaluation[88]. Loss-of-function tet2 zebrafish mutants, created by ZFNs, present abnormal myelopoiesis and differentiation blockage that resemble MDS phenotype[101].

TALENs are another nucleases system that can induce DNA breaks and recombination in endogenous genes of zebrafish[102]. This technique is carried out by assembling left and right-arm TALEN plasmids, in vitro transcription of mRNAs encoding TALEN pair, and injecting into one-cell stage embryos[98]. Zebrafish embryos injected with *idh1* TALEN mRNAs exhibited a high-efficiency knockout (97%), which developed a phenotype with significantly reduced definitive hematopoiesis and an increase in myeloid precursors reminiscent of the changes in primitive myelopoiesis[103].

CRISPR/Cas9 system consists of CRISPR RNA (crRNA), transactivating crRNA (tracrRNA), and Cas9 nuclease mRNA or protein. The principle is that the crRNA: tracrRNA duplex forms into a single guide RNA (sgRNA), and direct cleavage of target DNA by Cas9 protein[104,105]. In zebrafish, with CRISPR-mediated knockout, it can achieve an efficiency of 75–99% of indels[100]. Multiple sgRNAs up to 5 sets can be delivered simultaneously, resulting in a combination knockout within the same fish[106], bypassing the need for crossing multiple transgenic lines. Especially, with CRISPR/Cas9 genome editing, it can introduce biallelic mutations of multiple genes in the F0, allowing for phenotypic analysis directly in injected animals, saving two generations of time, and greatly improving the output of research. CRISPR/Cas9 technique combined with zebrafish has revolutionized

genome editing and gene functional studies and achieved efficiencies generally exceeding what has been attained by ZFNs or TALENs.

Transient models of leukemia and pre-leukemia were then established based on leukemic mutations and transient genetic tools, which primarily include antisense morpholino (MO)-mediated knockdown or mRNA-expressing vector-mediated transient overexpressions[107]. MOs are typically antisense oligomers of 25 bases that function via complementary binding to the mRNA of interest, thereby blocking translation[107]. Two consecutive studies done by Ma et al. demonstrated functions of *flt3* and *idh1* in zebrafish models by MO knockdown in parallel with transient overexpression of human AML mutations *FLT3-ITD* and *IDH R132H*, revealing their roles on the myeloid expansion[103,108]. As for mRNA, we and other groups have tested the functions of several key leukemic oncogenes, including zebrafish *wnt family member 10b* (*wnt10b*), zebrafish *Janus kinase 2a* (*jak2a*)$^{V581F}$, human *Calreticulin* (*CALR*), human *mixed-lineage leukemia 1* (*MLL*)-*AF9* fusion gene, human *NPM1c+*, human *FLT3-ITD*, and human *IDH*$^{R132H}$, in zebrafish which displayed leukemia- or pre-leukemia-like phenotypes shortly after injections[109]. Additionally, chemotherapeutics such as doxorubicin were evaluated in this model, proving its effects in reducing myeloid expansion and resuming hematopoiesis.

Zebrafish xenotransplantation was used as a pre-clinical therapeutic platform for chemical screening. The first leukemia xenotransplantation zebrafish model, in which K562 and NB-4 leukemia cells were transplanted into embryos, was subsequently used for chemotherapy tests[110]. Leukemia cells can survive in the recipient embryos, proliferate, and circulate within the embryonic vasculature for 7 days without rejection[111]. Adult xenotransplantation requires the zebrafish to be immunocompromised and used for 20-30 days before rejection could occur[112,113].

The generation of transparent adult zebrafish, also known as *Casper*, preserved the transparency of zebrafish from the embryonic stage to adulthood and offered a unique *in vivo* model. Together, these studies prove zebrafish transplanted with leukemia cells can provide an alternate pre-clinical model to rodents with unique advantages.

### 1.4 Zebrafish as a Model to Study Autophagy

Autophagy is a highly conserved cellular mechanism shared by a wide range of species from yeast to mammals. Zebrafish have recently emerged for studying autophagy. Almost all orthologs of autophagy components have been identified in the zebrafish genome, and most of them shared over 70% homology with humans among gene functional domains (e.g., *ATG7* 77%, *ATG5* 81%, *ATG3* 82%). Besides, zebrafish is especially feasible for genome editing by techniques like the Tol2, TALEN, and CRISPR systems. Together with its transparent and ex-utero embryonic stage, multiple reporter lines and mutants were created, making it convenient for observing autophagy during vertebrate development. Particularly, zebrafish transgenic *GFP-Lc3* and *GFP-Gabarap* fish lines tagged the autophagy markers and allow for direct monitoring of autophagic flux in live animals[114]. This model is further developed by using the *Elavl3* promoter specifically expressed in the central nervous system for monitoring autophagy in neurons[115], though zebrafish line with hematopoietic cells specifically expressing EGFP:Lc3 is awaiting creation.

Taking advantage of embryonic transparency, autophagy from different stages of development can be visualized in live cells from organs and tissues by light-sheet fluorescence microscopy[116]. Moreover, chemicals can be added directly into the medium for treatment, and are efficiently absorbed by the skin, thus allowing zebrafish for direct assays of drug-induced autophagy. In previous studies, many chemicals were found to regulate autophagy using zebrafish transgenic models. For example, the use of a zebrafish *GFP-Lc3* reporter line help reveals that 1-phenyl-2-thiourea/PTU, an anti-pigmentation chemical, induces autophagy in various tissues while it targets tyrosinase[117]. The pathogen infection and phagocytosis-related

autophagy are also well captured by using tissue-specific zebrafish reporter lines. Especially for the study of phagocytosis-related autophagy[50]. Lysosomes and mitochondria can also be easily detected in live embryos by the addition of LysoTracker™ Red or mito-Red to media before imaging. In addition, Lc3 expression levels and conjugation to PE can be monitored by western blot analysis against Lc3 proteins[118]. An advanced method has been developed to measure and quantify autophagosome accumulation in vivo[118].

Gene knockdown studies of ATGs by custom-designed morpholinos in zebrafish identified functions of *becn1*, *Atg5*, and *Atg7*[116,119,120]. Other regulatory proteins such as Mtor, Rubcn, and Raptor were characterized by morpholino treatment[50,121]. However, the off-target effects of this approach unavoidably induce cellular stress and may disrupt the phenotype reading[122–124]. Therefore, a more advanced technique like the CRISPR-Cas9 genome editing system was adopted for reliable targeted gene deletions of ATGs, *sqstm1*, *optn*[125,126]. For instance, we have recently examined the role of autophagy regulation during definitive hematopoiesis via CRISPR-Cas9 knockout of multiple ATGs (*atg2a*, *becn1*, *atg13*, *atg3*, *atg5*, *atg9a*, *atg12*), either individually or in combination[127].

In conclusion, due to the high-efficiency genome engineering and well-established hematopoietic assays, zebrafish is an ideal vertebrate model for studying the complex role of autophagy in hematopoiesis. Studies in zebrafish will greatly contribute to our understanding of the distinct roles of autophagy-associated genes in different aspects of hematopoiesis.

# 2. Research Aims and Objectives

## 2.1 Research Aims

FLT3-ITD$^+$ AML patients treated with TKIs only show transient remission and they soon encounter frequent relapses. It is believed that FLT3-ITD expression promotes basal autophagy in AML cells; thus, AML patients with FLT3-ITD mutation are more sensitive to proteasome inhibitors than the FLT3-WT counterparts. Autophagy is one of the resistance mechanisms of FLT3-ITD$^+$ AML. However, suppression or ablation of core autophagic regulators, such as Atg5, Atg7, Fip200, or Beclin1, is usually lethal and ultimately induces death in mouse models. In addition to targeting canonical autophagy pathways, exploring novel targets of autophagy in FLT3-ITD$^+$ AML is needed. Meanwhile, it is also vital to study the functions of these autophagy-related target genes in normal hematopoiesis. A comprehensive understanding of these genes mediating both malignant and normal hematopoiesis is helpful in developing improved therapeutic strategies.

Here I aimed to identify potential therapeutic targets and the underlying mechanisms using both AML cell lines and zebrafish models. Theoretically, the expression of potential gene target(s) is upregulated by autophagy specifically in FLT3-ITD$^+$ AML cells. Targeting this gene will inhibit autophagy and thereafter proliferation of leukemia cells. Consequently, the ubiquitous autophagy of healthy cells will be less affected. Furthermore, I also aimed to investigate the role of the gene(s) in controlling normal and malignant hematopoiesis in zebrafish models. Through this study, I aimed to broaden the perspectives and provide technical solutions on AML gene therapy. This study has shed light on more precise

understanding of the roles of autophagy in leukemia and provided insights into the development of novel therapeutic agents.

## 2.2 Objectives

1. To identify autophagy-associated protein(s) as therapeutic target candidates for AML using FLT3-ITD$^{+}$ AML cell lines.

2. To investigate the functional roles of novel autophagy-associated candidate proteins using AML cell lines.

3. To examine the functional roles of novel autophagy-associated candidate proteins in definitive hematopoiesis using zebrafish models.

# 3. Material and Methods

## 3.1 Cell Culture and Viability Test

The human acute myeloid leukemia cell lines MV4-11, MOLM-13, KG-1, Kasumi-1, NOMO-1, OCI-AML3, THP-1, ML2, and human chronic myeloid leukemia cell line K562 were originated from the DSMZ (German Collection of Microorganisms and Cell Cultures, Leibniz, Germany) and ATCC (American Type Culture Collection, USA). Cells were cultured in RPMI 1640 medium (Gibco, #11875119) supplemented with Glutamax (Thermo Fisher, #35050079), 10% fetal bovine serum (Thermo Fisher, #26140079), and 1% of penicillin and streptomycin (Gibco, #15070063) at 37°C in a humidified hood containing 5% CO2. The stock of cell lines was maintained in cryovials with 10% DMSO RPMI 1640 medium following the procedure by putting in a -20-degree fridge for 3 hours and overnight in a -80-degree fridge then transferred to a liquid nitrogen tank preservation for less than 2 years.

After resuscitation, cells were subculture in full RPMI medium for one day before cell viability was measured by the PrestoBlue reagent (Thermo Fisher, A13262). Cells medium mixed with PrestoBlue were incubated at 37°C in dark for 2 hours, then the fluorescence intensities at 590 nm were measured by a plate reader (BMG FLUOstar Optima). The fluorescence absorbance indicates the viable cell numbers. An automated cell counter (Thermo Fisher) was used to validate the viable cell number during the experiments. IC50 of drugs were obtained where the does inhibit cell growth by around 50% compared to the DMSO-treated control group after 24-hour incubation. Viability test was carried out in three independent triplicates.

### 3.2 Zebrafish Husbandry and Maintenance

Wild-type, Tg(*mpx*:EGFP), Tg(*Lc3*:GFP), Tg(*mfap4*:BFP), and Tg(*coro1a*: DsRed) zebrafish lines were raised and supported under regular light-dark cycle (14 hours light/ 10 hours dark), and standard aquatic conditions, and fed twice a day with living shrimp. By natural spawning, embryos were collected and kept in an E3 medium supplemented with methylene blue at 28.5 °C (**Fig. 3.1**). Embryos stage was decided by the hour past fertilization (hpf) according to the criteria in the guidelines[128] introduced by Kimmel et al.. All zebrafish-related experiments were conducted under the approval of the Animal Subjects Ethics Sub-Committee (ASESC) of The Hong Kong Polytechnic University.

### 3.3 Generation of Mutants by CRISPR/Cas9 System

Clustered regularly interspaced short palindromic repeats (CRISPR) and CRISPR-associated protein 9 (Cas9) system is an advanced technique for gene editing[106]. Custom-designed synthesized sgRNA and Cas9 nuclease were purchased from Integrated DNA Technologies (Iowa, USA) (**Table 3.1**). The items were stored at -20 °C upon arrival. The diluted Cas9 nuclease mixed with diluted sgRNA was activated by incubation at 37 °C for 10 minutes. Then the ribonucleoprotein (RNP) was delivered into embryos by microinjection or transfection. After 24 to 48 hours, genomic DNA was collected for restriction fragment length polymorphism (RFLP) assay for genotyping.

### 3.4 Microinjection

For zebrafish embryo injections, diluted sgRNAs and Cas9 nucleases were mixed and incubated to form the RNP complex. RNP mixture at a concentration of

3 uM was prepared in 20 mM HEPES solution. The material was delivered into one-cell stage embryos at the cell cytoplasm using a pressure-controlled PLI-90 Pico-Injector (Harvard Apparatus, Massachusetts, USA) and a stereomicroscope (Nikon SMZ800, USA) (**Fig. 3.1**).

### 3.5 Transfection

sgRNAs (44 uM) and Cas9 nucleases were mixed and transfected into M13, OCI-AML3, THP-1, MV4-11, and KG-1 cells (5X10^7) via the Neon Transfection system (Thermo Fisher, USA). Briefly, cells that reach 80% confluency were collected, washed with PBS, resuspended with Buffer R (Neon transfection system, Thermo Fisher), then mixed with the RNPs to make a 100ul cell mixture. The parameters of the electroporation are 1,700v, 20ms, and 1 pulse, with a transfection efficiency of up to 76%. Next, the transfected cells were cultured in RPMI medium supplemented with 10% FBS in a humidified 37°C/5% CO2 incubator for 48 hours before follow-up experiments.

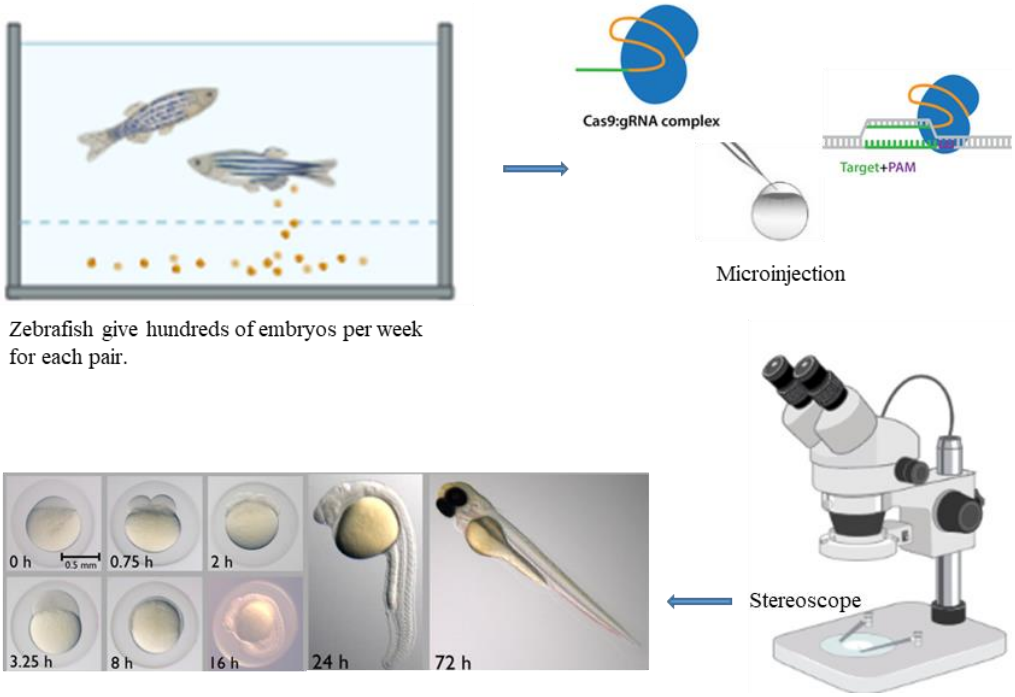


Figure 3.1 Natural spawning, microinjection, and CRISPR/Cas9 delivery in zebrafish.

### 3.6 Restriction Fragment Length Polymorphism Analysis and Sequencing

Leukemia cells after transfection and embryos after microinjection were collected and lysed with proteinase K (2 mg/ml, Thermo Fisher) in genome DNA extraction buffer and incubated for 2 hours at 55 °C followed by 98 °C inactivation for 5 minutes. The sequence of specific genes was PCR-amplified using pre-designed primers (BGI) following general PCR protocol (**Table 3.1**). AciI, HpaII, StyI, and MseI were ordered from the New England Biolabs (NEB) and stored at -20 °C upon receipt (NEB, USA). Amplified DNA was mixed with the corresponding restriction enzyme and incubated at 37 °C for 2 hours. Then the products were run on agarose gel (1.5% ) for electrophoresis. Mutations can be verified by cut or uncut bands. Mutants were PCR-amplified, cloned with pGEM-T Easy Vector Systems (Promega), then transformed into TOP competent cells (Thermo Fisher) following blue/white screening where white positive colonies were picked for plasmid extraction and Sanger sequencing (BGI, China).

### 3.7 Western Blot

The following antibodies were from *Cell Signaling Technology*: phosphor-FLT3 (Tyr591, #3461), FLT3 (#3462), phospho-STAT5 (Tyr694, #9352), phospho-AKT (Ser473, #9277), AKT (#9272), ERK (#9102), phospho-ERK (#4370), ATG5 (#8540), GAPDH (#2118), p62(#5114), PINK1 (#6946), ULK1 (#4776), Phospho-Histone H3 (Ser10) (D2C8) (#3465).

The following antibodies were from *Abcam*: LC3B (#ab48394), and goat Anti-Rabbit IgG H&L (HRP) (#ab6789). Antibodies from *Santa Cruz*: p16 (sc-1661), p21 (sc-6246), DOCK2, and BECN1 (sc-11427). SCPEP1 (MBS704649) antibody was from *MyBioSource*. ERMP1 (17321) antibody was from *Proteintech*.

Mammalian Protein Extraction Reagent (#78501) and protease inhibitors cocktail (#78429) were from *Thermo Fisher*. 10-12% polyacrylamide gel, non-fat milk, and enhanced chemiluminescence (ECL) detection reagents were from *Bio-Rad*. Polyvinylidene difluoride (PVDF, 0.45um) membrane was from *Millipore*. Rapamycin (autophagy inducer),3-MA (PI3K inhibitor), and chloroquine (CQ, autophagosome-lysosome fusion inhibitor) were from *Selleck Chemicals*. Chemicals (DMSO, IAA, DTT, Tris, Methanol, Ethanol) were from *Sigma-Aldrich* unless otherwise stated.

Cellular proteins were collected by lysing with MPER at 4°C for 30 minutes. After centrifugation and mixing with loading dye buffer, the protein lysates were denatured by boiling for 5 minutes. Proteins were deposited at -20°C and used within 2 weeks. Embryos were deyolked and extracted for proteins using lysis buffer, by using an insulin syringe needle from BD Biosciences (#324921). The concentration of the sample was measured by the BCA kit (Thermo Fisher, #23225). A similar mass of protein was loaded and run on a 12% acrylamide gel (TGX FastCast, Bio-Rad, #1610175). In 4 °C room, the proteins were transferred onto PVDF membrane at 250 mA, 300 V for 2.5 hours. In room temperature, the membranes were blocked by 5% non-fat milk in Tris-buffered saline with 0.1% Tween (TBST) for 2 hours. After washing with phosphate-buffered saline solution (PBST), membranes were blotted for 16 hours at 4 °C with the primary antibodies at 1:500-1:1000 ratio. Then the membranes were immersed with appropriate secondary antibodies at 1:2500, room temperature for 2 hours. The intensity of proteins was enhanced by ECL and imaged using ChemiDoc XRS+ System (Bio-Rad, USA). Then parameters were measured using ImageJ (NIH) and quantified

using GraphPad Prism 8 software. Three independent biological repeats were conducted.

### 3.8 Whole-mount In Situ Hybridization

*Dock2*, *ermp1*, and *scpep1* mRNA probes were generated as follows. Briefly, wild-type zebrafish cDNA was amplified, and PCR cloned into the vector (pGEM-T Easy system, Promega, A1360), the recombinant plasmid was synthesized by overnight incubation at 4 degree, then transformed into TOP10 competent cells. Positive colonies were picked and cultured and extracted for plasmids using the miniprep Kit (Qiagen, USA). Then the plasmids were verified via sequencing. The confirmed plasmids were linearized, purified, and *in vitro* synthesized for mRNA using T7 or SP6 RNA polymerase (Roche) supplemented with RNase inhibitor. The probes were labeled using DIG RNA Labeling Kit (Roche, #11175025910). Then the synthesized antisense RNA probe was precipitated with LiCl in an RNase-free water solution at -20 °C overnight. Then the solution was centrifuged for 10 minutes at 12,000xg, 4 °C, and the pellet was washed with pre-cooled 75% ethanol. The pellet was collected by centrifugation at 7,500g at 4 °C, and air-drying. RNase-free water was used to resuspend the RNA. The probe was stored at -20 degrees for further experiment.

To detect expression patterns of hematopoietic genes, WISH was performed as follows. Zebrafish embryos were immersed in 4% paraformaldehyde (PFA) for 16 hours at 4 degree to fix, followed by stepwise dehydration with ethanol of increasing concentration and stored at -20 °C overnight. After rehydration with ethanol of decreasing concentration, the embryos were treated with H2O2/KOH (1:1) solution to remove pigment. Then the embryos were permeabilized in

Proteinase K in PBST, then refixed with 4% PFA and incubated in a pre-hybridization buffer (PHB) for 4 hours at 65°C. Zebrafish embryos were then incubated at 65°C overnight with probes of *c-myb* (HSPC), *pu.1* (myeloid progenitor), *l-plastin* (pan-leukocyte), *hbae1* (erythrocyte), *mpx* (neutrophil), and *rag1* (T-lymphocyte) to examine definitive hematopoiesis. Next, the embryos were incubated with anti-digoxigenin in 2% lamb serum overnight at 4°C. Then the embryos were washed using PBST (0.1% Tween) and Alkaline phosphatase (AP) buffers, followed by staining with the nitro blue tetrazolium/5-bromo-4-chloro-3-indolyl phosphate solution (NBT/BCIP, Roche, # 11681451001) till the signal intensified [H282]. The embryos were then imaged using bright field light microscope. Positive cells were counted to determine the level of gene expression.

### 3.9 Phospho-Histone H3 (PH3) Immunostaining

Fixed zebrafish embryos (n=20) were permeabilized with pre-cooled acetone at -20 °C for half an hour. Embryos were then washed with PBST for 3 times and immersed in goat serum/bovine serum albumin PBS blocking solution for 4 hours. After washing with PBST, embryos were incubated with anti-rabbit phospho-Histone H3 (Ser10) antibody at a ratio of 1:500 overnight at 4 °C. Next, embryos were washed using PBST solution and immersed with goat anti-rabbit secondary antibody (Alexa Flour 594) for 3 hour prior to fluorescent imaging.

### 3.10 Flow Cytometry and Cell Sorting

Flow cytometry was used to measure cell cycle, autophagic flux, and apoptosis. To analyze cell death and cell cycle, 1x10^6 cells were washed and re-suspended in 500ul of PBS, and 5 ul of propidium iodide (Thermo Fisher, P3566) was added

avoiding light exposure. Cell samples in phosphate-buffered saline (PBS) with 1% FBS were then run on FACS: Calibur-Flow Cytometer (BD Pharmigen).

Zebrafish Tg(*coro1a*: DsRed) were crossed to collect embryos. On day 3, embryos were dissociated using Trypsin-EDTA solution (0.05%) (Thermo Fisher, #25300062) for 20 minutes at room temperature and dispersed by pipetting. Then trypsin was inactivated with CaCl2 (2mM), then the lysates were centrifuged and filtered by a 40 μm cell strainer (BD Biosciences, #352340) and transferred into PBS solution (1% fetal bovine serum). Cell sorting was conducted in a BD FACSAria III Cell Sorter following the user guide.

Selected hematopoietic cells were incubated using Hoechst and CYTO-ID mixed solution(Enzo Life Sciences, USA) for 30 minutes at 28.5 °C, in the dark. After washing with PBS 3 times, cells were placed on the confocal dish (35mm, SPL life sciences, #100350) and checked under Leica TCS SPE Confocal Microscope (Leica Microsystems, Wetzlar, Germany) at 40× (**Fig. 3.2**). Images were processed and analyzed using Leica LAS-X software (Leica, Germany).

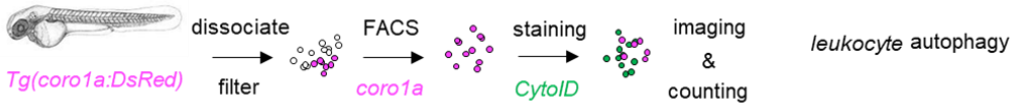


Figure 3.2 Schematic workflow of FACS-based cell sorting of zebrafish hematopoietic cells.

### 3.11 Autophagy Modulation and Lysotracker Staining

Zebrafish embryos from 2 dpf were incubated with 3-Methyladenine (10mM, Selleckchem, #S2767) or chloroquine (100uM, Selleckchem, #S4157) for 24 hours. Then 3 dpf Tg(*Lc3*:GFP) embryos were stained with 10uM Fluorescent dye LysoTracker™ Red DND-99 (Invitrogen, #L7528) in the dark at 28.5 °C for around 1 hour to monitor the lysosome. Next, embryos were washed with E3 buffer 3 times before imaging.

### 3.12 Lightsheet Imaging

Embryos raised to 3 or 4 dpf were immersed with tricaine solution (0.164 mg/ml, Sigma-Aldrich, A5040) and fixed in low-temperature agarose (1.5%, Sigma-Aldrich, A9045) within glass capillary, then imaged using Zeiss Lightsheet Z.1 Illumination Microscope (Zeiss, NY, USA). Captured images were analyzed and measured using a new version of ZEN (Carl Zeiss Microscopy, NY, USA) software. The positive signals of LysoTracker Red, GFP-Lc3 e, and GFP-Lc3 and LysoTracker Red double-stained signals were measured to calculate the number of autophagic structures following the standard described in a previous study[115].

### 3.13 CYTO-ID Staining and Confocal Imaging

Cyto-ID is a cationic amphiphilic tracer dye that can label autophagic structures including pre-autophagosomes, autophagosomes, and autolysosomes in live cells[129]. First, confluent cells were treated with DMSO, Rapamycin, or chloroquine at IC50 to induce or inhibit autophagy for around 24 hours. Then cells (10^6) were collected by centrifugation for 5 min at 1500g and washed with prewarmed PBS with 1% FBS. Cells were resuspended in Cyto-ID Green dye PBS solution (1:4000)

for 30 min at 37 °C in the dark. Autophagic flux was monitored by fluorescence microscopy or flow cytometry. For confocal imaging, the cells were mounted with Prolong Gold Antifade Mounting solution supplemented with 4′,6-diamidino-2-phenylindole (DAPI) (Invitrogen) in a confocal plate and monitored under a Zeiss LSM780 microscope using ZEN software.

### 3.14 Liquid Chromatography Mass Spectrometry

Cells at exponential growth were treated with autophagy modulators for 24 hours, then centrifuged, and washed with PBS. Proteins were then extracted using the MPER extraction buffer with protease and phosphatase inhibitors. Then protein samples were purified using Methanol/chloroform and resuspended in 4M urea solution. The purified protein samples were reduced with 10mM DTT at 37 °C for 30min and alkylated with 20mM IAA in the dark for 15min. 50mM ammonium bicarbonate was used to dilute the so that urea concentration is 1M. The protein concentration was measured using the BCA test. According to the concentration, the same amount of protein from different groups were digested with trypsin (mass protein: trypsin=40:1) at 37 °C for 16h. Peptides were next desalted using C18 columns (#P189870), cold-dried, and resuspended with 0.1% FA before putting on the Orbitrap MS coupled with LC (Thermo Fisher). Three independent replicate experiments were performed for each condition. MassHunter Quantitative Analysis software was used for the automatic processing of quantitative data. The raw m/z data was searched against the Uniprot database and analyzed using the Proteome Discoverer (Thermo Fisher) to produce the list of identified proteins and their normalized abundance. Then their z-scores (log 2) and p-values (-log 10) were plotted using GraphPad Prism 8.

### 3.15 Real-Time Quantitative PCR

RNA sample was obtained from zebrafish embryos by RNAiso Plus solution (Takara, #9108) extraction. Around 30 embryos were collected for each group. The sample was dissociated with 1ml Trizol, eluted with chloroform, and centrifuged. The supernatant was transferred to a new tube and incubated with isopropanol at room temperature for 10min. Then the RNA was collected by centrifugation at 14000g for 10 minutes and subsequently washed with 75% ethanol at 7500 g for 5 minutes at 4 °C. The RNA was air-dried and re-suspended in RNase-free water (20 ul). Yields of RNA were determined by the absorbance ratio at 260 nm and 280 nm using Nanodrop Spectrophotometer (Thermo Fisher). RevertAid First Strand cDNA Synthesis Kit was used to synthesize the cDNA (Thermo Fisher, K1622) following the manufacturer's protocol. Next cDNA as a PCR template was diluted and PCR using FastStart Universal SYBR Green Master reagents (Roche, #4913850001) and primers (**Table 3**.1). PCR amplification was performed on ABI 7300 Real-Time PCR System (Thermo Fisher). There are three biological replicates, and the experiment is performed in triplicates independently.

### 3.16 Statistical Analysis

Statistical analysis was performed via GraphPad Prism, version 8 (GraphPad Software, CA, USA). In the figures, the error bars stand for the standard error of the mean, and the data were displayed as mean ± standard error of the mean (SEM). Student t-test was performed for pairwise comparison. P-values less than 0.05 were considered statistically significant. The level of significance was indicated as *P<0.5, **P<0.01, ***P<0.001.

Table 3.1 List of sgRNAs and primers

| Name | Sequence |
|---|---|
| Human *DOCK2* sgRNA | TCTTAAACCAGATGGGTGAC |
| Zebrafish *dock2* sgRNA | GATCAGATCATCAAGTGAGT |
| Human *ERMP1* sgRNA | GTAGATGTACAACGGCCCAC |
| Zebrafish *ermp1* sgRNA | GTGGACGTCCAGAAGCCCACCGG |
| Human *SCPEP1* sgRNA | CCACGGGATTATCCACAAAT |
| Zebrafish *scpep1* sgRNA | AGCTTAAGGTCTCTGTCAAG |
| Human *PINK1* sgRNA | CCCTTGGCCATCAAGATGATGTG |
| Zebrafish *pink1* sgRNA | CCTCCGCTCGATGTCCATGGAGT |
| *DOCK2* genotyping Forward | AAGGTGCTAAAGGAGCCACC |
| *DOCK2* genotyping Reverse | GGGACAGAAGCCATGTTCCA |
| *dock2* genotyping Forward | GCACCTGGATGTGAATTGCG |
| *dock2* genotyping Reverse | GGACTGGGGATTGAGGTTTGAT |
| *ERMP1* genotyping Forward | ACATAACCTCCATTGGCCCC |
| *ERMP1* genotyping Reverse | TGGGCTGTGACAAGTTCCAA |
| *ermp1* genotyping Forward | TGGGGAAAATGTTAATGAAGAAGG |
| *ermp1* genotyping Reverse | TGAGTCGAAGTGGCAGTTAGC |
| *SCPEP1* genotyping Forward | GTCCTCTGGCTTCTTCGAGT |
| *SCPEP1* genotyping Reverse | TTGGCATAGGCACCACTACC |
| *scpep1* genotyping Forward | CCAATAGCTCCAGTGCCAGT |
| *scpep1* genotyping Reverse | TGTAACTGTATCCGGTGCCC |
| *PINK1* genotyping Forward | TGCTGCTGTGTATGAAGCCA |
| *PINK1* genotyping Reverse | TAGTCAGGTTACCTCCCCCTG |
| *pink1* genotyping Forward | GTGTCCATGAAAGAGCGGGA |
| *pink1* genotyping Reverse | ATGTGGATTGAGTCGGGTCG |
| Zebrafish *c-myb* probe Forward | CGGCACAGACACAGTGTTTACAGTA |

| | |
|---|---|
| Zebrafish *c-myb* probe Reverse | GATTCTCGAAGGCAACTTTGGACCT |
| Zebrafish *l-plastin* probe Forward | GAAGACCAGCGTCCATCTGC |
| Zebrafish *l-plastin* probe Reverse | CCAGCTCCACCGCATAGTTA |
| Zebrafish *mpx* probe Forward | CTCTGAACCCTGCTTCCCAAT |
| Zebrafish *mpx* probe Reverse | TGGAATCTCTATCAGTCTCTTTCCA |
| Zebrafish *hbae1* probe Forward | AGAGCCAGAGCTGAGAGGAA |
| Zebrafish *hbae1* probe Reverse | GTCTCTCTGCCAAAGACAAA |
| Zebrafish dock2 probe Forward | GCTTCGATGTGGATTGAGCG |
| Zebrafish dock2 probe Reverse | CTCATCCATATCCGGCAGCTC |
| Zebrafish ermp*1* probe Forward | CTGCTCGGCTTCGTTTGTTT |
| Zebrafish ermp*1* probe Reverse | ATCCAGATGCTTCCTGGCTCT |
| Zebrafish scpep*1* probe Forward | AGCTGAGGACGTGTTTGTCA |
| Zebrafish scpep*1* probe Reverse | ACCCACATCTCCTGACCCATC |
| *ATG3* qRT-PCR Forward | GATGGCGGATGGGTAGATACA |
| *ATG3* qRT-PCR Reverse | TCTTCACATAGTGCTGAGCAATC |
| *ATG5* qRT-PCR Forward | CACTTTGTCAGTTACCAACGTCA |
| *ATG5* qRT-PCR Reverse | TAGAGCGAACACGAACCATCC |
| *ATG7* qRT-PCR Forward | ATGATCCCTGTAACTTAGCCCA |
| *ATG7* qRT-PCR Reverse | CACGGAAGCAAACAACTTCAAC |
| *TP53* qRT-PCR Forward | CCGGCGCACAGAGGAAGAGA |
| *TP53* qRT-PCR Reverse | TGGGGAGAGGAGCTGGTGTTGT |
| *Dr.atg13-QF* | ATCACAAGGGTGACTCCTGC |
| *Dr.atg13-QR* | CGCACTGTCTGAAAGCCTTCC |
| *Dr.becn1-QF* | GGCTTTCCTTGACTGTGTCC |
| *Dr.becn1-QR* | CCTTTGTCCACATCCATTCTG |
| *Dr.atg9a-QF* | GTTTCTCCCAGTGGACGTGTG |
| *Dr.atg9a-QR* | TTGCCATGTGAAATAAGGAAGGTCC |

| | |
|---|---|
| *Dr.atg5-QF* | AGAGAGGCAGAACCCTACTATC |
| *Dr.atg5-QR* | CCTCGTGTTCAAACCACATTTC |
| *Dr.atg3-QF* | GGCTGTTTGGATATGATGAG |
| *Dr.atg3-QR* | AGCAGGTGGAGGGAGATTAG |
| *Dr.b-actin-QF* | TTCCTTCCTGGGTATGGAATC |
| *Dr.b-actin-QR* | GCACTGTGTTGGCATACAGG |
| *Dr.mTOR-QF* | TTATCGTGCTGGTCCGAGCT |
| *Dr.mTOR-QR* | AAGTGGGCCCTTATCGCTGT |
| *Dr.p62-QF* | CGATGTTTTTGTCGGTCTCA |
| *Dr.p62-QR* | CAAGAGCCAAACCCATCATT |
| *Dr.ATF6-QF* | ATGAGTGAGAACTCTGTGCT |
| *Dr.ATF6-QR* | TCATTGGACCCAAGTTGACA |
| *Dr.PERK-QF* | GCTCAAAGACGCAAGCACTG |
| *Dr.PERK-QR* | ATGAGTCCACAGGAGACGGA |
| *Dr.CHOP-QF* | TCTTCAGAGAAGGAGCCCGA |
| *Dr.CHOP-QR* | CTTGGTGGCGATTGGTGAAC |

# 4. Results

## 4.1 Leukemia Cell Line Profiling

To examine the role of autophagy in heterogeneous AML, a panel of leukemia cell lines with different genetic backgrounds, including MOLM-13 (M13), MV4-11, K562, OCI-AML3, THP-1, and KG-1 were studied (**Table 4.1**). MV4-11, KG-1, M13, and K562 cells showed doubling growth within a day (**Fig**. 4.1a). Next, half-maximal inhibitory concentration (IC50) of Rapamycin (RAPA, autophagy inducer), chloroquine (CQ, inhibitor of autophagosome and lysosome fusion), and TKIs like sorafenib, quizartinib, sunitinib, and midostaurin of each cell line were measured (**Table 4.2**). Fast-proliferating AML cell lines like MV4-11, M13, and KG-1 cells were more sensitive to CQ treatment than the CML cells (**Fig**. 4.1b, c). The cell number of all the AML cell lines (except K562, a CML cell line) was halved at a concentration of 75 uM (IC50=75 uM). While the response to the autophagy inducer, RAPA, was similar among AML cell lines, only the cell number of MV4-11 and NOMO-1 reduced by half at a concentration of 20uM (**Fig**. 4.1b). All cell lines showed dose-dependent growth inhibition to kinase inhibitors, but quizartinib showed the most potency for M13 cells (**Fig**. 4.1d-i).

To examine their autophagy level, two FLT3-ITD$^{+}$ AML cell lines, M13 and MV4-11 cells were treated with 20 uM and 75 uM of RAPA and CQ, then harvested for Western blot against the LC3 protein. During autophagy, the cytosolic LC3 protein (LC3-I) is conjugated to phosphatidylethanolamine (PE) to form the conjugated form of LC3 protein (LC3-II), which is later recruited to autophagosomal membranes[130]. Then LC3-II can be used to mark autophagy level in cells. However, since autophagy is a continuing process, LC3-II level fluctuates when the autophagosome is fused and degraded by lysosome. To measure the

autophagic flux, CQ is routinely used to block the autophagosome-lysosome fusion so that the actual level of autophagy is captured[118]. The result showed elevated LC3-II level after treatment of CQ among the AML cells, while MV4-11 cells were more sensitive to autophagy inhibitors compared to M13 cells, indicating by a higher LC3-II/GAPDH ratio (**Fig**. 4.2).

Table 4.1 Sequencing variations and origins of leukemia cell lines

| Cell line | Origin | Cell type | Featured mutations | Doubling time | Ref. |
|---|---|---|---|---|---|
| M13 | Adult acute myeloid leukemia, 20 Y male | Monocyte | MLL-AF9 gene fusion, FLT3 internal tandem duplication (**FLT3-ITD**) | 3-4 days | [131] |
| MV4-11 | Childhood AML, 10 Y male | Monocyte | **FLT3-ITD** | 32 hours | [132,133] |
| K562 | Chronic myelogenous leukemia, 53 Y male | Cancer cell line | BCR-ABL1 gene fusion, TP53 homozygous | 47 hours | [134] |
| OCI | AML, 73 Y female | Cancer cell line | DNMT3A R635W mutation | 3-4 days | [135] |
| THP-1 | Adult acute monocytic leukemia, 1 Y male | Monocyte | MLL-MLLT3; MLL-AF9, NARS | 60-70 hours | [136] |
| KG-1 | Macrophage, acute myelogenous leukemia, 59Y male | leukemia cell line | Gene fusion, FGFR1 + HGNC, a mutation in NARS, TP53 | 38 hours | [137] |
| NOMO-1 | Adult acute monocytic leukemia, 31 Y | Cancer cell line | MLL-AF9; TP53 Heterozygous | 55 hours | [138] |
| ML2 | Adult acute myeloid leukemia, 26 Y | Cancer cell line | MLL-AF6, KARS heterozygous | 60-70 hours | [139] |

Table 4.2 IC50 of leukemia cell lines to tyrosine kinase inhibitors

| Drug (uM) /cell lines | ML2 | THP-1 | KG-1 | MOLM13 |
|---|---|---|---|---|
| Sorafenib | >5 | 4~5 | 3 | <0.5 |
| Sunitinib | >5 | 4 | >5 | <1 |
| Midostaurin | 1 | 1 | 1 | <0.5 |
| Quizartinib | 4~5 | 2 | 4~5 | <0.5 |

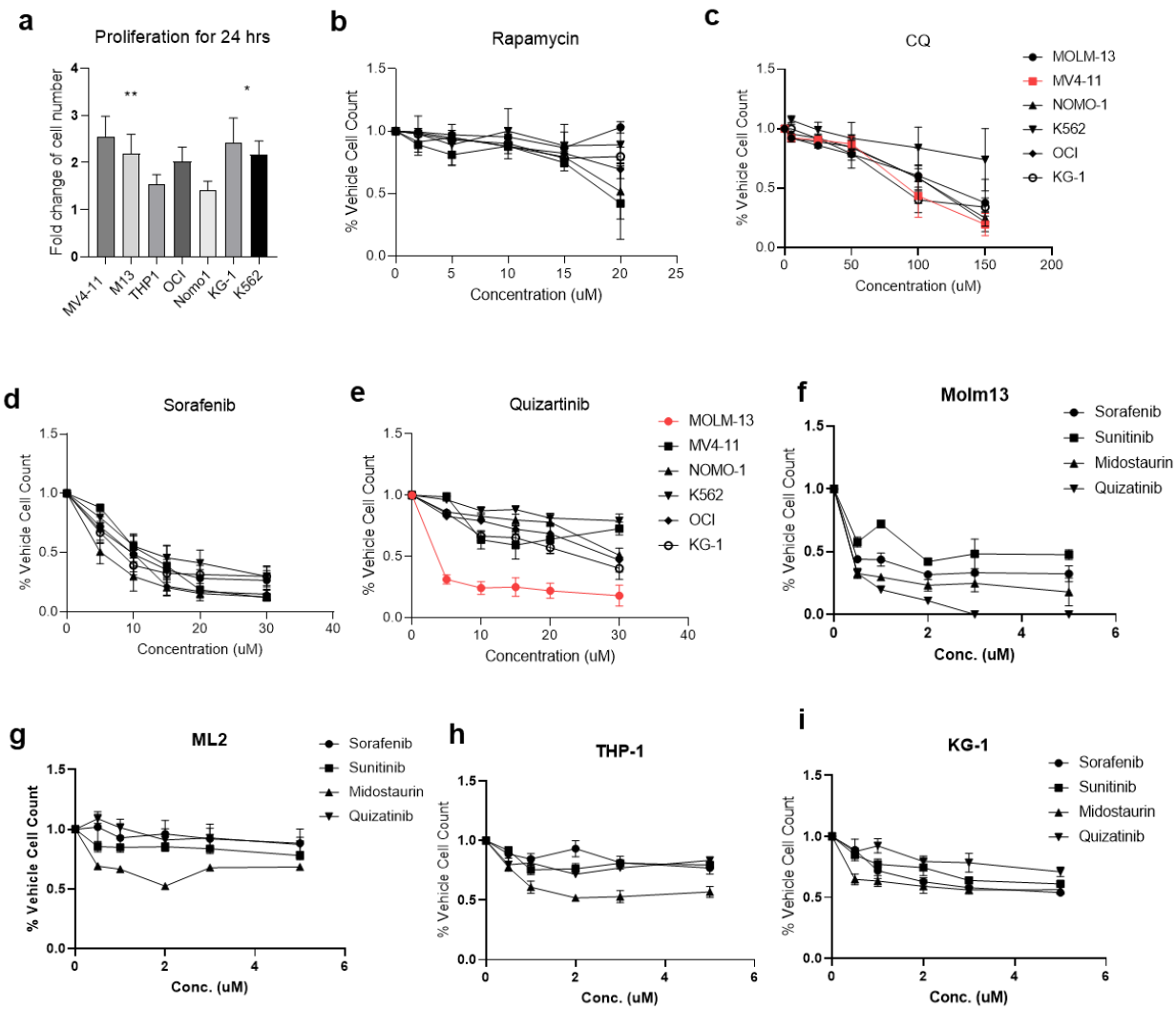


Figure 4.1 Dosage test of leukemia cell lines

a) Proliferation rate of different AML cell lines. b) Does-dependent viability test of different AML cell lines to Rapamycin. c) Dosage test of CQ. d) Dosage test of sorafenib. e) Dosage test of quizartinib. f) Does-dependent viability test of M13 cells to different inhibitors. g) Viability test of ML2. h) Viability test of THP-1. i) Viability test of KG-1 to inhibitors. Each cell line was cultured with full medium and grown to a confluency of 80%, then treated with inhibitors for 24h accordingly. Cell numbers were plotted and compared to the numbers before treatment. Student's t-test. *$p<0.05$, **$p<0.01$. CQ, chloroquine.

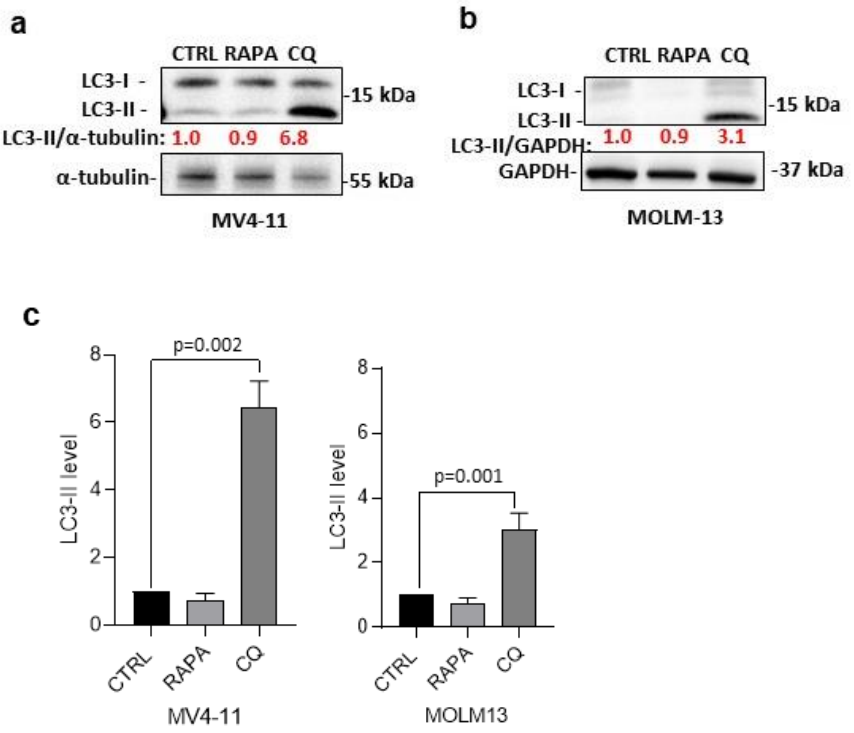


Figure 4.2 Autophagy of FLT3-ITD+ cell lines

a) Autophagy flux of MV4-11 cells indicated by LC3-II/a-tubulin after CQ treatment. b) Autophagy flux of M13 cells indicated by LC3-II/GAPDH. c) Statistical analysis. Each cell line was cultured with full medium and grown to a confluency of 80%, then treated with 20 uM Rapamycin and 75 uM CQ for 24h accordingly. Student's t-test. p values describe the significance of change between CQ-treated cells and the control. CTRL, control. RAPA, rapamycin. CQ, chloroquine.

## 4.2 Proteomics Screening

To further study the role of autophagy on FLT3-ITD$^{+}$ AML cells, in particular, to identify potential downstream protein effectors of autophagy in leukemic cells, M13 and MV4-11 cells were treated with autophagy modulators and harvested for proteomics analysis. Proteins that are oppositely regulated by autophagy inducer (RAPA) and inhibitors (3-MA/CQ) were considered as candidates that potentially act downstream of autophagy in regulating leukemogenesis. As shown in the volcano map, the y-axis stands for the values of -log(p-value), and the x-axis means the value of log2(fold change), negative value indicates a decreased expression of the treated group compared to the control, while the positive value means upregulated expression compared to the control. All the statistically significant proteins ($p<0.05$, $-\log10>1.3$) were plotted in the upper space of the graph in red or blue color. M13 and MV4-11 cells have different genetic mutation backgrounds. Thus, they showed different proteomics results when treated with the same autophagy modulators (**Fig**. 4.3a, b). M13 and MV4-11 were more responsive to CQ than RAPA, with more protein changes detected (**Fig**. 4.3). Since M13 cell line was more sensitive to kinase inhibitors than MV4-11 cells, I narrowed down the analysis on M13 cells to further investigate target genes related to FLT3-ITD (**Fig.** 4.4).

According to the pathway analysis, autophagy inhibitors like CQ and 3-MA greatly inhibited most of the cellular processes like cell proliferation, cell differentiation, kinase signaling, and lysosome-related endocytosis in M13 cells (**Fig**. 4.5). While rapamycin upregulated the expression of regulators in ubiquitin proteolysis and protein processing (folding, sorting, and degradation) in the endoplasmic reticulum (ER) (**Table 4.3**). CQ treatment downregulated pathways

including JAK/STAT, NF-kappa B, AMPK, VEGF signaling, and lysosome pathways (**Table 4.3**). A list of target proteins that exhibit opposite changes upon treatment with autophagy inducer and inhibitor was identified (**Table 4.4**), with a significant fold change over 2 ($p<0.05$). In this way, the listed effectors were primarily associated with autophagy-specific-regulated change rather than other secondary metabolic changes due to drug-induced stress. However, 3-MA blocks the formation of the phagophore at the beginning of autophagy while CQ inhibits the fusion of autophagosome and lysosome (later stage of autophagy), so the fold change value of protein (in the table) may be different and indicate the stage when the protein plays a role.

Dedicator of cytokinesis 2 (DOCK2), a protein specifically expressed in hematopoietic cells[140], decreased by 5-fold when M13 cells were treated with RAPA (the most downregulated protein after RAPA treatment), while increased by 2-fold when cells were treated with 3-MA (**Table 4.4**). Endoplasmic Reticulum Metallopeptidase 1 (ERMP1), a protein located on the ER membrane[141], increased by 16-fold when M13 cells were treated with RAPA (the most upregulated protein after RAPA treatment), while reduced by 2-fold when treated with CQ (**Table 4.4**). Retinoid-inducible serine carboxypeptidase 1 (SCPEP1) expression increased when M13 cells were treated with RAPA and reduced by 5-fold when treated with CQ (the most downregulated protein after CQ treatment compared to others in the list) (**Table 4.4**). Although PINK1 protein was not detected in the sample, the level of PINK1-mediated mitophagy related proteins such as VDAC1 (Voltage Dependent Anion Channel 1, component of the outer mitochondrial membrane) and TOM22/40 (Translocase of Outer Mitochondrial Membrane 22/40, component of the outer mitochondrial membrane) were significantly upregulated by RAPA

treatment, while downregulated by 3-MA treatment in FLT3-ITD AML cells (**Table 4.4**).

DOCK2 loss-of-function mutations were found to be associated with combined immunodeficiencies, patients of which showed defective T, B, and NK cells[142]. Although ERMP1 is differentially expressed in the ovary of rat, no related inborn genetic disease was found[143]. SCPEP1 mutations were not related to any inborn genetic disease previously[144]. Meanwhile, there are knowledge gaps between these proteins and hematopoiesis, so I decided to investigate further on functions of DOCK2, ERMP1, and SCPEP1 in normal hematopoiesis and AML progression. I also added PINK1, a known mitophagy regulator, to study their roles in autophagy-mediated hematopoietic cell development (**Table 4.5**).

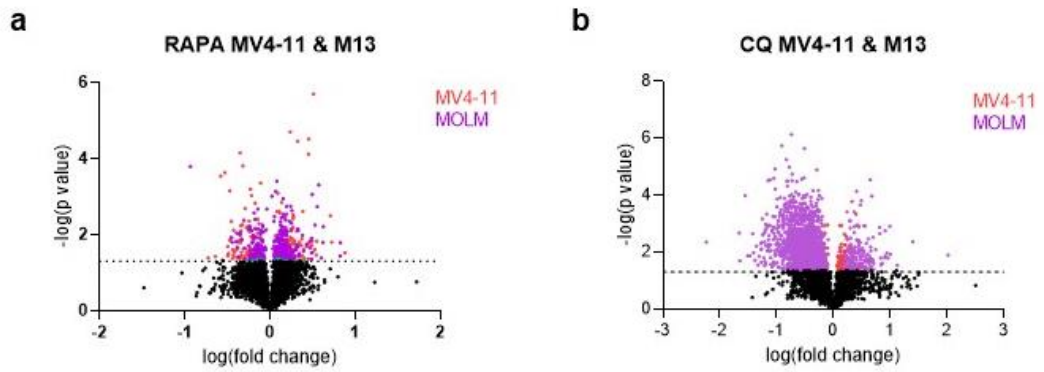


Figure 4.3 Proteomics of M13 and MV4-11 cells

a) Volcano plot of p-values (-log10) and z-scores (log2) in quantified proteins between CTRL and RAPA treated MV4-11or M13 cells. Significantly changed proteins were plotted in red or purple color. b) Volcano plot of CQ-treated MV4-11 or M13 cells. Significantly altered proteins were plotted in blue or red color. M13, MOLM-13 cells. RAPA, rapamycin. CQ, chloroquine. Cells were incubated with rapamycin (20 uM) or chloroquine (75uM) for 24h, with DMSO as the solvent and control treatment. Student's t-test.

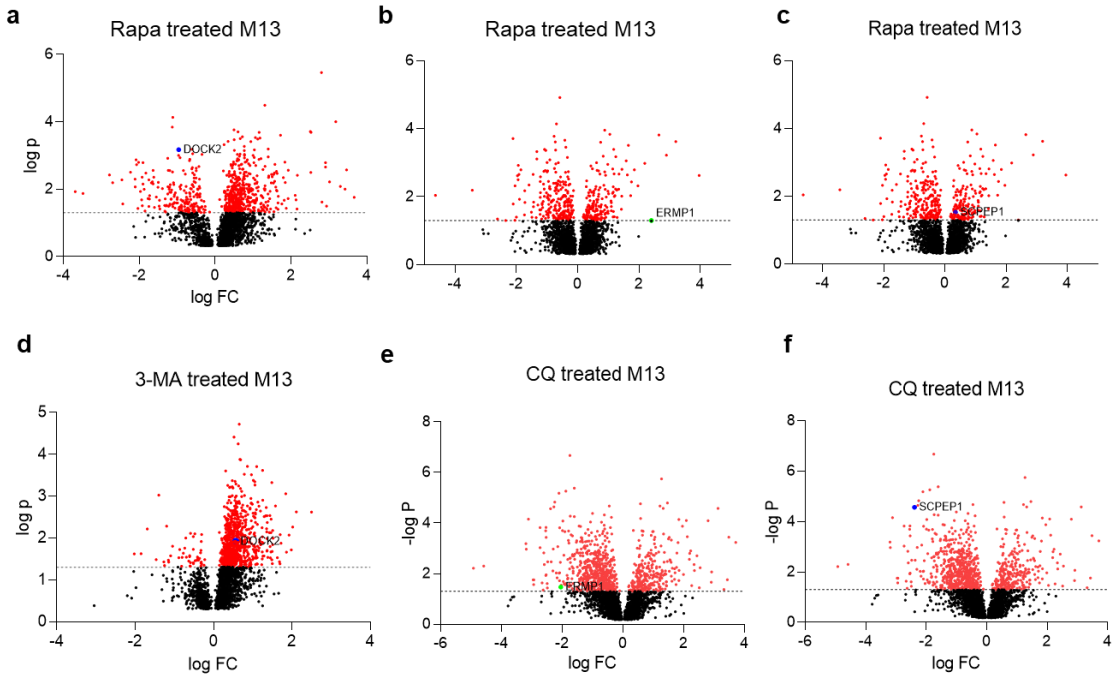


Figure 4.4 Proteomics of M13 cells treated with autophagy modulators

M13, MOLM-13 cells. Rapamycin, an autophagy inducer, targets mTOR. 3-MA, autophagy inhibitor that inhibits PI3K. CQ, chloroquine, autophagy inhibitor that inhibits fusion of autophagosome and lysosome. X=values of log (fold change), Y=values of -log (p-value). Dots in red meaning significantly altered (either increased or decreased) proteins, which have the p-value less than 0.05. Cells were incubated with rapamycin (20 uM), 3-MA (100 mM), or chloroquine (75uM) for 24h, using DMSO as the solvent. Student's t-test.

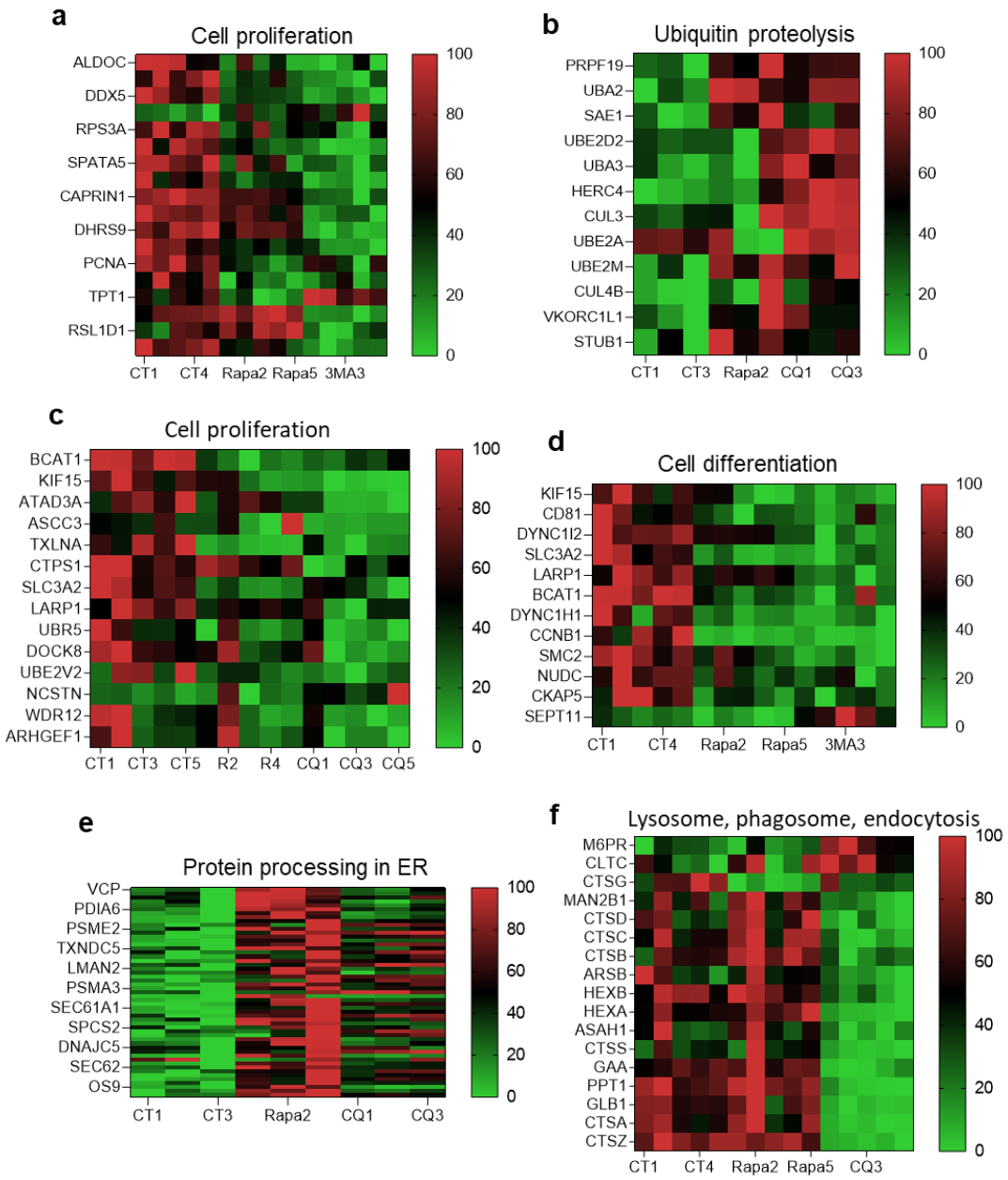


Figure 4.5 Heatmap of pathway analysis

Cell proliferation, ubiquitin proteolysis, cell differentiation, protein processing, lysosome, phagosome, and endocytosis. In the heatmap, proteins were plotted in red (upregulated) or green (downregulated) after RAPA, CQ, or 3-MA treatment.

Table 4.3 KEGG pathway analysis of RAPA or CQ-treated M13 cells

| RAPA-Upregulated pathways | CQ-Downregulated pathways |
|---|---|
| Aminoacyl-tRNA biosynthesis | JAK-STAT signaling pathway |
| RNA transport | NF-kappa B signaling pathway |
| Ribosome biogenesis | AMPK signaling pathway |
| Folding, sorting, and degradation | VEGF signaling pathway |
| Protein processing in ER | TNF signaling pathway |
| Ubiquitin mediated proteolysis | Wnt signaling pathway |
| Carbohydrate digestion and absorption | mTOR signaling pathway |
| Aging and longevity regulating pathway | Autophagy |
| Lysosome and endocytosis | Lysosome |

Table 4.4 Potential autophagy regulators and effectors in FLT3-ITD$^{+}$ AML cells

| Protein | Description | 3-MA/DMSO | CQ/DMSO | RAPA/DMSO | Expression |
|---|---|---|---|---|---|
| DOCK2 | Dedicator of cytokinesis | 1.8 | 1.1 | 0.2 | specific in hematopoietic cells |
| ERMP1 | Endoplasmic Reticulum Metallopeptidase 1 | 1.2 | 0.6 | 16 | located on the ER membrane, expressed within the ovary |
| SCPEP1 | Retinoid-inducible serine carboxypeptidase | 1 | 0.2 | 1.5 | mediated hemodynamics and vascular resistance |
| STK10 | Serine/threonine-protein kinase | 1.6 | 1.1 | 0.4 | high in bone marrow, membrane |
| NCAPG | Condensin complex subunit 3 | 2.7 | 2.5 | 0.4 | broad expression in bone marrow, Nucleus |
| BRI3BP | BRI3-binding protein | 1.8 | 0.5 | 3.6 | found in bone marrow, mitochondria |
| THOC5 | THO complex subunit 5 homolog | 0.5 | 1.2 | 1.4 | ubiquitous expression, Cytoplasm, Nucleus |
| LGALS9 | Galectin-9 | 1.9 | 1.9 | 0.1 | broad expression in the spleen, blood, and others |
| BAG6 | Large proline-rich protein | 1.6 | 1.3 | 0.4 | broad expression, Cytoplasm, Nucleus, Secreted |

Table 4.5 The selected target genes of investigation

| Gene | Related disorder | Molecular function | Pathways | Expression |
|---|---|---|---|---|
| DOCK2 | Immunodeficiency | cytoskeletal rearrangements, lymphocyte migration | Regulation of RAC1 activity, Chemokine signaling pathway (CCR5) | overexpressed in lymph nodes, monocytes, and lymphocyte |
| ERMP1 | Acute myeloid leukemia, | protein binding, peptidase, hydrolase activity, and metallopeptidase activity | unfolded protein response (UPR) | ovary, nasal epithelium, peripheral blood |
| SCPEP1 | Galactosialidosis | carboxypeptidase activity, peptidase, hydrolase activity | No Data Available | overexpressed in peripheral blood, bone marrow |
| PINK1 | Parkinson's disease (Autosomal Recessive) | Function with Parkin to mediate mitophagy | Mitophagy, autophagy | overexpressed in muscle and serum |

### 4.3 TCGA-Based Expression Analysis

From The Cancer Genome Atlas (TCGA) database, we retrieved microarray data (mRNA expression) to analyze the gene expression levels of *DOCK2, ERMP1*, *SCPEP1,* and *PINK1* among normal hematopoiesis and AML subtypes. Previously, due to elevated expression of FLT3 found in AML patients, it was identified as a prognostic marker[145]. The expression of PINK1 was lower in AMLs compared to the normal hematopoiesis samples, though the level varied among different types of blood cells (**Fig.** 4.6a). DOCK2 expression was similar among AML patient samples, HSCs, myeloid progenitors, and normal blood cell samples (**Fig.** 4.6b). Level of ERMP1 expression was lower in AML samples compared to the HSCs and myeloid progenitors according to another dataset from TCGA (**Fig.** 4.6c). While the expression level of SCPEP1 was higher in AML samples compared to the HSCs, multipotential progenitors, and common myeloid progenitors (**Fig.** 4.6d).

Combined with the proteomic data, PINK1, DOCK2, ERMP1, and SCPEP1 are potential regulators of cell proliferation involved in autophagy in FLT3-ITD$^+$ AML cells. They are potential chemotherapeutic targets for treating the FLT3-ITD$^+$ AML subtype and further demonstrating how these effectors mediate autophagy-related regulation in AML progression will bring novel insights into AML therapy targeting autophagy-related pathways.

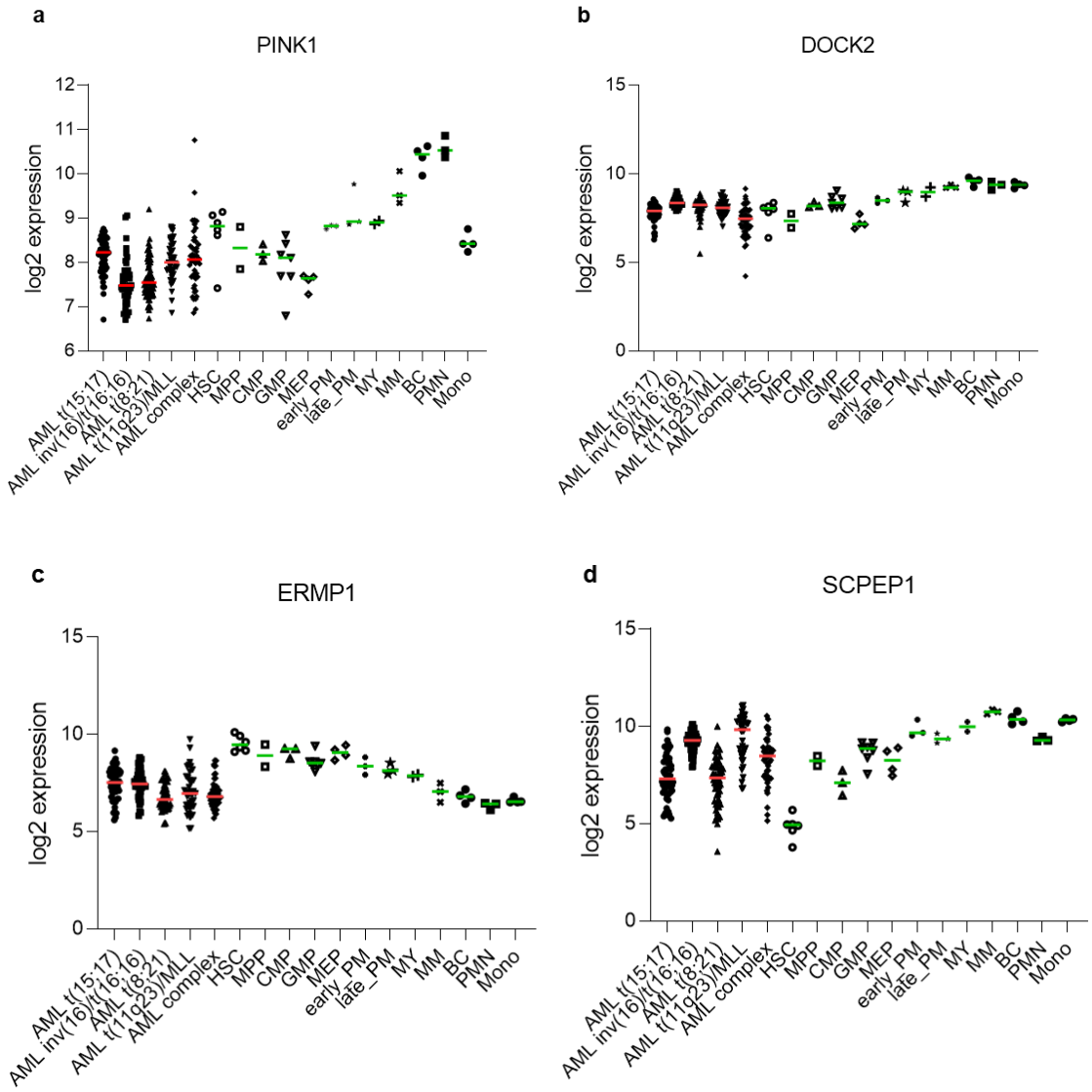


Figure 4.6 mRNA expression data of normal hematopoiesis and AMLs from TCGA

a) PINK1 expression. b) DOCK2 expression. c) ERMP1 expression. d) SCPEP1 expression. Among subtypes of AMLs, HSC, and PB cells. TCGA, The Cancer Genome Atlas. AML subtypes with chromosomal abnormalities: AML t(15;17), AML inv(16)/t(16;16), AML t(8;21), AML t(11q23)/MLL. AML complex, AML with complex aberrant karyotype. HSC, hematopoietic stem cell. MPP, multipotential progenitors. CMP, common myeloid progenitor cell. GMP, granulocyte monocyte progenitors. MEP, megakaryocyte-erythroid progenitor cell.

Early_PM, early promyelocyte. Late_PM, late promyelocyte. MY, myelocyte. MM, metamyelocytes. BC, band cell. PMN, polymorphonuclear cells. Mono, monocytes.

### 4.4 Role of *DOCK2* in AML Cell Lines

DOCK2, as a guanine exchange factor (GEF), is specifically expressed in the hematopoietic cells, including myeloid cells and lymphocytes, and regulates polarization and migration of immune cells through activating Ras-related C3 botulinum toxin substrate (Rac)[140]. Results from mass spectrometry show that the DOCK2 level was mediated by the mTOR signaling pathway as the mTOR inhibitor RAPA significantly inhibited DOCK2 expression. To study the role of *DOCK2* in AML, a *DOCK2* loss-of-function mutant M13 cell line was created via CRISPR/Cas9 genome editing (**Fig.** 4.7a).

Sequencing results of the *DOCK2* gene from *DOCK2*$^{Mut}$ cells revealed 1bp deletion or insertion (within a MseI cut site) near the PAM sequence (**Fig.** 4.7a), indicating frameshift mutation that produces truncated proteins. The genotyping result showed the mutation rate was nearly 100%, while the Western blot showed the DOCK2 protein level reduced significantly (**Fig**. 4.7b,c). *DOCK2*$^{Mut}$ M13 cells showed inhibited proliferation compared to the CTRL cells (**Fig**. 4.7d). Next, we measured the kinase signaling activation by Western blot. *DOCK2*$^{Mut}$ cells exhibit higher STAT5 and ERK activation while lower levels of AKT phosphorylation (**Fig**. 4.7f, g). Meanwhile, increased LC3-II/GAPDH level in *DOCK2*$^{Mut}$ M13 cells compared to the control suggests a disrupted autophagy (**Fig.** 4.7f, g), though whether it was due to autophagy inhibition or lysosomal degradation inhibition requires more studies. RT-qPCR results suggest the expressions of BECN, TP53, KARS, or RAF were not affected by DOCK2 deficiency (**Fig.** 4.7e).

To confirm our findings, we generated the *DOCK2*$^{Mut}$ MV4-11 cells. Again, genome editing induced mutation close to 90% (**Fig.** 4.8a), and significantly reduced DOCK2 protein expression (**Fig.** 4.8c). *DOCK2*$^{Mut}$ MV4-11 cells showed inhibited growth compared to the CTRL cells (**Fig**. 4.8b). *DOCK2*$^{Mut}$ MV4-11 cells also exhibited increased LC3-II level and reduced FLT3 phosphorylation (**Fig**. 4.8c, d).

*DOCK2*$^{Mut}$ THP-1 and KG-1 cells were also created using the same sgRNA and transfection method (**Fig**. 4.9a). Loss of *DOCK2* did not affect the growth of THP-1 and KG-1 cells (**Fig**. 4.9b). Both *DOCK2* mutant cells showed more LC3-II level, ERK, or FLT3 activation (**Fig**. 4.9c, d). DOCK2 deficiency suppressed the activity of some signaling pathways (AKT/FLT3) while promoting another signaling (STAT5/ERK) according to the cell types.

Next, we performed proteomics analysis on *DOCK2*$^{Mut}$ M13 cells to evaluate the effects of DOCK2 deficiency on the cellular pathways of FLT3-ITD$^{+}$ AML. Significantly changed proteins were plotted as downregulated (left panel, red) and upregulated (right panel, red) (**Fig**. 4.10a). *DOCK2*$^{Mut}$ M13 cells showed generally elevated levels of protein markers from cell signaling and metabolism, while mostly reduced levels of markers from cell cycle and proliferation (**Fig**. 4.10b-d).

The Ingenuity pathway analysis (IPA) showed that EIF2 and mTOR signaling pathways were significantly inhibited in *DOCK2*$^{Mut}$ M13 cells, while RHOA signaling and the Isoleucine degradation I pathways were upregulated (**Fig**. 4.11). Key regulators and correlations from mTOR signaling were shown in the schematic pathway graph (**Fig**. 4.11).

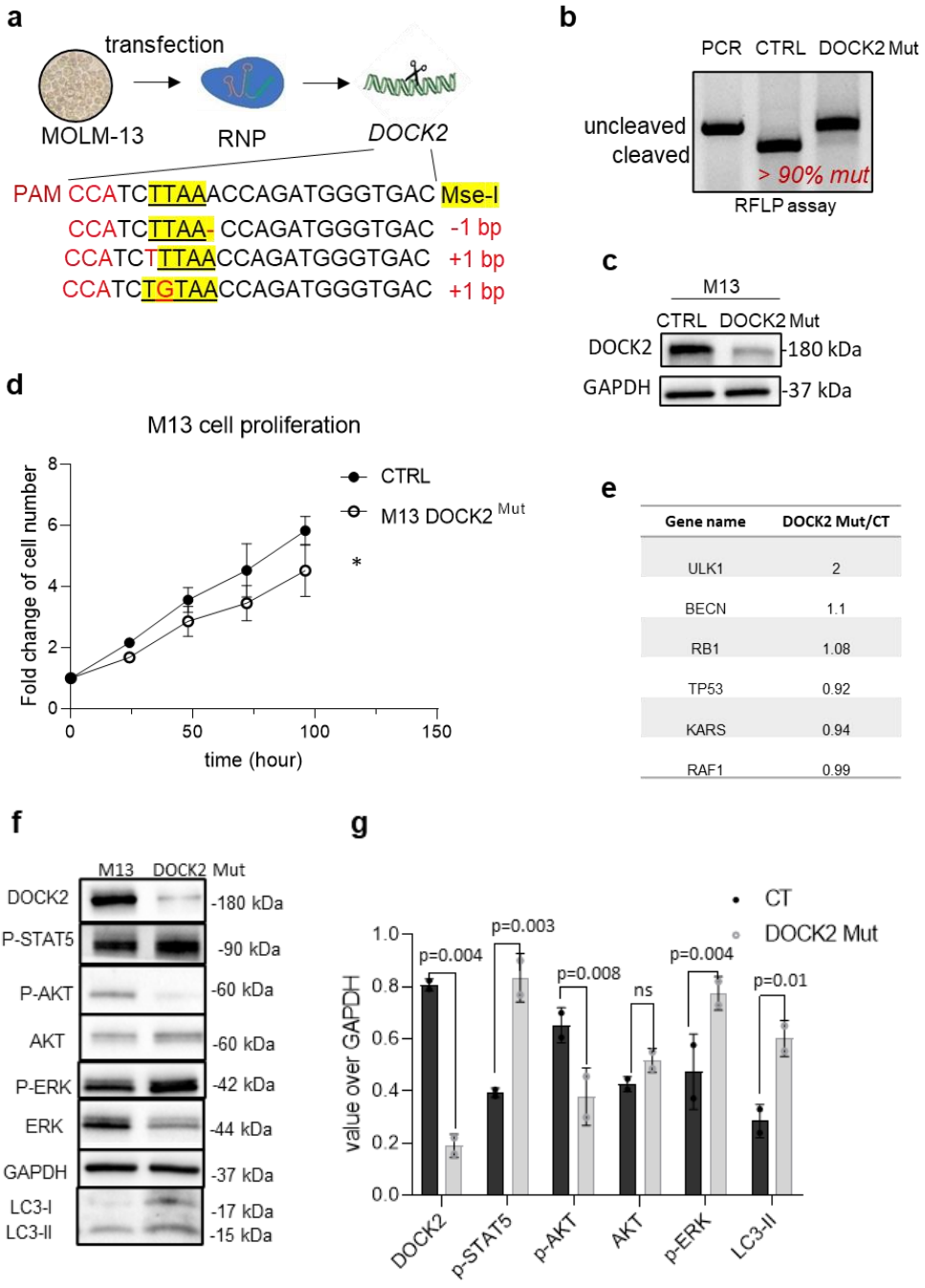


Figure 4.7 Effects of DOCK2 deficiency on cell proliferation, kinase signaling, and autophagy in FLT3-ITD$^{+}$ AML cells

a) Schematic graph of targeting *DOCK2* in M13 cell line via CRISPR/cas9 technique. b) The result of restriction fragment length polymorphism (RFLP) assay. c and d) Western blot against DOCK2 protein. GAPDH protein serves as the internal control. LC3II/GAPDH ratio after CQ treatment indicates autophagic flux. e) Result of RT-

qPCR. f and g) Western blot against DOCK2, p-STAT5, p-AKT, AKT, p-ERK, ERK, and LC3II. GAPDH protein serves as the internal control. RNP, ribonucleoprotein. CT, control. Mut, mutant. Student's t-test. p values describe the significance of change between *DOCK2* mutant and control cells. *$p<0.05$. ns, not significant.

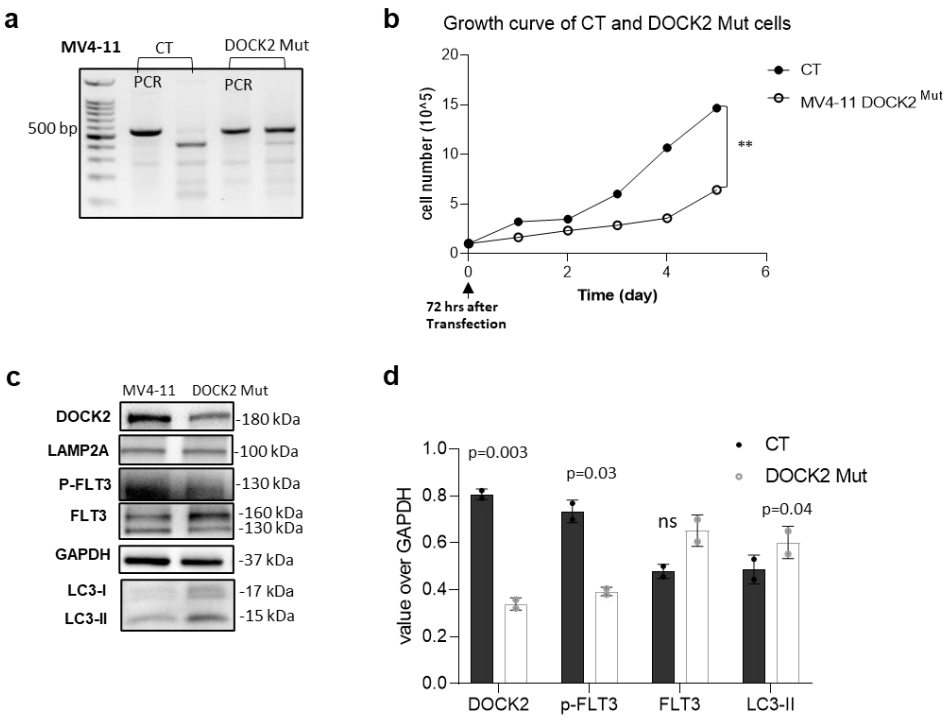


Figure 4.8 Effects of DOCK2 deficiency on cell proliferation and FLT3 phosphorylation in FLT3-ITD$^{+}$ AML cells

a) Result of genotyping. b) Statistical result of cell proliferation. c and d) Western blot against DOCK2, p-FLT3, FLT3, and LC3-I/II. GAPDH protein serves as the internal control. CT, control. Mut, mutant. Student's t-test. p values describe the significance of change between *DOCK2* mutant and control cells. **p<0.01. ns, not significant.

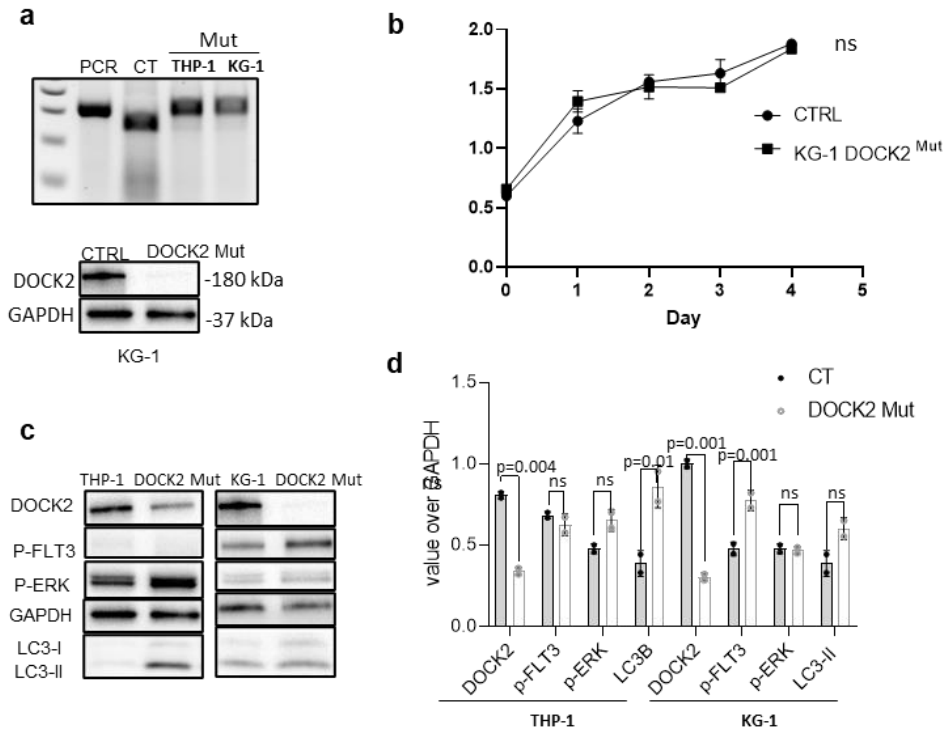


Figure 4.9 Effects of DOCK2 deficiency on cell proliferation and kinase signaling in FLT3-WT AML cells

a) The result of genotyping. Western blot against DOCK2 confirmed the knockout. b) Plot of the cell proliferation. c and d) Western blot against DOCK2, p-FLT3, p-ERK, and LC3I/II. GAPDH protein serves as the internal control. CT, control. Mut, mutant. Student's t-test. p values describe the significance of change between *DOCK2* mutant and control cells. ns, not significant.

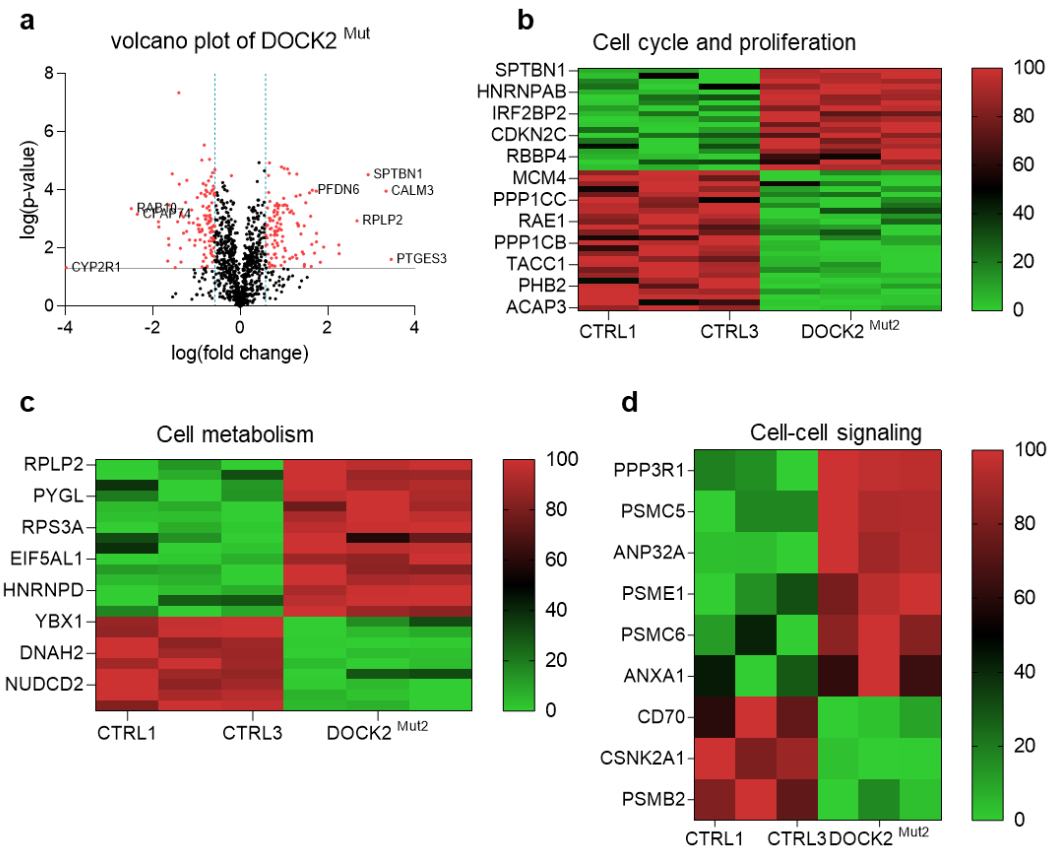


Figure 4.10 Effects of DOCK2 deficiency on proteomics in M13 cells

a) Volcano plot of proteomics. b) Heatmap of proteins from cell cycle and proliferation. c) Heatmap of proteins from cellular metabolism. d) Heatmap of proteins from cell signaling. CTRL, control. Mut, mutant. CTRL, control. Mut, mutant. Student's t-test.

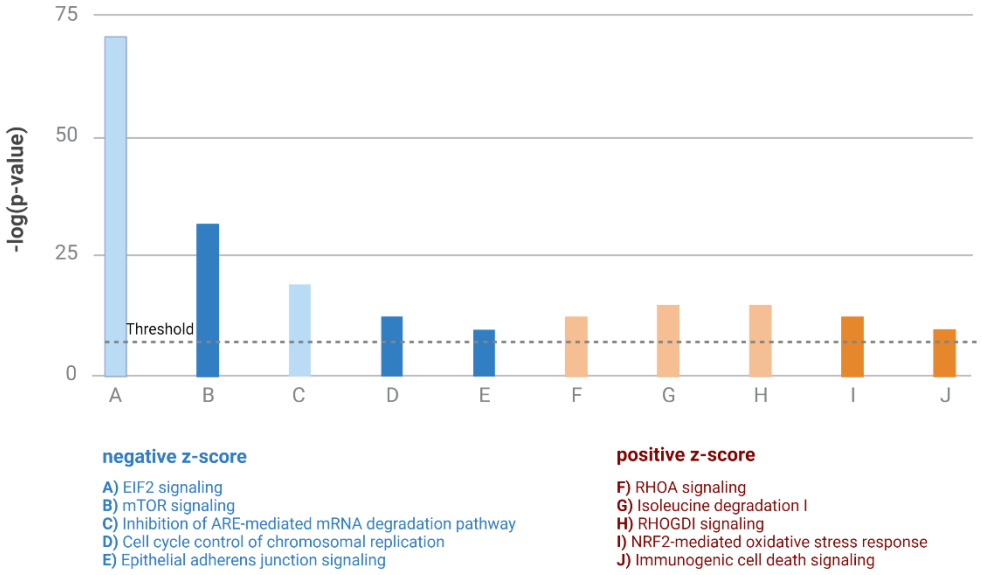


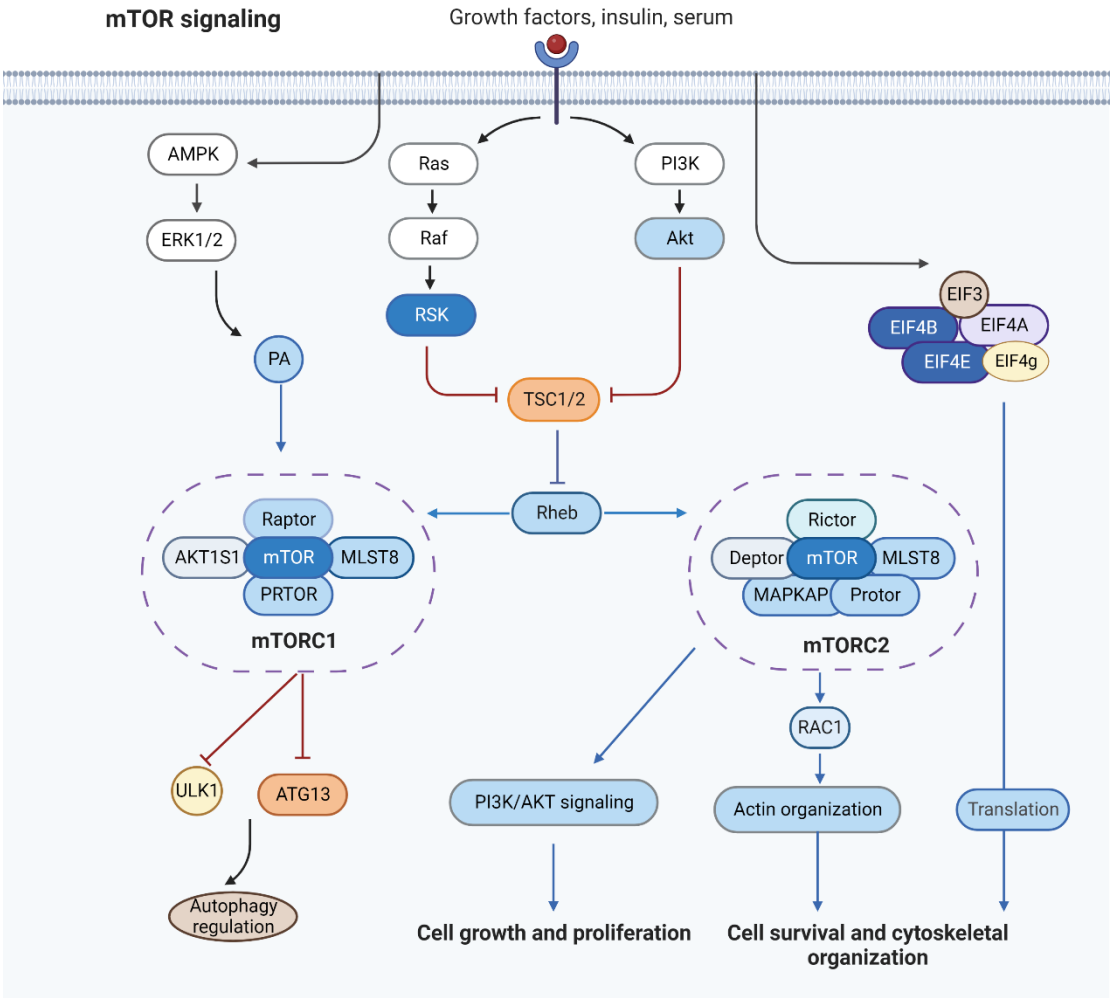


Figure 4.11 Ingenuity pathway analysis of DOCK2 deficiency-induced proteomics changes

Proteins from specified pathways were clustered and ranked by the correlation efficiency in positive or negative z-score. The mTOR signaling pathway was significantly downregulated, and cell proliferation and cytoskeletal organization were inhibited in the *DOCK2*$^{Mut}$ M13 cells. mTOR, mammalian target of rapamycin. PI3K, phosphatidylinositol 3-kinase-related kinase. mTORC1, mTOR complex 1. mTORC2, mTOR complex 2. TSC1/2, tuberous sclerosis complex subunit 1/2. EIF, eukaryotic translation initiation factor.

### 4.5 Role of *dock2* in Zebrafish Hematopoiesis

*DOCK2* gene in zebrafish duplicates into *dock2 like* and *dock2*, proteins of which share 74% and 65% sequence identity to the human DOCK2 protein (**Fig.** 4.12a). The creation of the *dock2*$^{Mut}$ zebrafish line was validated by the genotyping and sequencing result, which shows a 5bp deletion in the target site (**Fig.** 4.12b, c). The *dock2* mutation is consistent and inherited in the F2 generation (a mix of heterozygous, homozygous mutants, and wild-type siblings) (**Fig.** 4.12d). By using a *dock2* mRNA probe, the expression of dock2 during embryonic development was analyzed. The result suggested the expression of *dock2* increased (especially in the thymus region) at around 5 days past fertilization, when the lymphopoiesis started (**Fig.** 4.12e).

Hematopoiesis was evaluated on the *dock2*$^{Mut}$ embryos and the wild-type siblings from the F2 generation by WISH. We found that expressions of *pu.1* and *c-myb*, markers of the myeloid progenitor and HSCs, significantly increased in the *dock2*$^{Mut}$ embryos from 24 hpf and 36 hpf (**Fig.** 4.13a, c). The number of neutrophils (*lyz*) and lymphocytes (*rag1*) decreased, while the number of leukocytes (*l-plastin*) and erythroid (*hbae1*) did not change compared to the WT control (**Fig.** 4.13d, e). These results show that loss of *dock2* induced expansion in myeloid progenitors and HSC population while blocking the differentiation of neutrophils and lymphocytes.

Then I moved on to the analysis of hematopoietic cell proliferation in zebrafish embryos. Phospho-histone 3 (PH3) is a marker of mitosis that stains cells in late G2 and mitosis, where PH3 marks the condensed chromatin just before chromosomal segregation[146]. The results suggested that the loss of *dock2* did not affect the proliferation of hematopoietic cells from the 48 hpf embryos (**Fig.** 4.14a).

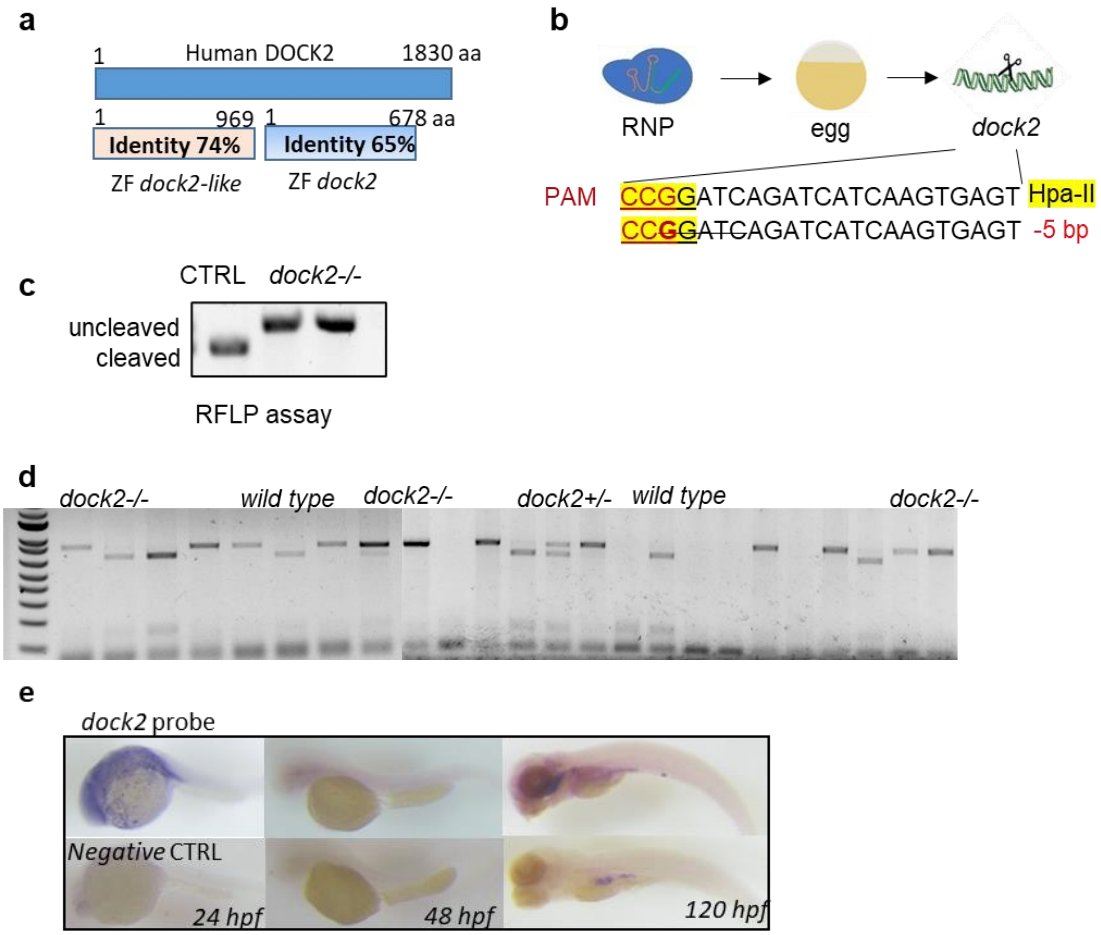


Figure 4.12 Generation of *dock2* mutant zebrafish line

a) Schematic graph of the protein structure of human and zebrafish DOCK2. Identity is shared by the protein sequence shown in percentage. b) Schematic graph of sgRNA targeting zebrafish *dock2* gene, within which the enzyme Hpa-II was used for the restriction fragment length polymorphism (RFLP) assay. c) Genotyping result of *dock2* mutant and CTRL siblings. d) Genotyping result of mixed embryos from *dock2* mutants F2 generation. e) Expression of *dock2* during embryonic development of zebrafish. CTRL, control. ZF, zebrafish. RNP, ribonucleoprotein. hpf, hour past fertilization.

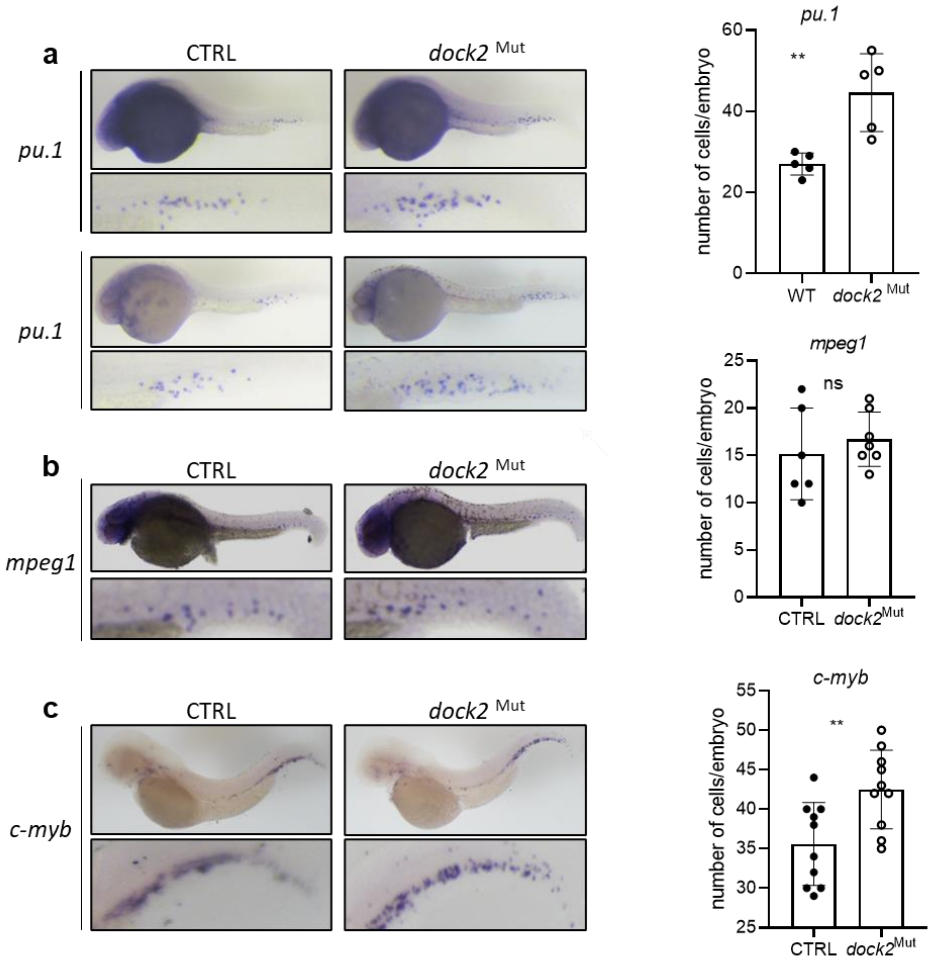
a
CTRL
dock2 Mut
pu.1
pu.1
b
CTRL
dock2 Mut
mpeg1
c
CTRL
dock2 Mut
c-myb
pu.1
number of cells/embryo
**
WT
dock2 Mut
mpeg1
number of cells/embryo
ns
CTRL
dock2Mut
c-myb
number of cells/embryo
**
CTRL
dock2Mut

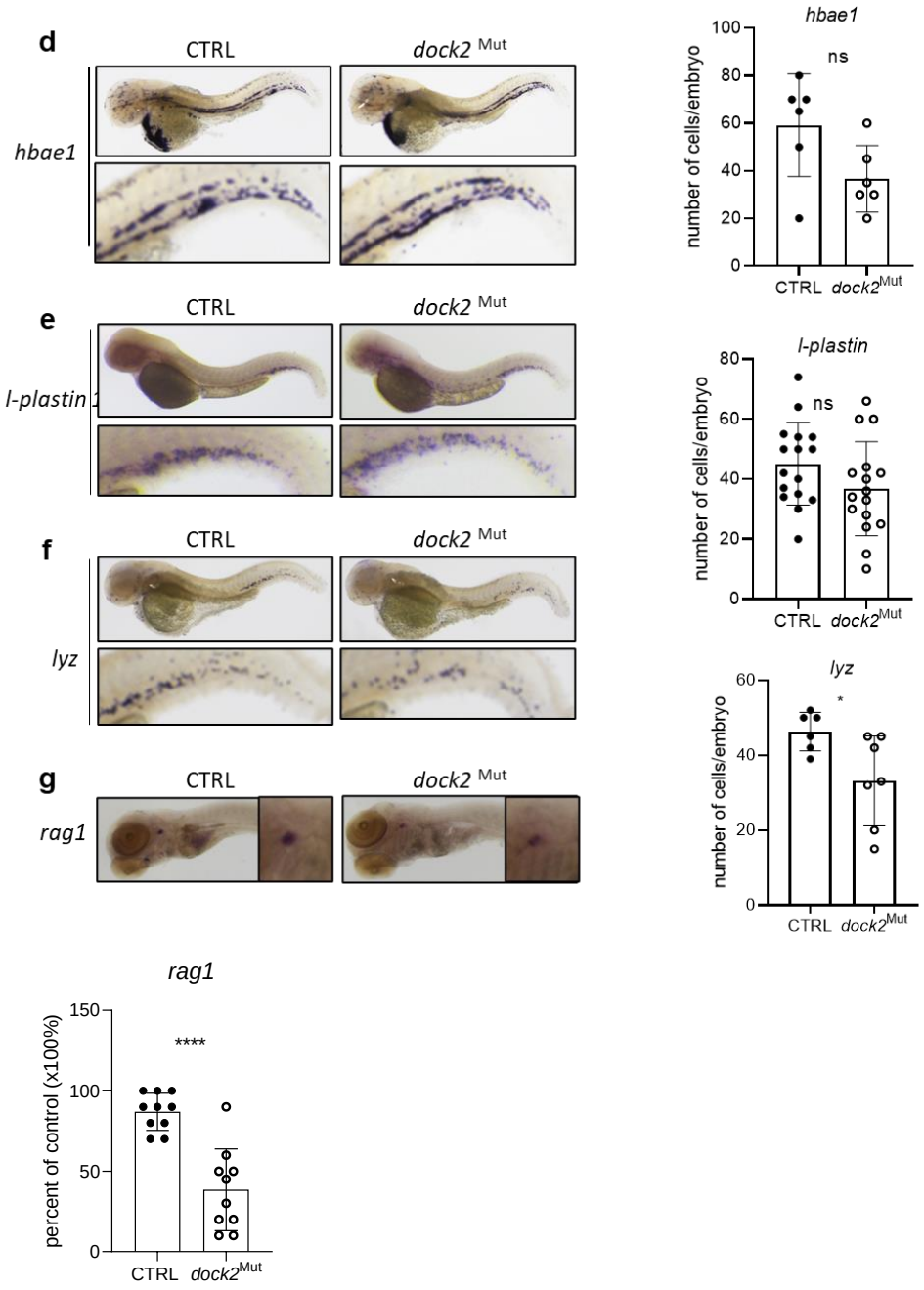


Figure 4.13 Hematopoiesis analysis on *dock2* mutant zebrafish embryos

Expression pattern and quantity of *pu.1*, *mpeg1*, *hbae1*, *c-myb*, *l-plastin*, *lyz*, and *rag1* in CHT of zebrafish embryos at 24 hpf, 36 hpf, and 48 hpf. Lateral view, head to left, CTRL, and mutants (siblings). Line denotes the mean value. $p<0.01$, n=20~40. CTRL, control. Mut, mutant. Student's t-test, $*p \leqslant 0.05$, $**p \leqslant 0.01$, ns, not significant, compared to CTRL.

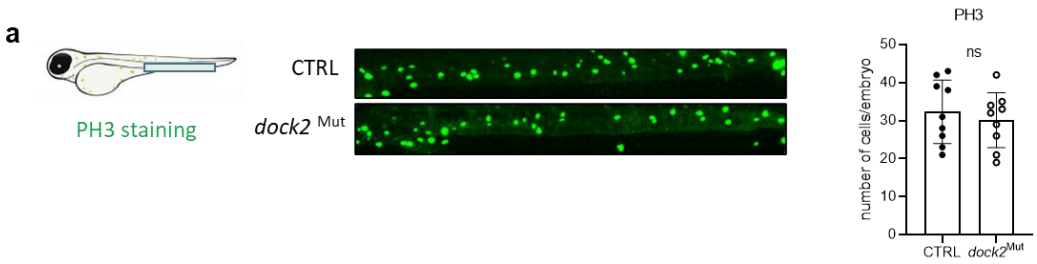


Figure 4.14 Effects of *dock2* mutation on hematopoietic cell proliferation in zebrafish embryos

a) Phosphorylated histone H3 (PH3) staining showed the proliferation of hematopoietic cells in the caudal hematopoietic tissue from 48 hpf zebrafish embryos. Student's t-test, ns, not significant, compared to CTRL. CTRL, control. Mut, mutant.

### 4.6 Role of *ERMP1* in AML Cell Lines

Among the listed proteins, the ERMP1 increased the most (~20 folds) in RAPA-treated M13 cells, which was in the same direction as autophagy regulation in FLT3-ITD$^{+}$ leukemia cells. A previous study showed that the expression level of *ERMP1* was elevated in high-risk childhood AML[147]. This ER-located peptidase is highly associated with the unfolded protein response (UPR) and oxidative stress defense[148].

To evaluate the role of the ERMP1 protein in AML proliferation, *ERMP1* gene of M13 cells was targeted with CRISPR/Cas9 RNP (**Fig**. 4.15a). The genotyping result showed a mutation of over 90% (**Fig**. 4.15b). Western blot against ERMP1 protein showed more than a 50% reduction in expression (**Fig.** 4.15c). The *ERMP1*$^{Mut}$ cells showed suppressed growth compared to the CTRL cells (**Fig**. 4.15d). Results of Western blot showed that levels of FLT3 and LC3-II significantly decreased in *ERMP1*$^{Mut}$ cells (**Fig**. 4.15e).

Mass spectrometry-based proteomics was performed to analyze the proteomics of *ERMP1* mutated cells (**Fig.** 4.15f). Specifically, cell cycle arrest marker (SMC2) and transcription inhibitor (SLTM) were significantly upregulated. While mitochondrial trifunctional enzymes from the oxidation pathway (HADHB), membrane trafficking effector (EHD), and cell signaling and transcription co-regulator (PHB2) significantly reduced (**Fig.** 4.15f). As for pathways regulation, the heatmap showed most proteins from the proliferation and metabolism pathway were downregulated in the *ERMP1*$^{Mut}$ cells compared to the CTRL M13 cells (**Fig**. 4.15g, h).

The ingenuity pathway analysis (IPA) showed that EIF2 signaling, BAG2 signaling, and mTOR signaling were generally downregulated in the *ERMP1*$^{Mut}$

cells. While inhibition of AAE-mediated mRNA degradation, actin cytoskeleton signaling, and Isoleucine degradation pathways were upregulated from the *ERMP1*$^{Mut}$ cells compared to the CTRL M13 cells (**Fig**. 4.16). As shown in the schematic graph of the BAG2 signaling pathway, ERMP1 deficient cells displayed downregulated autophagy, protein processing, and cell proliferation, which align with the CQ-induced signaling inhibition (**Fig**. 4.16).

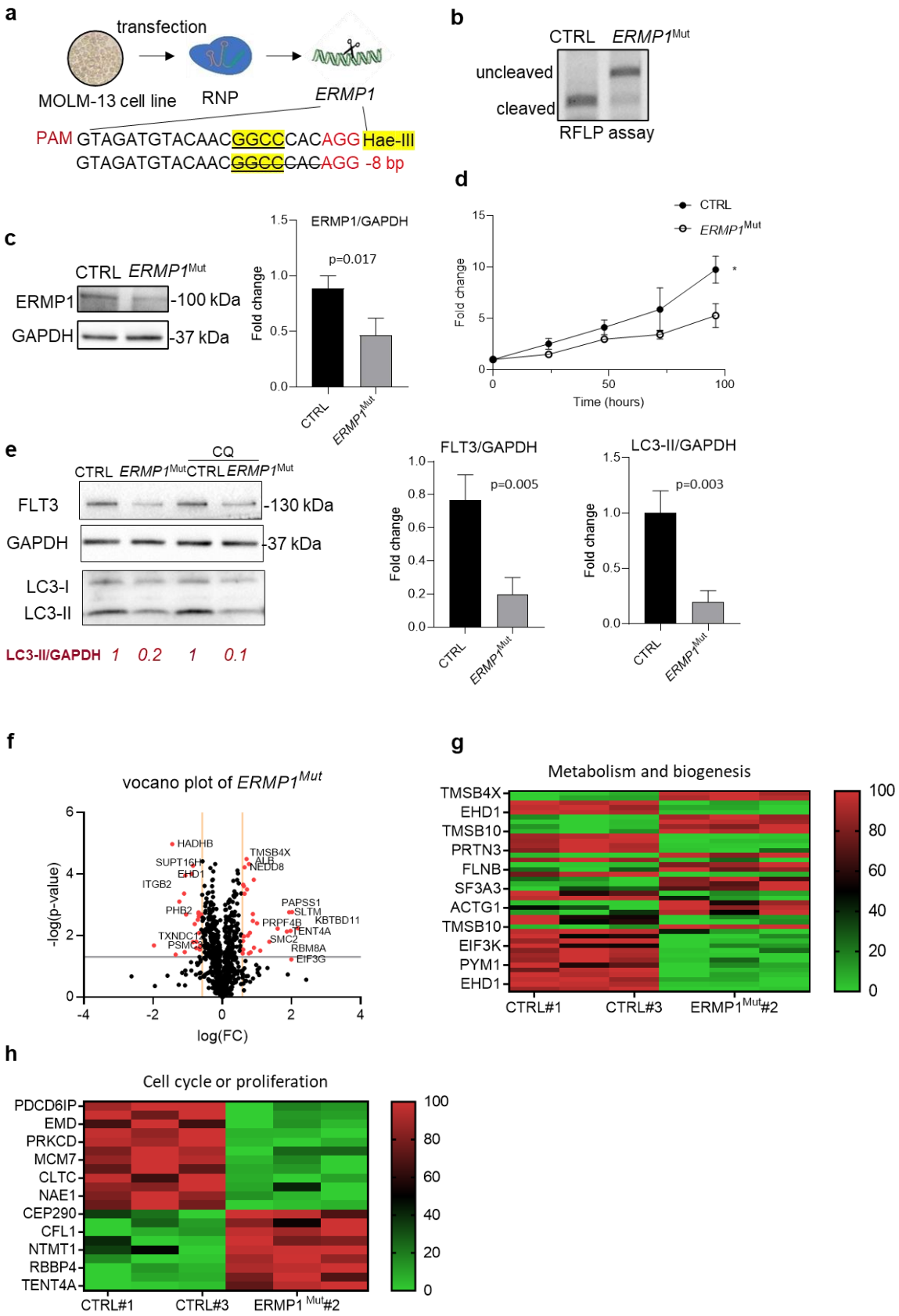


Figure 4.15 Effects of ERMP1 deficiency on cell proliferation and autophagy in FLT3-ITD$^{+}$ AML cells

a) Schematic graph of targeting *ERMP1* in M13 cell line via CRISPR/Cas9 technique. b) Result of genotyping. c) Western blot against ERMP1 protein. GAPDH serves as the internal control. d) Plot of the cell proliferation. e) Western blot of FLT3, LC3B, and GAPDH. f) Volcano plot of proteomics data. g) Heatmap of proteins from metabolism and biogenesis. h) Heatmap of proteins from cell cycle and proliferation. CTRL, control. Mut, mutant. Student's t-test. *$p<0.05$.

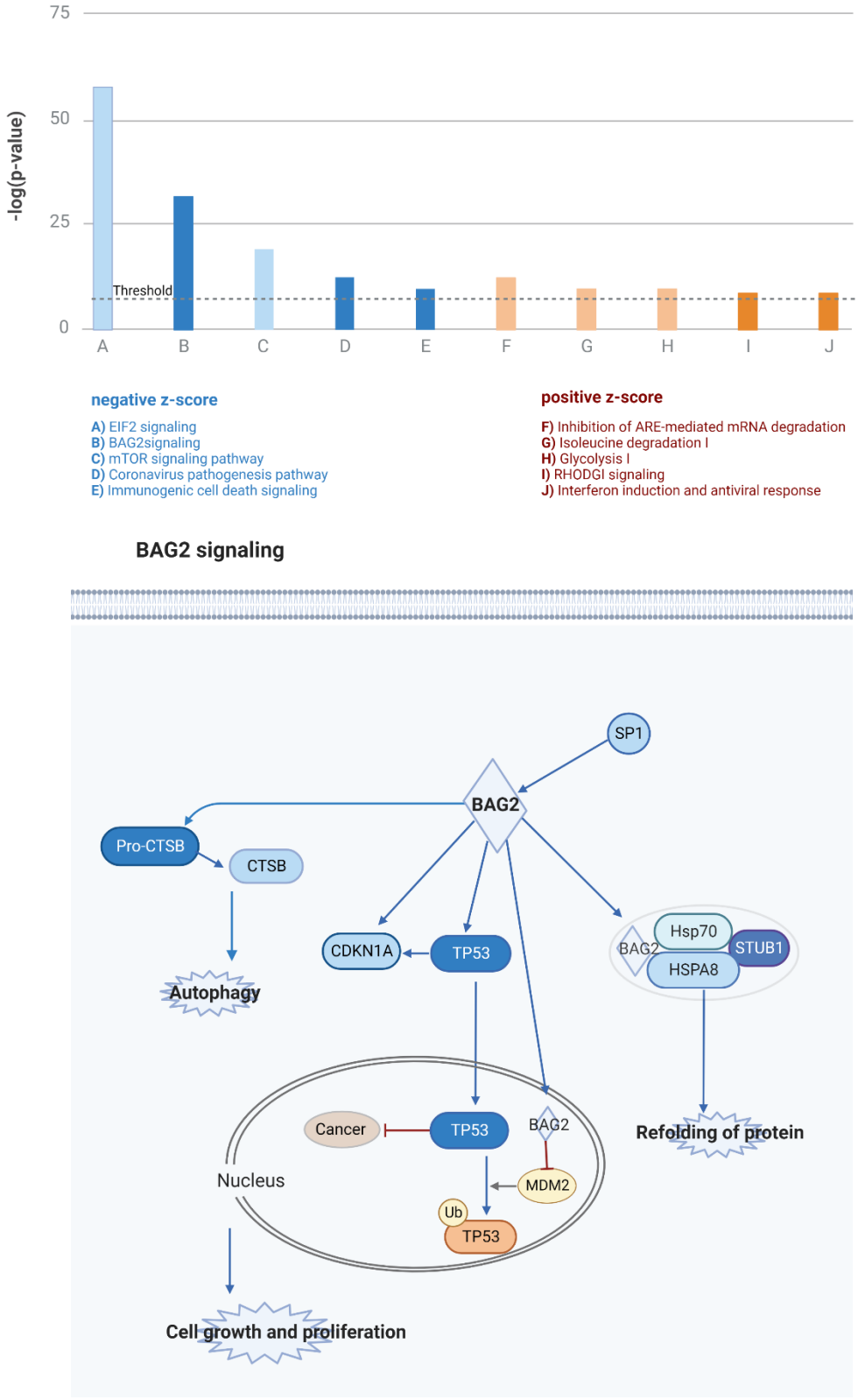


Figure 4.16 Ingenuity pathway analysis of ERMP1 deficiency-induced proteomics changes

Proteins from specified pathways were clustered and ranked by the correlation efficiency in positive or negative z-score. The BAG2 signaling pathway was significantly downregulated. Autophagy pathway and cell proliferation were inhibited in the *ERMP1* mutant M13 cells. BAG2, Bcl2-associated athanogene 2. CTSB, cathepsin B. SP1, specificity protein 1, a transcription factor that promotes cell proliferation. TP53, tumor suppressor 53. CDKN1A, cyclin-dependent kinase inhibitor 1A. STUB1, STIP1 homology, and U-box containing protein 1, an E3 ubiquitin ligase, promoting protein degradation. Ub, ubiquitination. HSPA8, heat shock protein family A (Hsp70) member 8.

### 4.7 Role of *ermp1* in Zebrafish Hematopoiesis

The zebrafish *ermp1* gene encodes a protein that shares 63% sequence identity with human homolog (**Fig**. 4.17a). A zebrafish *ermp1* mutant line was created by CRISPR/Cas9 system, and the sequencing result of the mutant gene confirmed a 17bp deletion in the targeted exon (**Fig**. 4.17b). RFLP assay of the mixed embryos from the F2 generation showed Mendelian randomization of *ermp1* mutation inheritance (heterozygous or homozygous) (**Fig**. 4.17c). The RNA probe of *ermp1* was synthesized to test the expression pattern of *ermp1* in zebrafish embryo development, during which *ermp1* is ubiquitously expressed at 24 hpf, 48 hpf, and 120 hpf (**Fig.** 4.17d).

To evaluate the loss of *ermp1* on hematopoiesis, whole-mount in situ hybridization of *l-plastin*, *c-myb*, *mpx*, and *rag1* probes were performed (**Fig.** 4.18). The numbers of leukocytes (*l-plastin),* neutrophils (*mpx*), and lymphocytes (*rag1*) reduced (**Fig.** 4.18a, c, d). While no significant change was found in the number of HSCs (**Fig.** 4.18b). Then the cell proliferation was measured via PH3 staining. The number of proliferating hematopoietic cells decreased in the CHT of 48 hpf *ermp1* mutant embryos compared to the wild-type siblings (**Fig**. 4.19a). RT-qPCR results showed that the expression of *ddit3*, which encodes a key regulator of the unfolded protein response pathway, significantly increased, while the expression of *perk*, which represents another branch of the pathway, reduced in the *ermp1* mutants compared to the wild-type embryos (**Fig**. 4.19b).

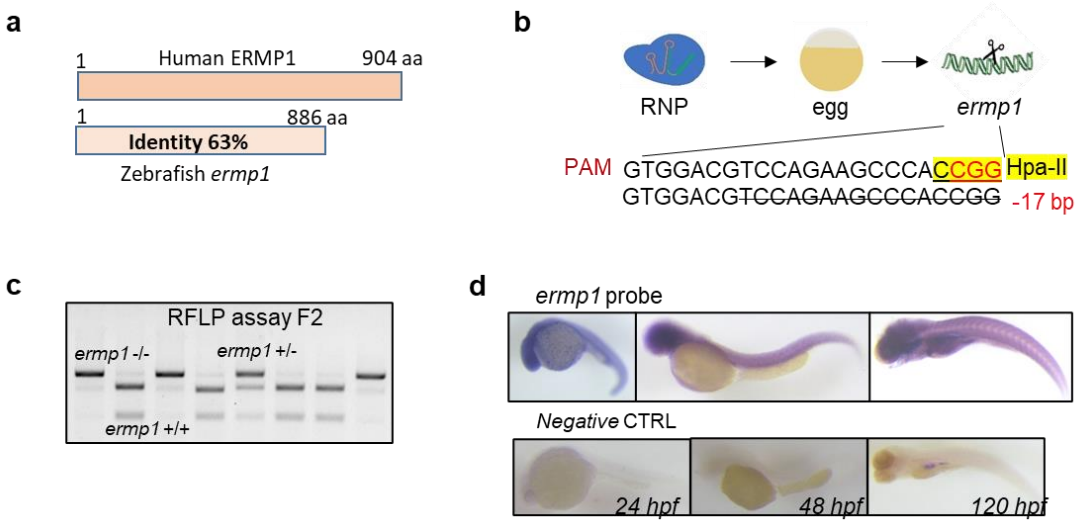


Figure 4.17 Generation of *ermp1* mutant zebrafish line

a) Schematic graph shows the sequence identity of human and zebrafish ermp1 protein. b) Schematic graph of sgRNA targeting zebrafish *ermp1* gene, within which the enzyme Hpa-II was used for the restriction fragment length polymorphism (RFLP) assay. c) Result of genotyping in the F2 generation of mixed embryos. d) *ermp1* expression in zebrafish embryos at 24 hpf, 48 hpf, and 120 hpf. aa, amino acids. bp, base pairs. hpf, hour past fertilization. RNP, ribonucleoprotein.

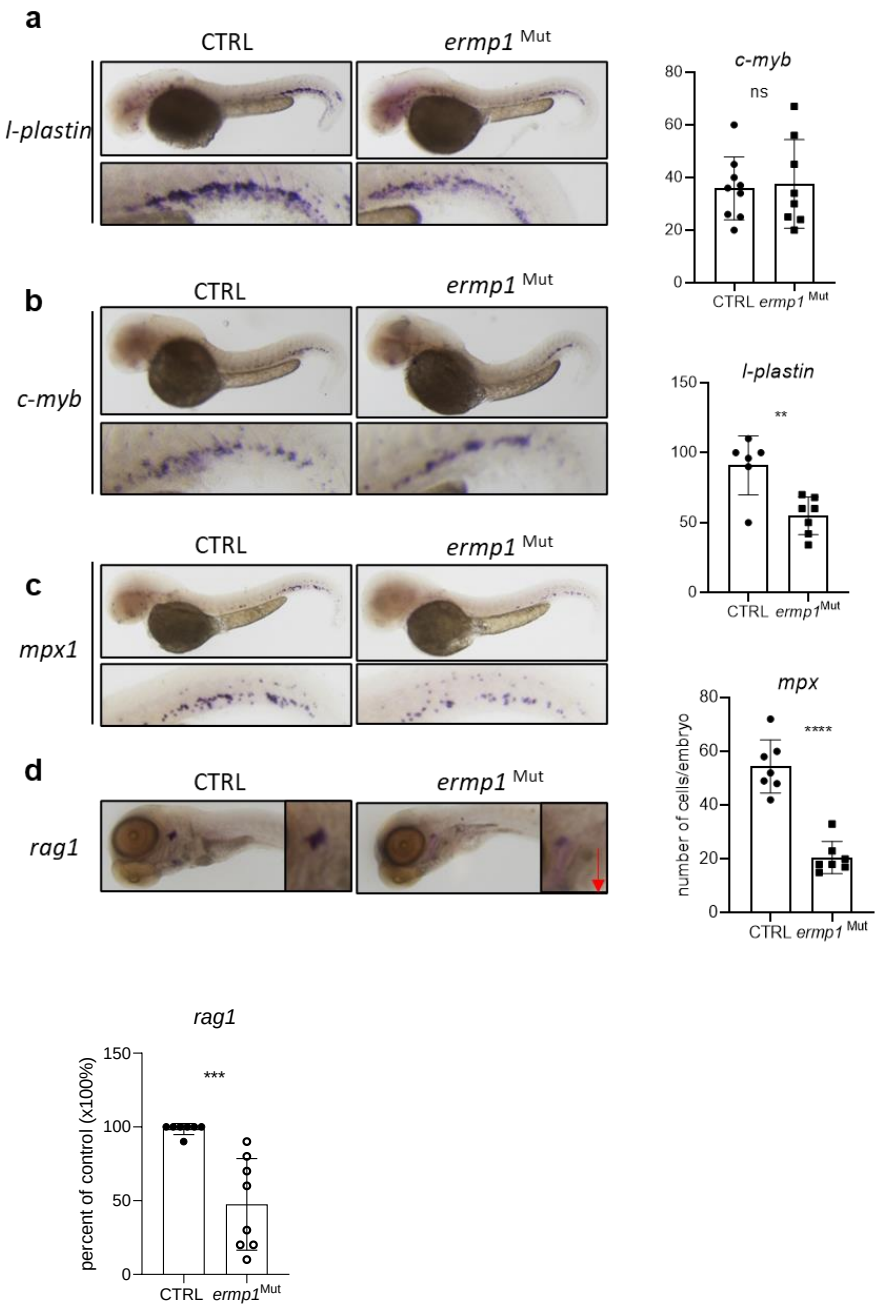


Figure 4.18 Hematopoiesis analysis of *ermp1* mutant embryos

Expression pattern and quantity of *pu.1*, *mpeg1*, *hbae1*, *c-myb*, *l-plastin*, *lyz*, and *rag1* in CHT of zebrafish embryos at 24 hpf, 36 hpf, and 48 hpf. Lateral view, head to left, CTRL, and mutants (siblings). Line denotes the mean value. $p<0.01$, n=20~40. CTRL, control. Mut, mutant. Student's t-test, $^{**}p\leq0.01$, $^{****}p\leq0.0001$, ns, not significant, compared to CTRL.

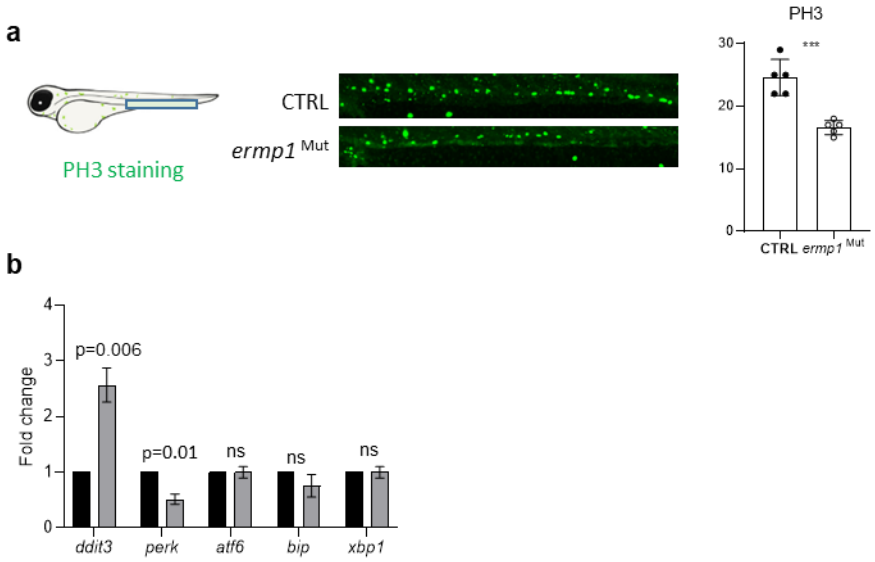


Figure 4.19 Effects of *ermp1* mutation on hematopoietic cell proliferation in zebrafish embryos

a) Phosphorylated Histone H3 staining showed the proliferation of hematopoietic cells in the CHT from 48 hpf zebrafish embryos. b) RT-qPCR of the unfolded protein response markers. *ddit3, DNA damage inducible transcript 3*. *perk, protein kinase RNA-like ER kinase*. *atf6, activating transcription factor 6*. *xbp1, x-box binding protein 1*. CTRL, control. Mut, mutant. Student's t-test, ***p≤0.001, ns, not significant.

### 4.8 Role of *SCPEP1* in AML Cell Lines

The expression of *retinoid-inducible serine carboxypeptidase* (*SCPEP1*) decreased around 5 folds in MOLM-13 cells treated with CQ while increasing by 1.5-fold after RAPA treatment. Previously, it was reported that SCPEP1 participated in the regulation of endothelin-1-mediated hemodynamics and vascular resistance[149]. Our proteomics data suggested that SCPEP1 is a downstream effector of the autophagy pathway in FLT3-ITD$^{+}$ AML cells. To further evaluate its role in AML cells, we induced loss-of-function mutation of the *SCPEP1* gene in M13 cells via CRISPR/Cas9 system (**Fig**. 4.20a).

The sequencing result showed that the CRISPR/Cas9 RNP induced a 4bp or 1 bp deletion around the designated PAM sequence from the early exon of *SCPEP1* in M13 cells (**Fig**. 4.20a). RFLP assay showed the rate of mutation is over 90% in the leukemia cells (**Fig**. 4.20b). Western blot against SCPEP1 suggested a 50% reduction of SCPEP1 protein level in *SCPEP1*$^{Mut}$ cells compared to the CTRL leukemia cells (**Fig**. 4.20b). Meanwhile, LC3-II/GAPDH significantly increased in *SCPEP1*$^{Mut}$ cells treated with CQ (**Fig**. 4.20c, d).

Results of the cell viability test showed that loss of *SCPEP1* suppressed the growth of M13 cells (**Fig**. 4.20e). The mutant and control M13 cells showed no difference in response to RAPA treatment (**Fig**. 4.20f). While SCPEP1-deficient cells became more resistant to the CQ treatment (**Fig**. 4.20g).

Next, MS-based proteomics was performed to analyze the protein changes caused by the SCPEP1 deficiency. Significantly altered proteins were marked in red on the above area in the volcano plot (**Fig**. 4.21a). It showed that protein expressions of splicing factor 3A (SF3A1), heterochromatin protein 1-binding protein 3 (HP1BP3), RNA metabolism and transcription (RBM8A), and cell cycle

or proliferation (NUP98) were significantly upregulated. While levels of Rho GTPase-activating protein (ARHGAP9), protein binding and folding (NUDCD2), and Ras-Related GTP-Binding Protein (RAB10) were significantly decreased in the SCPEP1 deficient leukemia cells (**Fig**. 4.21a).

Heatmap analysis showed protein effectors from cell cycle and proliferation, cellular transport, and biogenesis was generally downregulated, as indicated in green color from the analysis in the *SCPEP1*$^{Mut}$ cells (**Fig**. 4.21b-d). The ingenuity pathway analysis showed that glycolysis, unfolded protein response, phagocytosis in macrophage and monocytes, and NAD signaling pathways were significantly downregulated, leading to inhibition of general translation and protein degradation in the SCPEP1 deficient cells (**Fig.** 4.22).

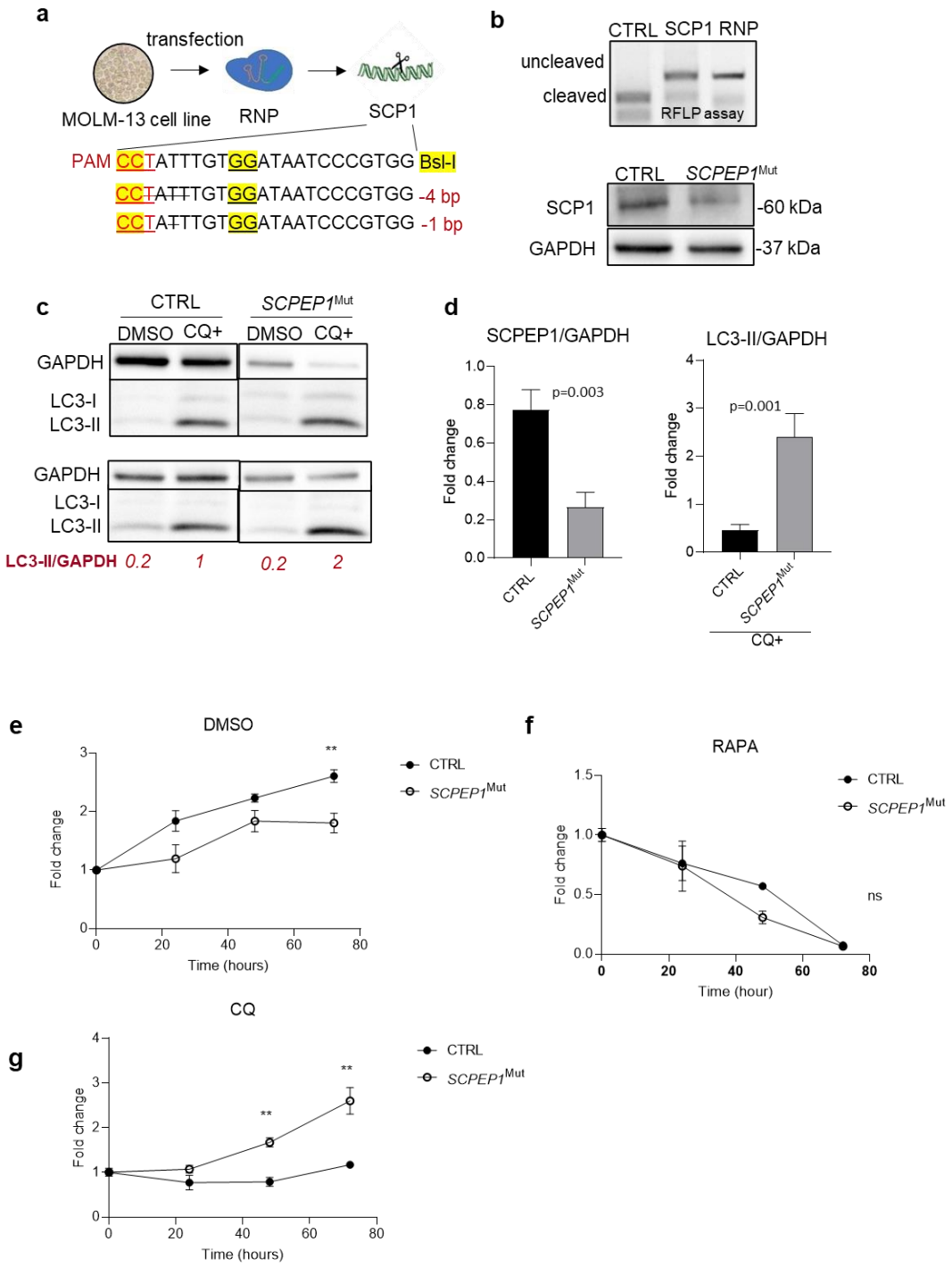


Figure 4.20 Effects of SCPEP1 deficiency on cell proliferation and autophagy in FLT3-ITD$^{+}$ AML cells

a) Schematic graph of targeting *SCPEP1* gene in M13 cell line via CRISPR/cas9 technique. b) The result of genotyping confirmed over 90% mutation. Western blot against SCPEP1 antibody confirmed over 50% reduction. c) Result of Western blot

against LC3-I/II, *SCPEP1*$^{Mut}$ and CT cells treated with or without CQ. d) Statistical analysis of SCPEP1 and LC3-II levels. GAPDH as an internal control protein. e) Plot of cell proliferation. f) Cell viability test with RAPA treatment. g) Cell viability test with CQ treatment. CTRL, control. Mut, mutant. Student's t-test, **p≤0.01, ns, nonsignificant.

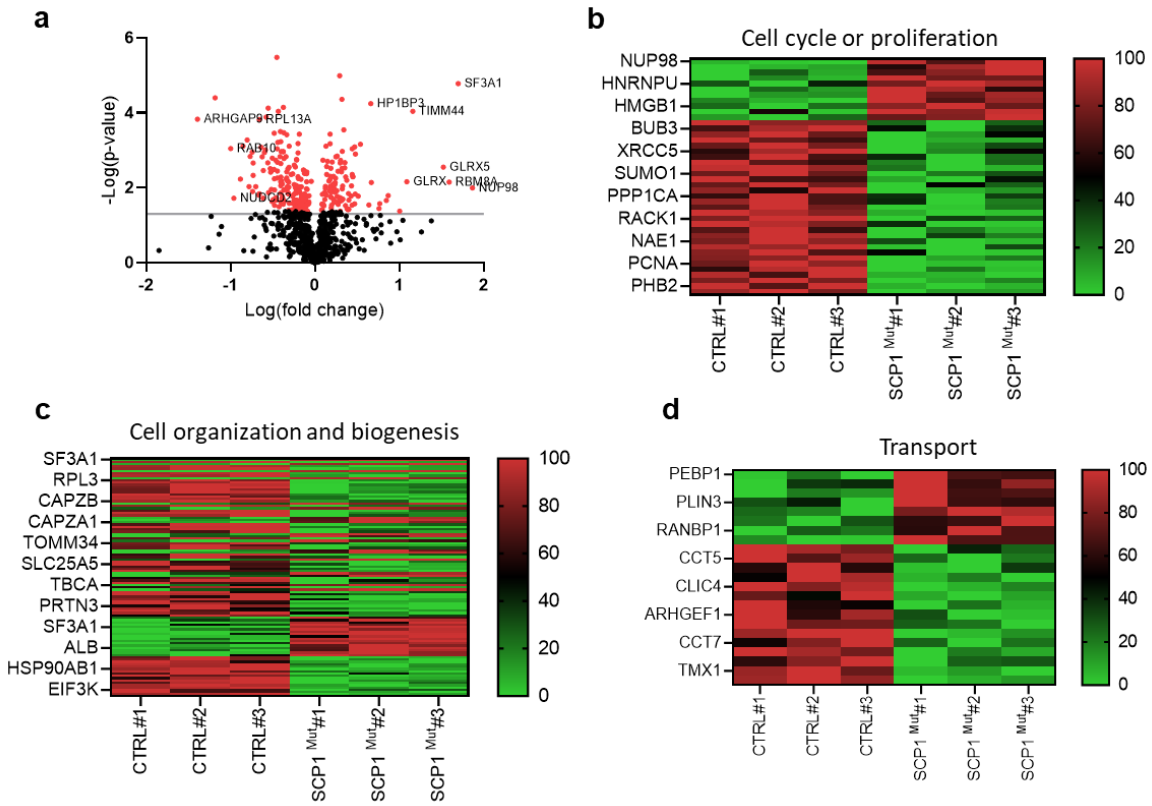


Figure 4.21 Proteomics analysis of *SCPEP1* mutant AML cells

a) Volcano plot of proteomics. b) Heatmap of proteins from cell cycle and proliferation. c) Heatmap of proteins from cell organization and biogenesis. d) Heatmap of proteins from transport. CTRL, control. Mut, mutant.

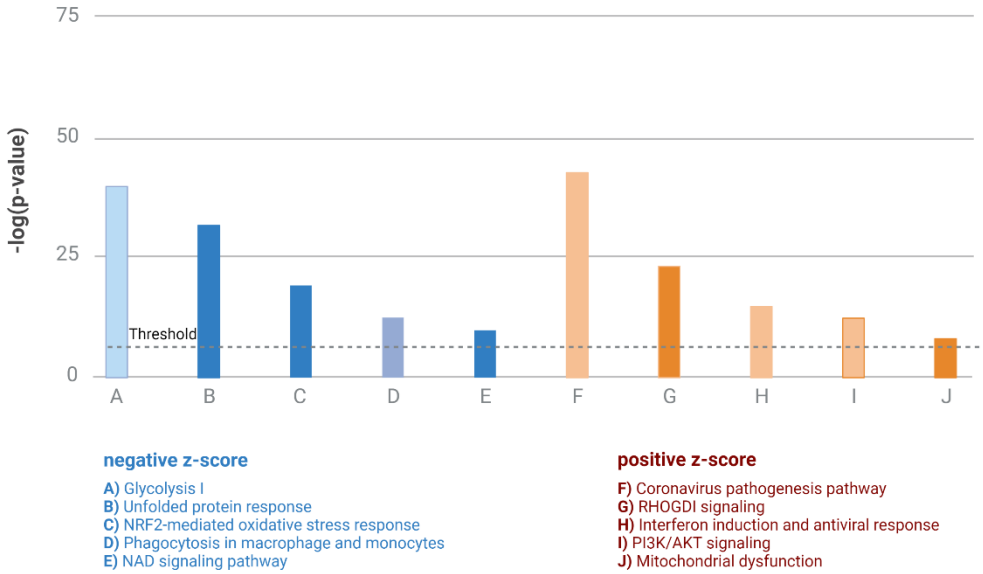


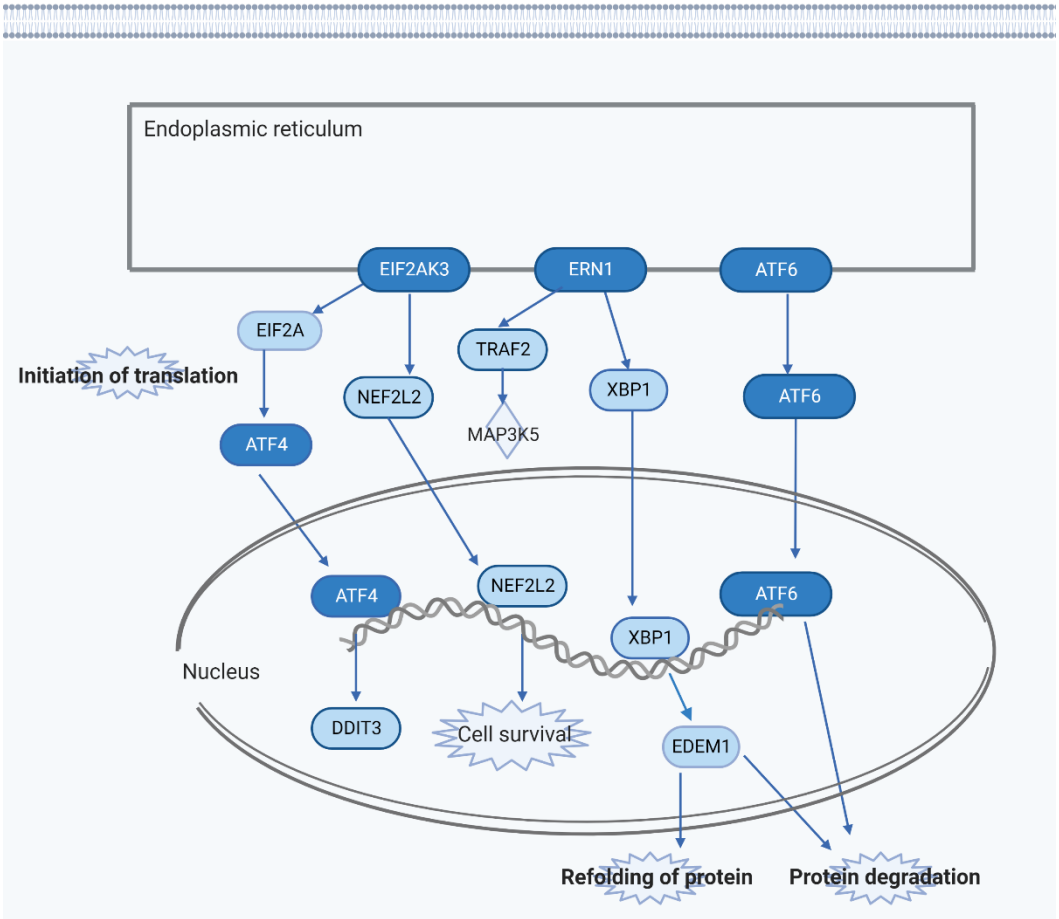


Figure 4.22 Ingenuity pathway analysis of SCPEP1 deficiency-induced proteomics changes

Proteins from specified pathways were clustered and ranked by the correlation efficiency in positive or negative z-score. The unfolded protein response (UPR) pathway was significantly downregulated in the *SCPEP1*$^{Mut}$ M13 cells compared to the CT cells. General translation and endoplasmic reticulum-associated protein degradation were inhibited. EIF2AK3, eukaryotic translation initiation factor 2 alpha kinase 3. ERN1, endoplasmic reticulum to nucleus signaling 1. ATF6, activating transcription factor 6. DDIT3, DNA damage-inducible transcript 3, a transcription factor from the C/EBP family. XBP1, X-box binding protein 1. NEF2L2, NFE2 like bZIP transcription factor 2. EDEM2, ER degradation enhancing alpha-mannosidase like protein 2.

### 4.9 Role of *scpep1* in Zebrafish Hematopoiesis

Zebrafish *scpep1* encodes a protein that shares 66% sequence identity with human homolog (**Fig.** 4.23a). We generated the *scpep1* mutant zebrafish embryos via CRISPR/Cas9. The gene mutation rate in *scpep1* is nearly 100%, while the sequencing result of *scpep1* from mutant embryos showed a 5bp deletion near the PAM sequence (**Fig.** 4.23b, c). Western blot against scpep1 protein indicated a 50% deficiency in the *scpep1* mutant zebrafish embryos (**Fig.** 4.23d). WISH analysis using the designed *scpep1* probe showed ubiquitous expression throughout embryonic development (**Fig.** 4.23e).

Next, we analyzed the changes in hematopoiesis caused by *scpep1* deficiency. Results showed that the number of neutrophils (*mpx*) and lymphocytes (*rag1*) decreased (**Fig.** 4.24a, c). While the number of myeloid progenitors (*pu.1*), HSCs (*c-myb*), and leukocytes (*l-plastin*) did not change (**Fig.** 4.24b, d).

The reduction in *mpx* positive (neutrophils) cells was again shown in *scpep1* mutant Tg (*mpx*: GFP) zebrafish embryos (**Fig**. 4.25a). Loss of *scpep1* inhibited hematopoietic cell proliferation as indicated by decreased PH3 signals (**Fig.** 4.25b).

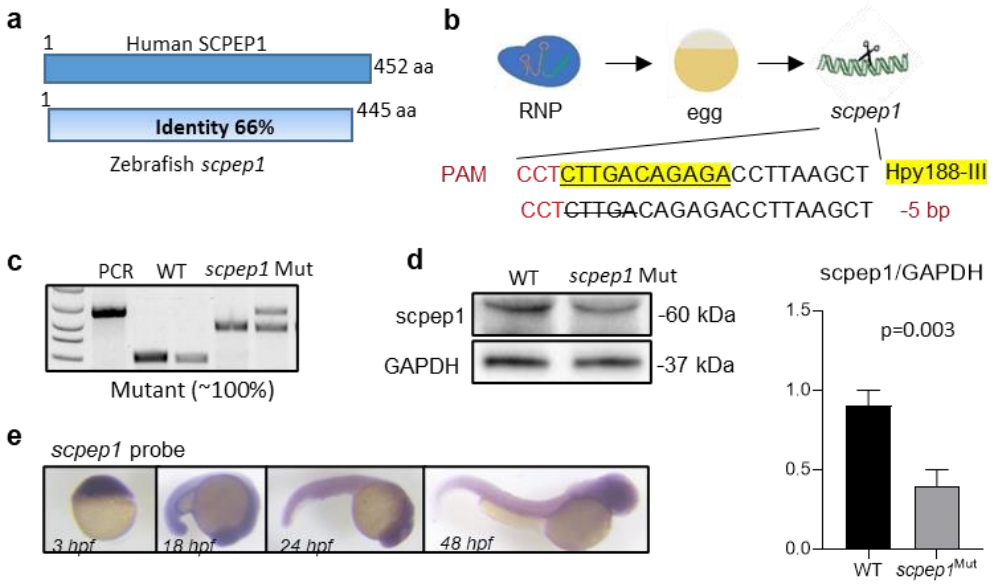


Figure 4.23 Generation of *scpep1* mutant embryos

a) Schematic graph of the protein structure of human and zebrafish *scpep1*. Identity shared by the protein sequence shown in percentage. b) Schematic graph of sgRNA targeting zebrafish *scpep1* gene. c) Result of RFLP assay. d). Western blot of scpep1 in zebrafish embryos. Statistical analysis. e) *scpep1* expression in zebrafish embryos at 3hpf, 18 hpf, 24 hpf, and 48 hpf. WT, wild type. Mut, mutant. hpf, hour past fertilization. Student's t-test.

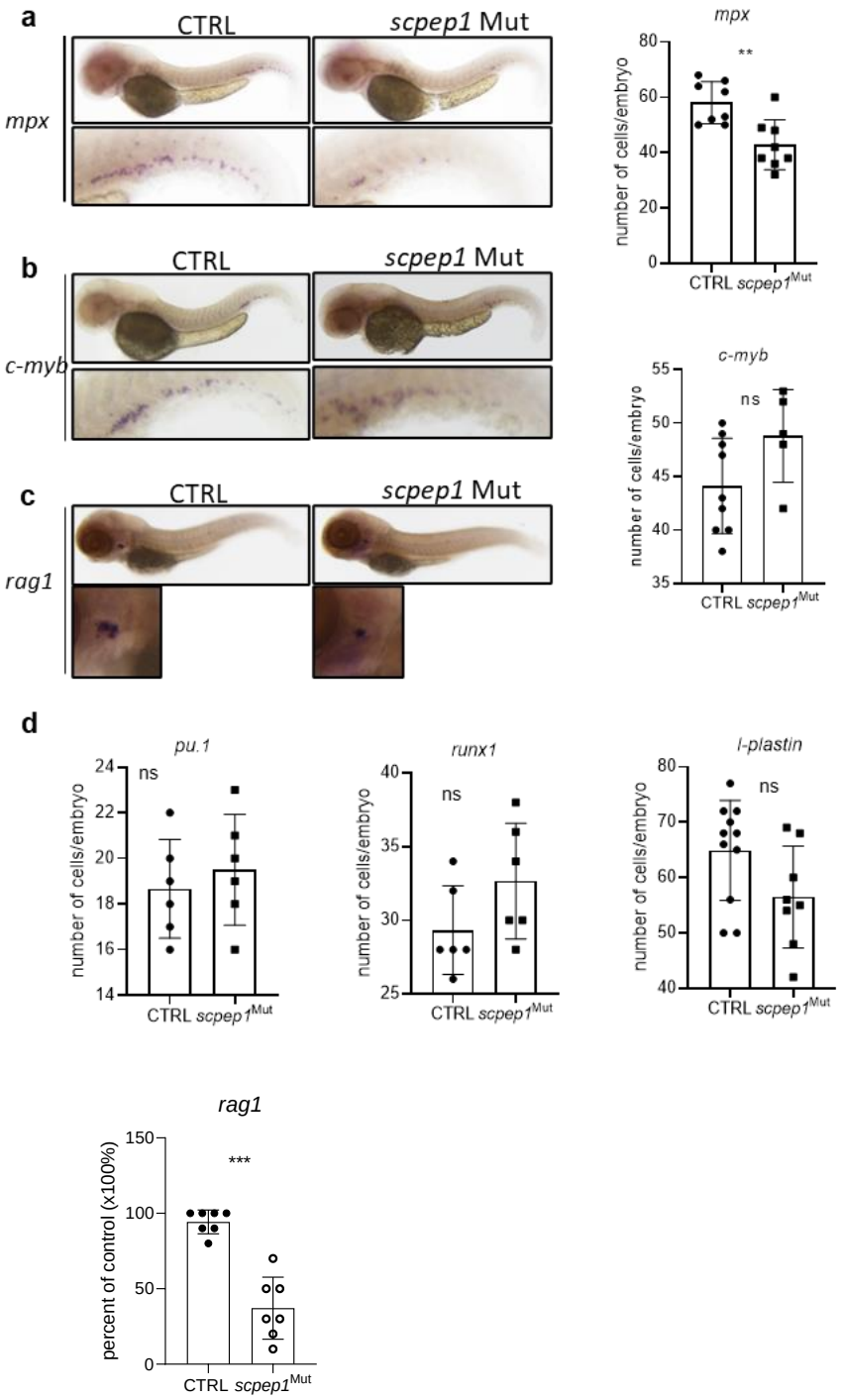


Figure 4.24 Hematopoiesis analysis in *scpep1* mutant embryos

a-d) Expression pattern and quantity of *mpx, c-myb, l-plastin, rag1, pu.1, runx1, l-plastin* in caudal hematopoietic tissue region of zebrafish embryos. Lateral view, head to the left. Line denotes the mean value. $p<0.01$, n=20~40. CTRL, control. Mut, mutant. Student's t-test, **$p \leqslant 0.01$. ns, not significant.

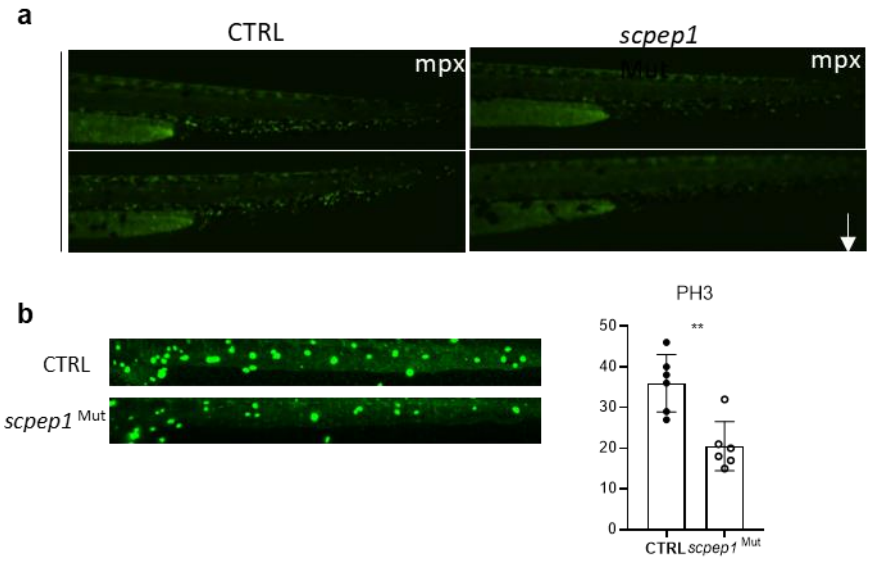


Figure 4.25 Effects of *scpep1* mutation on hematopoietic cell proliferation in zebrafish embryos

a) Image of *mpx*+ cells in caudal hematopoietic tissue region from *scpep1* mutant Tg (*mpx*: GFP) zebrafish embryos. b) PH3 staining showed the proliferation of hematopoietic cells in the caudal hematopoietic tissue from 48 hpf zebrafish embryos Student's t-test, ns, not significant, **p⩽0.01, compared to the control.

## 4.10 Role of *PINK1* in AML Cell Lines

PTEN-induced putative kinase 1 (PINK1) protein functions as a mitochondrial-located serine/threonine kinase. It is reported that PINK1 controls mitochondrial quality via mitophagy and protects cells under adverse conditions[32,150,151]. Meanwhile, PINK1 kinase also plays an important role in classic macroautophagy, deficiency of which upregulates canonical autophagy in cells by interacting with Beclin1[152].

To investigate the potential roles of PINK1 in AML progression, a *PINK1*-deficient AML cell line was created through CRISPR/Cas9 genome editing (**Fig**. 4.26a). Genotyping and sequencing results showed 1 bp insertion mutation in the *PINK1* gene from the mutant (**Fig**. 4.26b) and Western blot showed a significant reduction in PINK1 protein level (**Fig.** 4.26c). Results of CYTO-ID staining and flow cytometry indicated increased autophagic flux in *PINK1* mutant leukemic cells (**Fig.** 4.26d). Autophagic vacuoles significantly increased in *PINK1* mutant leukemic cells compared to the control as shown by Confocal imaging (**Fig**. 4.26e). Loss of *PINK1* moderately promoted cell proliferation (**Fig.** 4.26f). While results from RT-qPCR suggest no significant change of expressions of many autophagic genes including *ATG3*, *ATG5*, or *ATG7* (**Fig**. 4.26g). Notably, in parallel with the upregulated cell proliferation, the expression of *TP53* reduced in the *PINK1* mutant cells (**Fig**. 4.26g).

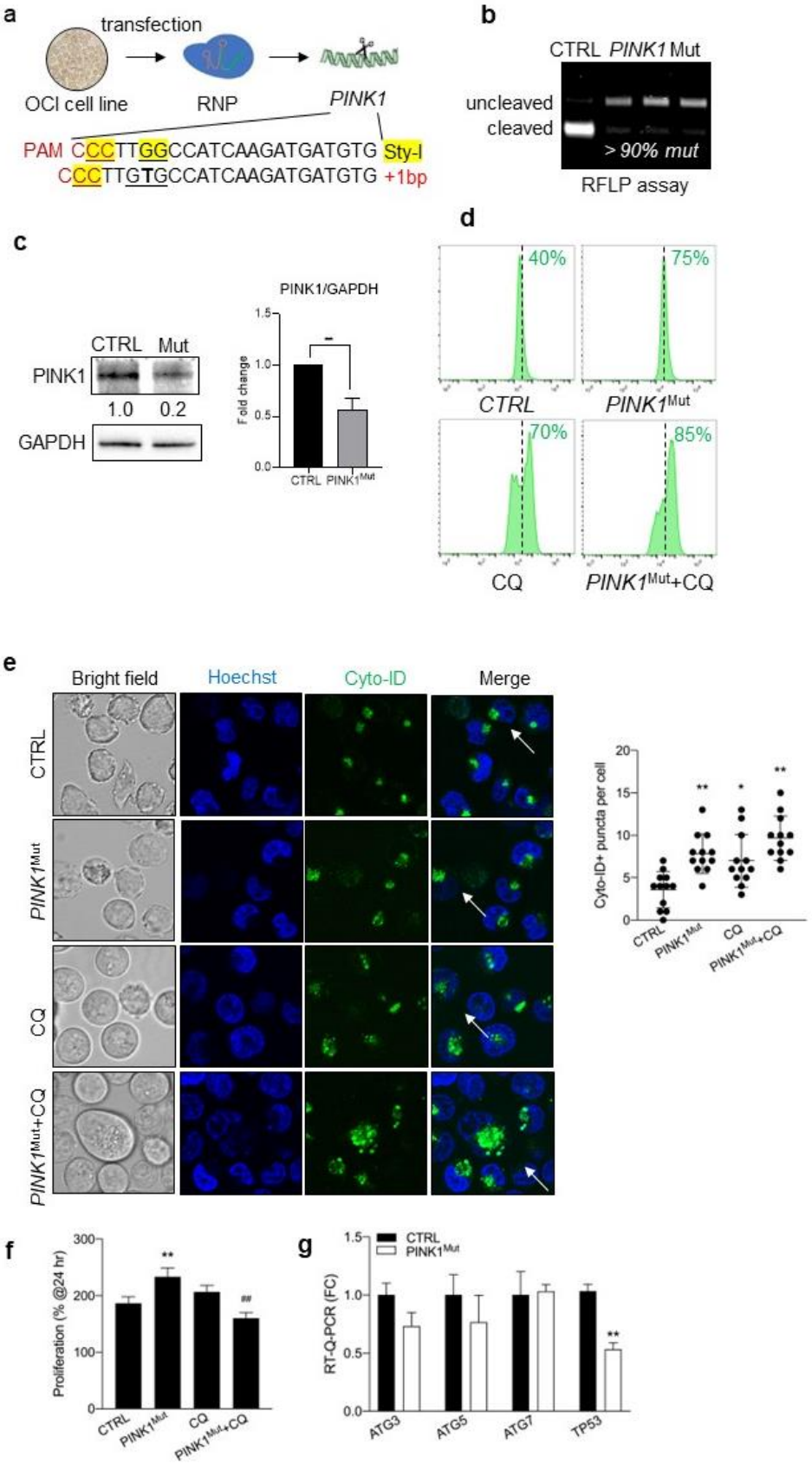


Figure 4.26 Effects of PINK1 deficiency on autophagy and cell proliferation in AML cells

a) The schematic graph of targeting *PINK1* in AML cell line via CRISPR/cas9. b) The result of genotyping. c) Western blot against the PINK1, GAPDH protein serves as the internal control. Statistical analysis. d) Flow cytometry of autophagic flux after CYTO-ID staining. e) Confocal imaging after CYTO-ID staining. Statistical analysis of autophagic flux. f) Statistical result of cell proliferation rate. g) Statistical result of RT-qPCR. CT, control. Mut, mutant. Student's t-test. *$p<0.05$. **$p<0.01$.

### 4.11 Role of *pink1* in Zebrafish Hematopoiesis

Zebrafish *pink1* encodes a protein of 574 amino acids, which shares 73% similarity with the PINK1 from humans among the functional sequence of protein (**Fig**. 4.27a). To investigate the role of *PINK1* in hematopoietic cell development, *pink1* mutant zebrafish embryos (*pink1*$^{Mut}$) were created by the CRISPR/Cas9 gene editing system. Results of the RFLP assay showed more than 90% mutagenic efficiency in RNP-injected F0 embryos (**Fig**. 4.27b), as previously reported that CRISPR/Cas9 editing achieved bi-allelic mutation was with nearly 100% efficiency in F0 embryos [100]. Results of sequencing validated that *pink1* mutation is a 4 bp deletion, that induced frameshift truncation in protein translation (**Fig**. 4.27c). Western blot confirmed a significant reduction in the level of pink1 in the mutant embryos (**Fig**. 4.27d). Although *pink1*$^{Mut}$ displayed normal morphology and growth during embryogenesis, the scale of Lc3-II/GAPDH enhanced significantly compared to the wild-type siblings at 48 hpf (**Fig**. 4.27d).

Next, we monitored the autophagic flux in the leukocytes of zebrafish embryos. Results showed that the number of autophagic vacuoles significantly increased in hematopoietic cells of *pink1*$^{Mut}$ embryos (**Fig**. 4.28). WISH against various hematopoietic cell probes was performed to analyze definitive hematopoiesis in zebrafish embryos. In 48 hpf *pink1*$^{Mut}$ embryos, the number of HSCs (*c-myb*+), erythroid cells (*hbae1*+), and pan-leukocytes (*l-plastin*+) significantly expanded (**Fig**. 4.29a). However, no significant change in the number of neutrophils (*mpx*) was observed (**Fig**. 4.29b). To investigate the correlation between autophagy and hematopoiesis in *pink1*$^{Mut}$ embryos, zebrafish embryos were treated with 3-MA to inhibit autophagy. WISH results showed that 3-MA treatment only induced subtle changes in various hematopoietic cells from the control group, but significantly

attenuated the development of HSCs, leukocytes, and erythroid cells in *pink1*$^{Mut}$ zebrafish embryos (**Fig**. 4.29).

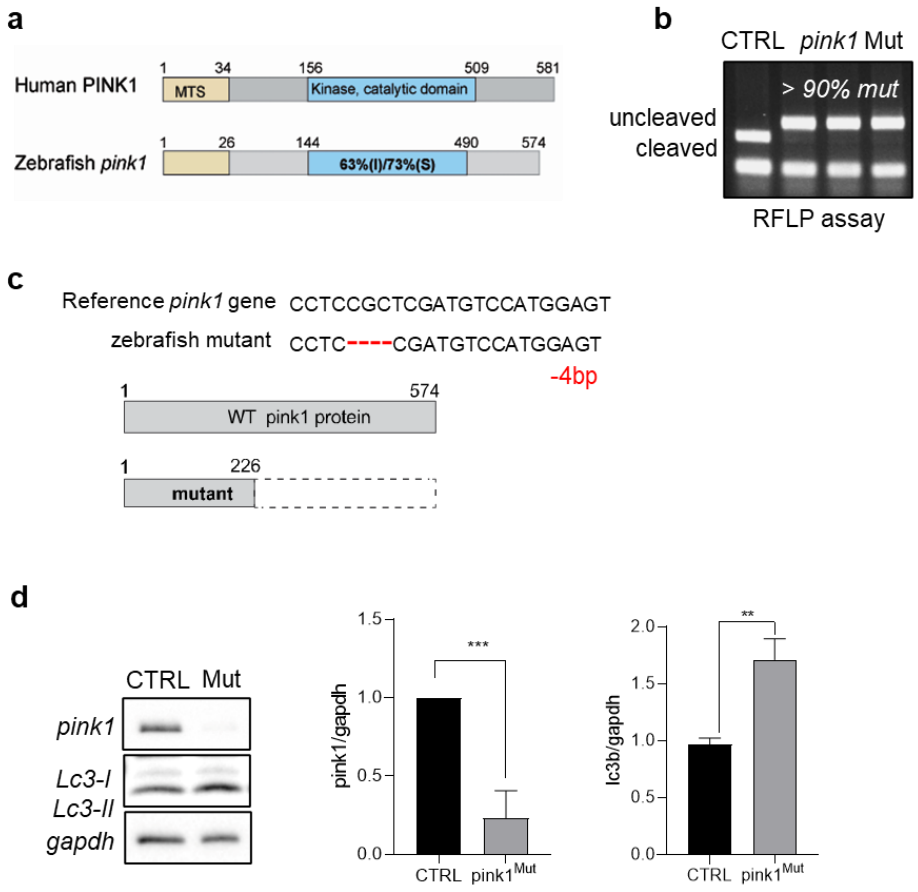


Figure 4.27 Generation of *pink1* mutant zebrafish embryos

a) The protein structure of human and zebrafish pink1. b) Result of genotyping by RFLP assay. c) The schematic graph of sequencing validation of zebrafish *pink1* mutation. d) Western blot against pink1 and lc3 protein, gapdh as the internal control. Statistical analysis of fold change in proteins. I, identity. CTRL, control. Mut, mutant. Student's t-test. **p<0.01. ***p<0.001.

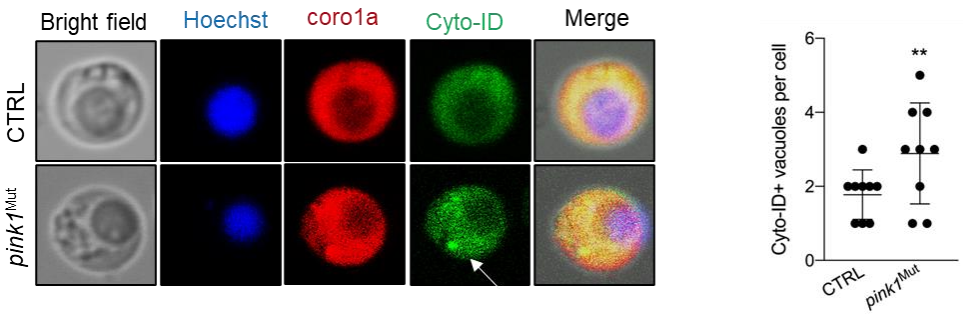


Figure 4.28 Effects of *pink1* mutation on autophagy in hematopoietic cells from zebrafish embryos

Imaging of autophagic structures indicated by CYTO-ID stain in coro1a: DsRed positive cells sorted from Tg (*coro1a*:DsRed) zebrafish embryos. Statistical analysis of number of autophagic vacuoles. dpf, days-past-fertilization. CTRL, control. Mut, mutant. Student's t-test. **p<0.01. ***p<0.001.

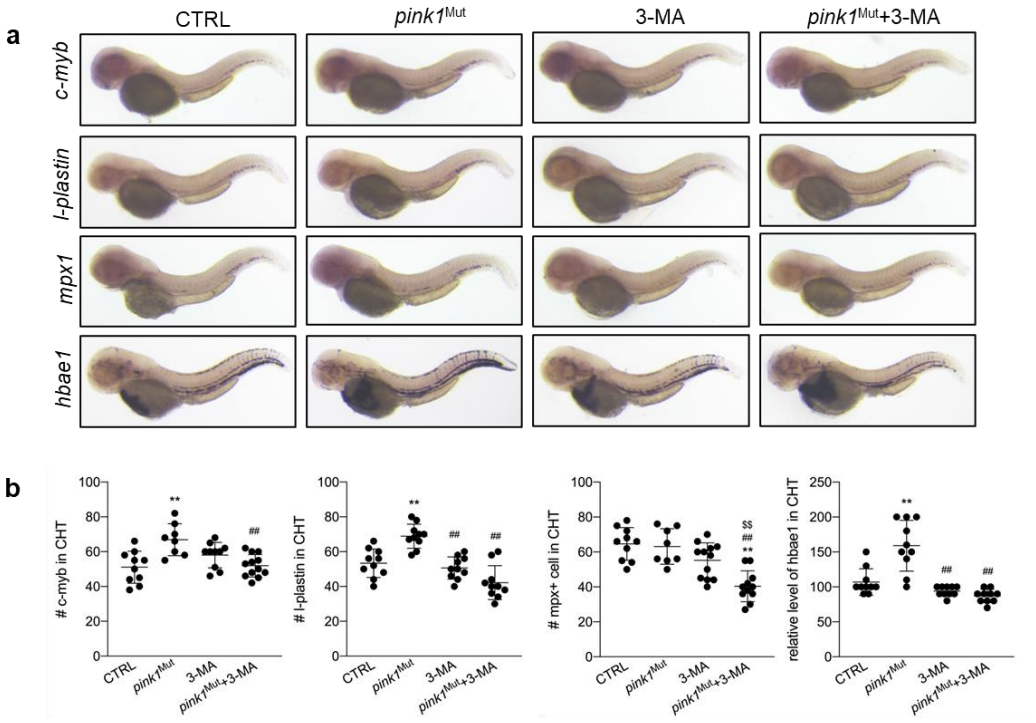


Figure 4.29 Effects of *pink1* mutation on hematopoiesis in zebrafish embryos

a) Whole mount in situ hybridization (WISH) analysis of *c-myb*, *l-plastin*, *mpx*, and *hbae1* probes in 2 dpf zebrafish embryos. b) Statistical analysis of the number of cells with positive signals. dpf, days-past-fertilization. CTRL, control. Mut, mutant. Student's t-test. **p<0.01, compared to the control group. ## p≤0.01, compared to mutant. $$ p≤0.01, compared to the 3-MA group.

# 5. Discussion

FLT3-ITD is one of the most frequently found gene mutations among AML patients. This gain of function mutation triggers constitutive autophosphorylation, which promotes the signaling cascade of PI3K, MAPK, and JNK/STAT signaling[21]. Tyrosine kinase inhibitors (e.g., quizartinib) that target FLT3-ITD and multiple kinases have been developed and approved by the administration[145]. However, patients treated with quizartinib only showed transient remission at initial doses and quickly encountered relapses.

Complex compensating signaling feedback is one of the reasons for TKI resistance in the FLT3-ITD$^+$ AML cells. The concurrent mutations of other genes including IHD1/2, DNMT3A, and NPM1 also contribute to the poor response to treatments. Thus, researchers have demonstrated that quizartinib acts synergistically with (1) Panobinostat, the histone deacetylase inhibitor; (2) 5-azacitidine, the DNA methyltransferase inhibitor; (3) Dasatinib or sorafenib to achieve a better outcome in relapsed FLT3-ITD$^+$ AMLs, against their resistance[153–155].

Moreover, several studies demonstrated that FLT3-ITD promoted autophagy regulation pathways in AML cells. For example, one study suggested that FLT3-ITD triggered an increase in autophagic flux in AML via *activating transcription factor 4* (*ATF4*) activation[156]. Targeting ATF4 inhibits autophagy and impairs AML cell growth. Another study suggested FLT3-ITD promoted leukemia cell proliferation through upregulating ULK1[157]. ULK1 inhibition induced apoptosis in FLT3-ITD$^+$ AML while having minimal effects on FLT3-WT or normal CD34$^+$ cells. Recently, Qiu et al. showed that autophagy is vital for leukemia stem cell maintenance of FLT3-ITD$^+$ AML since autophagy inhibition led to increased

oxidative phosphorylation and mitochondria accumulation[158]. Another recent study utilized the translatome proteomics with phosphoproteomics to analyze the resistance mechanism behind FLT3-inhibitors-treated AML, concluding that autophagy is dominantly resisting the therapies[159]. These findings demonstrated the AKT-mTORC1-ULK1-dependent autophagy pathway as the main mechanism behind FLT3-autophagy-targeted therapy. However, treating AMLs with classic autophagy inhibitors was not feasible due to the lack of specificity and severe side effects.

In this project, we found that fast-proliferating AML cell lines like MV4-11, M13, and KG-1 were more sensitive to autophagy inhibitors than CML cells. Consistently, AML cells conferring robust proliferation were addicted to a high level of autophagy. Autophagy induction promoted ubiquitin proteolysis and protein processing in ER, while autophagy inhibition suppressed signaling pathways and cell proliferation. Proteomics analysis upon treatment with autophagy modulators identified potential autophagy-related targets in FLT3-ITD$^+$ AML cells, including DOCK2, ERMP1, SCPEP1, and PINK1. However, direct evidence between autophagy and protein regulation is lacking, and it is highly possible that these autophagy effectors are regulated by other signaling pathways and transcription factors simultaneously. Proteomics results from RAPA, CQ, or 3-MA treatment might be due to autophagy-independent regulation, for example, oxidative stress induced by heavy doses of drugs.

Based on our proteomic analysis, DOCK2, ERMP1, SCPEP1, and PINK1 were chosen as potential autophagy-related targets from FLT3-ITD$^+$ cells according to the following criteria. First, these proteins are highly expressed in the hematopoietic system[140,141,144]. Second, these proteins were oppositely regulated by autophagy

inducer and inhibitor in the FLT3-ITD$^+$ cells, in which case the observed regulation was more likely due to autophagy-induced changes rather than other secondary metabolic effects. Although PINK1 was not in the table, it is well-known for controlling mitophagy, and the proteomics result suggested that mitochondrial membrane proteins such as VDAC1 and TOMM20 were oppositely regulated by autophagy inducer and inhibitor in the FLT3-ITD$^+$ cells too. DOCK2 protein level significantly reduced upon treatment with rapamycin, while elevated when treated with autophagy inhibitor, 3-MA. On the other hand, ERMP1 and SCPEP1 protein levels significantly increased after autophagy induction, while decreased after autophagy inhibition in FLT3-ITD$^+$ AML cells. Interestingly, CRISPR/Cas9 targeting these genes also affected autophagy, for example, DOCK2 deficiency induced autophagy while ERMP1 deficiency inhibited autophagy, which suggested that DOCK2 and ERMP1 may act downstream of autophagy modulators to regulate autophagy flux, which warrants further investigation.

DOCK2 belongs to the CDM (Caenorhabditis elegans CED-5, human DOCK180, and Drosophila melanogaster Myoblast City) family, functions as an atypical guanine exchange factor that regulates Rac activation[160]. In this study, we found DOCK2 is indispensable to FLT3-ITD$^+$ AML cell proliferation, probably due to its correlation with FLT3 and mTOR proteins. Loss of DOCK2 inhibited the AKT pathway while promoting STAT5-ERK signaling. DOCK2 deficiency significantly impaired FLT3 phosphorylation and mTOR signaling, which partially explains the inhibited cell growth and disrupted autophagy in FLT3-ITD$^+$ cells. While the promoted RHOA signaling can be associated with abnormal kinase signaling. In this study, the microtubule-associated protein 1A/1B-light chain 3 (LC3) levels were measured to indicate autophagy levels. LC3-II is the

phosphatidylethanolamine-form of LC3-I, and was shown to be a ubiquitin-like structure that binds and drags autophagic substrate to the autophagosome[161]. The increased LC3-II levels can be due to increased conversion of LC3-I to LC3-II, or due to decreased clearance of LC3-II by the lysosomes (like in the case of CQ treatment). In the DOCK2 mutant FLT3-ITD AML cells, both LC3-I and LC3-II levels increased (LC3-I/II also increased), indicating a blockage in normal LC3-I/II function. Meanwhile, proteomics analysis suggested downregulated autophagy. For explanation, it may be because DOCK2 plays a substrate or adaptor role in the LC3-II binding and autophagosome formation process. Considering DOCK2 is indeed a key player of cytoskeleton reorganization and membrane polarity, it is possible that the autophagosomal membrane extension is dependent on DOCK2 function. These finding are consistent with studies indicating that DOCK2 expression is correlated with poor prognosis of AML or CML[162,163]. The number of T and B cells, but not monocytes, markedly decreased in *Dock2*-/- mice that finally led to B cell defects and T lymphocytopenia[140]. Tomoko et al. found that although the number of B lymphocytes decreased, the number of common lymphoid progenitors (CLP) and HSCs remained normal in *Dock2*-/- mice[164]. These findings suggest that DOCK2 is important for lymphopoiesis, but dispensable for HSC engraftment and self-renewal. In our study, hematopoiesis analysis showed that the number of myeloid progenitors and HSCs expanded in *dock2* mutant zebrafish embryos. The number of neutrophils and lymphocytes decreased while the number of leukocytes and erythrocytes did not change in zebrafish *dock2* mutants. The reduction of neutrophils and lymphocytes in *dock2* mutant embryos can be partially explained by its functional role in the chemokine signaling and cytoskeleton reorganization,

however, the detailed reason for up and drop in the hematopoietic cell number requires more studies.

*ERMP1* gene encodes a protein of 898 aa, consisting of 8 putative transmembrane domains that resemble a zinc Metallo-aminopeptidase localized to the endoplasmic reticulum (ER). A previous study suggests ERMP1 is vital for follicle development[143]. *ERMP1* is reported as a candidate oncogene in breast cancers[141]. *ERMP1* is also found to be overexpressed in a high-risk group of childhood AML[147]. Loss of *ERMP1* suppressed autophagy activity and cell proliferation of FLT3-ITD$^+$ AML cells, suggesting that leukemia cell proliferation depends on ERMP1-mediated autophagy. Considering ERMP1 is an ER membrane protein, while ER plays a functional role in the formation of autophagosome[165], it is possible that ERMP1 plays a supporting role in the autophagosome development. ERMP1 deficiency also induced cell cycle arrest and general translation inhibition, indicated by the suppressed EIF2, BAG2, and mTOR signaling pathways in ERMP1 deficient FLT3-ITD$^+$ AML cells. In the zebrafish model, loss of *ermp1* reduced the number of leukocytes, neutrophils, and lymphocytes, but not HSCs, which may be explained by the decrease of proliferating cells in CHT. Consistent with previous *in vitro* studies reported that *ERMP1* silencing impaired cancer cell growth via inhibiting PERK pathway[148], *ermp1* deficiency in zebrafish also induced the expression of *ddit3*, while reducing the expression of *perk*, the key regulators of unfolded protein response (UPR). It is possible that leukocyte and lymphocyte development relies on the normal function of ER and UPR, which was disrupted by *ermp1* mutation in the zebrafish embryos. These findings suggested a previously undescribed role of the Autophagy-Ermp1-UPR axis in regulation of normal hematopoiesis, which warrants further investigations.

Serine carboxypeptidase (SC) is a family of lysosomal glycoproteins featured with substrate binding and catalytic domains that exhibit carboxyl-terminal proteolytic activity at acidic pH[144]. SCPEP1 belongs to the SC family and shares a conserved catalytic triad with the lysosomal proteins[166]. However, *Scpep1*-deficient mice did not exhibit phenotypes of lysosomal storage or reduction in lysosomal activity[167]. Loss of *SCPEP1* suppressed leukemia cell growth while upregulated autophagy compared to the control cells. In this study, LC3-II levels also increased in the *SCPEP1* mutant FLT3-ITD AML cells. The degradation of autophagic cargo (LC3-II-bond substrate) depends on lysosomes, therefore fusion of autophagosomes and lysosomes is a rate-limiting step[168]. The increased level of autophagic marker LC3-II may be due to the inhibition of lysosome-associated degradation, which caused an insufficient autophagic degradation that restrained the autophagy. Only use of LC3-II to represent autophagy activity is not sufficient. It is likely that *SCPEP1* plays a role in restoring autophagosome-lysosome fusion during autophagy, which may explain cells desensitization to CQ treatment. Combined with findings from DOCK2 and ERMP1 mutant leukemic cells, it indicates that essentially all cellular membranes contribute to the autophagosome development, such as plasma membrane, ER, lysosome, and mitochondrial membranes. Indeed, deep understanding of autophagy requires further exploration on the roles of key membrane proteins. In zebrafish, loss of *scpep1* only significantly reduced the number of neutrophils and lymphocytes while other hematopoietic lineages remained unchanged. Similar to *ermp1* knockout, the number of proliferating cells in CHT also reduced in *scpep1* mutants, which may partly explain the reduction in neutrophils. It is possible that neutrophil and lymphocyte development depends on the normal function of lysosome, which was

impaired by *scpep1* mutation in the zebrafish embryos. Here I identified a previously undescribed role of *scpep1* in hematopoiesis. However, the precise roles of *dock2*, *ermp1*, and *scpep1* require more studying of hematopoietic cell profiles in adult zebrafish's spleen and kidney marrow.

Other than the candidates identified from our proteomic analysis, previous research has underlain the function of PINK1 in mitophagy-mediated cellular stability of hematopoietic stem cells[169]. Pink1 deficient mice displayed enhanced oxidative respiration and improved proliferation in bone marrow cells[170]. Treatments with the autophagy inhibitors like bafilomycin A1, CQ, and Lys05 inhibited leukemia cell growth while significantly increased the expression of *PINK1*[70]. Our results show that PINK1 deficiency induced autophagic flux and promoted cell proliferation in AML cells. In zebrafish embryos, pink1 deficiency induced overall autophagy activity and expansion of hematopoietic cells during definitive hematopoiesis. In both cases, PINK1 is likely to function as a negative regulator of autophagy and proliferation, thus its role should be facilitated in the AML treatments. Similarly, our recent study on roles of *atgs* in zebrafish embryonic hematopoiesis showed that loss-of-function mutation of *becn1* induced hematopoietic cell expansion, which aligned with previous finding that *Beclin-1* is a tumor suppressor gene[127,171].

Targeting *dock2*, *ermp1*, *scpep1* and *pink1* in zebrafish exhibited differential effects in embryonic hematopoiesis, similar to the well-described discrepancy between targeting different autophagy-related genes (ATGs) in regulating vertebrate hematopoiesis[127]. For instance, our recent study demonstrated that vertebrate definitive hematopoiesis is regulated in an *atgs*-dependent manner[127]. However, how the four candidate genes interact with *atgs* in canonical as well as

non-canonical autophagy during normal hematopoiesis remains to be further investigated. Despite our findings in FLT3-ITD$^{+}$ AML cells and zebrafish normal hematopoiesis, roles of potential autophagy-related targets should be further studied mechanistically in zebrafish leukemia models such as Tg(*Runx1*:*FLT3*$^{ITD}$*IDH2*$^{R172K}$)[85], which will provide important insights about the role of autophagy and these candidates in leukemogenesis.

While the specificity of these candidates towards AML as well as their potential as novel therapeutic targets remains further investigation, our findings strengthen the idea of combination treatment with multiple inhibitors in FLT3-ITD$^{+}$ AML. Inhibition of autophagy attenuated the hematopoietic cell expansion, suggesting that hematopoietic cell expansion is induced via autophagy activation. Furthermore, we have identified several autophagy-related targets and demonstrated their involvement in leukemic cell growth, normal hematopoiesis, and autophagy using leukemia cell lines and zebrafish models. Nevertheless, this study provides evidence that DOCK2, ERMP1, and SCPEP1 can be potentially targeted for AML treatment, while the role of PINK1 requires guarantee. Meanwhile, this study has translational significance and lays the basis for clinical investigations of autophagy-associated target treatments.

# 6. Conclusions

In this project, I generated convincing data confirming that fast-proliferating AML cell lines, such as MV4-11, M13, and KG-1, are sensitive to autophagy inhibitors, and fast-proliferating AML cells are addicted to a higher level of autophagy. In AML cells, autophagy induction promotes ubiquitin proteolysis and protein processing in ER, while autophagy inhibition suppresses kinase signaling pathways and cell proliferation. Using relevant experimental methodologies, potential autophagy-related targets in FLT3-ITD$^+$ AML cells, including DOCK2, ERMP1, SCPEP1, and PINK1, are identified. Next, I revealed the roles of these genes in leukemia cell proliferation and zebrafish hematopoiesis. DOCK2 expression is highly correlated with FLT3-ITD activity and cell survival, while ERMP1 and SCPEP1 are indispensable for FLT3-ITD-related autophagy and cell proliferation. In contrast, PINK1 negatively regulates leukemia cell growth and hematopoietic cell expansion via autophagy.

In conclusion, my thesis work has certainly updated our understanding of the disease regulatory mechanisms of AML with solid experimental data. These findings, with translational significance, will pave the way for the future development of novel autophagy-related therapeutic agents against AML. Importantly, the rational design of novel autophagy-mediated treatment strategies as presented in my thesis work may also be further exploited for targeting other types of malignancies.

# 7. References


1. DiNardo CD, Cortes JE. Mutations in AML: prognostic and therapeutic implications. *Hematol. Am. Soc. Hematol. Educ. Progr.* 2016;2016(1):348–355.
2. Pui C-H, Yang JJ, Hunger SP, et al. Childhood Acute Lymphoblastic Leukemia: Progress Through Collaboration. *J. Clin. Oncol. Off. J. Am. Soc. Clin. Oncol.* 2015;33(27):2938–2948.
3. Döhner H, Estey E, Grimwade D, et al. Diagnosis and management of AML in adults: 2017 ELN recommendations from an international expert panel. *Blood*. 2017;129(4):424–447.
4. Leith CP, Kopecky KJ, Godwin J, et al. Acute myeloid leukemia in the elderly: Assessment of multidrug resistance (MDR1) and cytogenetics distinguishes biologic subgroups with remarkably distinct responses to standard chemotherapy. A Southwest Oncology Group Study. *Blood*. 1997;89(9):3323–3329.
5. Welch JS, Ley TJ, Link DC, et al. The origin and evolution of mutations in acute myeloid leukemia. *Cell*. 2012;150(2):264–278.
6. Paschka P, Du J, Schlenk RF, et al. Secondary genetic lesions in acute myeloid leukemia with inv(16) or t(16;16): a study of the German-Austrian AML Study Group (AMLSG). *Blood*. 2013;121(1):170–177.
7. Döhner H, Weisdorf DJ, Bloomfield CD. Acute Myeloid Leukemia. *N. Engl. J. Med.* 2015;373(12):1136–1152.
8. Löwenberg B, Downing JR, Burnett A. Acute myeloid leukemia. *N. Engl. J. Med.* 1999;341(14):1051–1062.
9. Papaemmanuil E, Gerstung M, Bullinger L, et al. Genomic Classification and

Prognosis in Acute Myeloid Leukemia. *N. Engl. J. Med.* 2016;374(23):2209–2221.

10. Olney HJ, Le Beau MM. The cytogenetics of myelodysplastic syndromes. *Best Pract. Res. Clin. Haematol.* 2001;14(3):479–495.
11. Marando L, Huntly BJP. Molecular Landscape of Acute Myeloid Leukemia: Prognostic and Therapeutic Implications. *Curr. Oncol. Rep.* 2020;22(6):61.
12. Okano M, Bell DW, Haber DA, Li E. DNA methyltransferases Dnmt3a and Dnmt3b are essential for de novo methylation and mammalian development. *Cell*. 1999;99(3):247–257.
13. Rosnet O, Schiff C, Pébusque MJ, et al. Human FLT3/FLK2 gene: cDNA cloning and expression in hematopoietic cells. *Blood*. 1993;82(4):1110–1119.
14. Wakita S, Sakaguchi M, Oh I, et al. Prognostic impact of CEBPA bZIP domain mutation in acute myeloid leukemia. *Blood Adv.* 2022;6(1):238–247.
15. De Kouchkovsky I, Abdul-Hay M. "Acute myeloid leukemia: a comprehensive review and 2016 update". *Blood Cancer J.* 2016;6(7):e441.
16. Dang L, White DW, Gross S, et al. Cancer-associated IDH1 mutations produce 2-hydroxyglutarate. *Nature*. 2009;462(7274):739–744.
17. Ward PS, Lu C, Cross JR, et al. The potential for isocitrate dehydrogenase mutations to produce 2-hydroxyglutarate depends on allele specificity and subcellular compartmentalization. *J. Biol. Chem.* 2013;288(6):3804–3815.
18. Rohle D, Popovici-Muller J, Palaskas N, et al. An inhibitor of mutant IDH1 delays growth and promotes differentiation of glioma cells. *Science*. 2013;340(6132):626–630.
19. Grisendi S, Bernardi R, Rossi M, et al. Role of nucleophosmin in embryonic development and tumorigenesis. *Nature*. 2005;437(7055):147–153.

20. Ley TJ, Miller C, Ding L, et al. Genomic and epigenomic landscapes of adult de novo acute myeloid leukemia. *N. Engl. J. Med.* 2013;368(22):2059–2074.

21. Meshinchi S, Appelbaum FR. Structural and functional alterations of FLT3 in acute myeloid leukemia. *Clin. Cancer Res.* 2009;15(13):4263–4269.

22. Meshinchi S, Woods WG, Stirewalt DL, et al. Prevalence and prognostic significance of Flt3 internal tandem duplication in pediatric acute myeloid leukemia. *Blood*. 2001;97(1):89–94.

23. Smith CC, Wang Q, Chin C-S, et al. Validation of ITD mutations in FLT3 as a therapeutic target in human acute myeloid leukaemia. *Nature*. 2012;485(7397):260–263.

24. Kornblau SM, Singh N, Qiu Y, et al. Highly phosphorylated FOXO3A is an adverse prognostic factor in acute myeloid leukemia. *Clin. cancer Res. an Off. J. Am. Assoc. Cancer Res.* 2010;16(6):1865–1874.

25. Zimmerman EI, Turner DC, Buaboonnam J, et al. Crenolanib is active against models of drug-resistant FLT3-ITD2positive acute myeloid leukemia. 2013;

26. Chan SM, Thomas D, Corces-Zimmerman MR, et al. Isocitrate dehydrogenase 1 and 2 mutations induce BCL-2 dependence in acute myeloid leukemia. *Nat. Med.* 2015;21(2):178–184.

27. Wu YT, Tan HL, Shui G, et al. Dual role of 3-methyladenine in modulation of autophagy via different temporal patterns of inhibition on class I and III phosphoinositide 3-kinase. *J. Biol. Chem.* 2010;285(14):10850–10861.

28. Mauthe M, Orhon I, Rocchi C, et al. Chloroquine inhibits autophagic flux by decreasing autophagosome-lysosome fusion. *Autophagy*. 2018;14(8):1435–1455.

29. Maiuri MC, Zalckvar E, Kimchi A, Kroemer G. Self-eating and self-killing:

crosstalk between autophagy and apoptosis. *Nat. Rev. Mol. Cell Biol.* 2007;8(9):741–752.

30. Mortensen M, Watson AS, Simon AK. Lack of autophagy in the hematopoietic system leads to loss of hematopoietic stem cell function and dysregulated myeloid proliferation. *Autophagy*. 2011;7(9):1069–1070.
31. Deretic V. Autophagy in inflammation, infection, and immunometabolism. *Immunity*. 2021;54(3):437–453.
32. Geisler S, Holmström KM, Skujat D, et al. PINK1/Parkin-mediated mitophagy is dependent on VDAC1 and p62/SQSTM1. *Nat. Cell Biol.* 2010;12(2):119–131.
33. Pohl C, Dikic I. Cellular quality control by the ubiquitin-proteasome system and autophagy. *Science*. 2019;366(6467):818–822.
34. Mai S, Muster B, Bereiter-Hahn J, Jendrach M. Autophagy proteins LC3B, ATG5 and ATG12 participate in quality control after mitochondrial damage and influence lifespan. *Autophagy*. 2012;8(1):47–62.
35. Jung CH, Seo M, Otto NM, Kim DH. ULK1 inhibits the kinase activity of mTORC1 and cell proliferation. *Autophagy*. 2011;7(10):1212–1221.
36. Mizushima N, Levine B, Cuervo AM, Klionsky DJ. Autophagy fights disease through cellular self-digestion. *Nature*. 2008;451(7182):1069–1075.
37. Liu Q, Chen L, Atkinson JM, Claxton DF, Wang HG. Atg5-dependent autophagy contributes to the development of acute myeloid leukemia in an MLL-AF9-driven mouse model. *Cell Death Dis.* 2016;7(9):e2361-12.
38. Piya S, Kornblau SM, Ruvolo VR, et al. Atg7 suppression enhances chemotherapeutic agent sensitivity and overcomes stroma-mediated chemoresistance in acute myeloid leukemia. *Blood*. 2016;128(9):126–1269.

39. Tanida I, Ueno T, Kominami E. LC3 conjugation system in mammalian autophagy. *Int. J. Biochem. Cell Biol.* 2004;36(12):2503–2518.

40. Scarlatti F, Maffei R, Beau I, Codogno P, Ghidoni R. Role of non-canonical Beclin 1-independent autophagy in cell death induced by resveratrol in human breast cancer cells. *Cell Death Differ.* 2008;15(8):1318–1329.

41. Shu L, Hu C, Xu M, et al. ATAD3B is a mitophagy receptor mediating clearance of oxidative stress-induced damaged mitochondrial DNA. *EMBO J.* 2021;40(8):e106283.

42. Koschade SE, Brandts CH. Selective Autophagy in Normal and Malignant Hematopoiesis. *J. Mol. Biol.* 2020;432(1):261–282.

43. Youle RJ, Narendra DP. Mechanisms of mitophagy. *Nat. Rev. Mol. Cell Biol.* 2011;12(1):9–14.

44. Joshi A, Kundu M. Mitophagy in hematopoietic stem cells: The case for exploration. *Autophagy*. 2013;9(11):1737–1749.

45. Cao Y, Cai J, Zhang S, et al. Loss of autophagy leads to failure in megakaryopoiesis, megakaryocyte differentiation, and thrombopoiesis in mice. *Exp. Hematol.* 2015;43(6):488–494.

46. Liu F, Lee JY, Wei H, et al. FIP200 is required for the cell-autonomous maintenance of fetal hematopoietic stem cells. *Blood*. 2010;116(23):4806–4814.

47. Gomez-Puerto MC, Folkerts H, Wierenga ATJ, et al. Autophagy Proteins ATG5 and ATG7 Are Essential for the Maintenance of Human CD34(+) Hematopoietic Stem-Progenitor Cells. *Stem Cells*. 2016;34(6):1651–1663.

48. Nishimura T, Kaizuka T, Cadwell K, et al. FIP200 regulates targeting of Atg16L1 to the isolation membrane. *EMBO Rep.* 2013;14(3):284–291.

49. Kim JK, Kim YS, Lee H-M, et al. GABAergic signaling linked to autophagy enhances host protection against intracellular bacterial infections. *Nat. Commun.* 2018;9(1):4184.

50. Masud S, Prajsnar TK, Torraca V, et al. Macrophages target Salmonella by Lc3-associated phagocytosis in a systemic infection model. *Autophagy*. 2019;15(5):796–812.

51. Sandoval H, Thiagarajan P, Dasgupta SK, et al. Essential role for Nix in autophagic maturation of erythroid cells. *Nature*. 2008;454(7201):232–235.

52. Ouseph MM, Huang Y, Banerjee M, et al. Autophagy is induced upon platelet activation and is essential for hemostasis and thrombosis. *Blood*. 2015;126(10):1224–1233.

53. Fujiwara Y, Browne CP, Cunniff K, Goff SC, Orkin SH. Arrested development of embryonic red cell precursors in mouse embryos lacking transcription factor GATA-1. *Proc. Natl. Acad. Sci. U. S. A.* 1996;93(22):12355–12358.

54. Kundu M, Lindsten T, Yang C-Y, et al. Ulk1 plays a critical role in the autophagic clearance of mitochondria and ribosomes during reticulocyte maturation. *Blood*. 2008;112(4):1493–1502.

55. Mortensen M, Simon AK. Nonredundant role of Atg7 in mitochondrial clearance during erythroid development. *Autophagy*. 2010;6(3):423–425.

56. Schweers RL, Zhang J, Randall MS, et al. NIX is required for programmed mitochondrial clearance during reticulocyte maturation. *Proc. Natl. Acad. Sci. U. S. A.* 2007;104(49):19500–19505.

57. Miller BC, Zhao Z, Stephenson LM, et al. The autophagy gene ATG5 plays an essential role in B lymphocyte development. *Autophagy*. 2008;4(3):309–314.

58. Salio M, Puleston DJ, Mathan TSM, et al. Essential role for autophagy during

invariant NKT cell development. *Proc. Natl. Acad. Sci. U. S. A.* 2014;111(52):E5678-87.

59. Wang S, Xia P, Huang G, et al. FoxO1-mediated autophagy is required for NK cell development and innate immunity. *Nat. Commun.* 2016;7:11023.

60. Watson AS, Riffelmacher T, Stranks A, et al. Autophagy limits proliferation and glycolytic metabolism in acute myeloid leukemia. *Cell death Discov.* 2015;1:15008-.

61. Piya S, Kornblau SM, Ruvolo VR, et al. Atg7 suppression enhances chemotherapeutic agent sensitivity and overcomes stroma-mediated chemoresistance in acute myeloid leukemia. *Blood*. 2016;128(9):1260–1269.

62. Altman BJ, Jacobs SR, Mason EF, et al. Autophagy is essential to suppress cell stress and to allow BCR-Abl-mediated leukemogenesis. *Oncogene*. 2011;30(16):1855–1867.

63. Qiu L, Zhou G, Cao S. Targeted inhibition of ULK1 enhances daunorubicin sensitivity in acute myeloid leukemia. *Life Sci.* 2020;243:117234.

64. Nguyen TD, Shaid S, Vakhrusheva O, et al. Loss of the selective autophagy receptor p62 impairs murine myeloid leukemia progression and mitophagy. *Blood*. 2019;133(2):168–179.

65. Du W, Xu A, Huang Y, et al. The role of autophagy in targeted therapy for acute myeloid leukemia. *Autophagy*. 2021;17(10):2665–2679.

66. Zou Q, Tan S, Yang Z, et al. NPM1 mutant mediated PML delocalization and stabilization enhances autophagy and cell survival in leukemic cells. *Theranostics*. 2017;7(8):2289–2304.

67. Xu D, Chen Y, Yang Y, et al. Autophagy activation mediates resistance to FLT3 inhibitors in acute myeloid leukemia with FLT3-ITD mutation. *J.*

*Transl. Med.* 2022;20(1):300.

68. Bosnjak M, Ristic B, Arsikin K, et al. Inhibition of mTOR-dependent autophagy sensitizes leukemic cells to cytarabine-induced apoptotic death. *PLoS One*. 2014;9(4):1–12.

69. Visser N, Lourens HJ, Huls G, Bremer E, Wiersma VR. Inhibition of Autophagy Does Not Re-Sensitize Acute Myeloid Leukemia Cells Resistant to Cytarabine. *Int. J. Mol. Sci.* 2021;22(5):.

70. Dykstra KM, Fay HRS, Massey AC, et al. Inhibiting autophagy targets human leukemic stem cells and hypoxic AML blasts by disrupting mitochondrial homeostasis. *Blood Adv.* 2021;5(8):2087–2100.

71. McAfee Q, Zhang Z, Samanta A, et al. Autophagy inhibitor Lys05 has single-agent antitumor activity and reproduces the phenotype of a genetic autophagy deficiency. *Proc. Natl. Acad. Sci. U. S. A.* 2012;109(21):8253–8258.

72. Torgersen ML, Engedal N, Bøe S-O, Hokland P, Simonsen A. Targeting autophagy potentiates the apoptotic effect of histone deacetylase inhibitors in t(8;21) AML cells. *Blood*. 2013;122(14):2467–2476.

73. Matsuo H, Nakatani K, Harata Y, et al. Efficacy of a combination therapy targeting CDK4/6 and autophagy in a mouse xenograft model of t(8;21) acute myeloid leukemia. *Biochem. Biophys. reports*. 2021;27:101099.

74. Bellodi C, Lidonnici MR, Hamilton A, et al. Targeting autophagy potentiates tyrosine kinase inhibitor-induced cell death in Philadelphia chromosome-positive cells, including primary CML stem cells. *J. Clin. Invest.* 2009;119(5):1109–1123.

75. Putyrski M, Vakhrusheva O, Bonn F, et al. Disrupting the LC3 Interaction Region (LIR) Binding of Selective Autophagy Receptors Sensitizes AML Cell

Lines to Cytarabine. *Front. cell Dev. Biol.* 2020;8:208.

76. Pei S, Minhajuddin M, Adane B, et al. AMPK/FIS1-Mediated Mitophagy Is Required for Self-Renewal of Human AML Stem Cells. *Cell Stem Cell*. 2018;23(1):86-100.e6.

77. Allende-Vega N, Villalba M. Metabolic stress controls mutant p53 R248Q stability in acute myeloid leukemia cells. *Sci. Rep.* 2019;9(1):5637.

78. Howe K, Clark MD, Torroja CF, et al. The zebrafish reference genome sequence and its relationship to the human genome. *Nature*. 2013;496(7446):498–503.

79. Davidson AJ, Zon LI. The "definitive" (and 'primitive') guide to zebrafish hematopoiesis. *Oncogene*. 2004;23(43):7233–7246.

80. Travnickova J, Tran Chau V, Julien E, et al. Primitive macrophages control HSPC mobilization and definitive haematopoiesis. *Nat. Commun.* 2015;6:6227.

81. Bertrand JY, Chi NC, Santoso B, et al. Haematopoietic stem cells derive directly from aortic endothelium during development. *Nature*. 2010;464(7285):108–111.

82. Ransom DG, Haffter P, Odenthal J, et al. Characterization of zebrafish mutants with defects in embryonic hematopoiesis. *Development*. 1996;123:311–319.

83. Fontana BD, Mezzomo NJ, Kalueff A V, Rosemberg DB. The developing utility of zebrafish models of neurological and neuropsychiatric disorders: A critical review. *Exp. Neurol.* 2018;299(Pt A):157–171.

84. Yi Z-N, Chen X-K, Ma AC-H. Modeling leukemia with zebrafish (Danio rerio): Towards precision medicine. *Exp. Cell Res.* 2022;421(2):113401.

85. Wang D, Zheng L, Cheng BYL, et al. Transgenic IDH2(R172K) and IDH2(R140Q) zebrafish models recapitulated features of human acute myeloid

leukemia. *Oncogene*. 2023;

86. Craven SE, French D, Ye W, de Sauvage F, Rosenthal A. Loss of Hspa9b in zebrafish recapitulates the ineffective hematopoiesis of the myelodysplastic syndrome. *Blood*. 2005;105(9):3528–3534.

87. Payne EM, Bolli N, Rhodes J, et al. Ddx18 is essential for cell-cycle progression in zebrafish hematopoietic cells and is mutated in human AML. *Blood*. 2011;118(4):903–915.

88. Kawakami K, Takeda H, Kawakami N, et al. A transposon-mediated gene trap approach identifies developmentally regulated genes in zebrafish. *Dev. Cell*. 2004;7(1):133–144.

89. Suster ML, Sumiyama K, Kawakami K. Transposon-mediated BAC transgenesis in zebrafish and mice. *BMC Genomics*. 2009;10:477.

90. Langenau DM, Traver D, Ferrando AA, et al. Myc-induced T cell leukemia in transgenic zebrafish. *Science*. 2003;299(5608):887–890.

91. Langenau DM, Feng H, Berghmans S, et al. Cre/lox-regulated transgenic zebrafish model with conditional myc-induced T cell acute lymphoblastic leukemia. *Proc. Natl. Acad. Sci. U. S. A.* 2005;102(17):6068–6073.

92. Yeh J-RJ, Munson KM, Chao YL, et al. AML1-ETO reprograms hematopoietic cell fate by downregulating scl expression. *Development*. 2008;135(2):401–410.

93. Deguchi K, Ayton PM, Carapeti M, et al. MOZ-TIF2-induced acute myeloid leukemia requires the MOZ nucleosome binding motif and TIF2-mediated recruitment of CBP. *Cancer Cell*. 2003;3(3):259–271.

94. Onnebo SMN, Rasighaemi P, Kumar J, Liongue C, Ward AC. Alternative TEL-JAK2 fusions associated with T-cell acute lymphoblastic leukemia and

atypical chronic myelogenous leukemia dissected in zebrafish. *Haematologica*. 2012;97(12):1895–1903.

95. Forrester AM, Grabher C, McBride ER, et al. NUP98-HOXA9-transgenic zebrafish develop a myeloproliferative neoplasm and provide new insight into mechanisms of myeloid leukaemogenesis. *Br. J. Haematol.* 2011;155(2):167–181.

96. Lu J-W, Hou H-A, Hsieh M-S, Tien H-F, Lin L-I. Overexpression of FLT3-ITD driven by spi-1 results in expanded myelopoiesis with leukemic phenotype in zebrafish. *Leukemia*. 2016;30(10):2098–2101.

97. Miller JC, Holmes MC, Wang J, et al. An improved zinc-finger nuclease architecture for highly specific genome editing. *Nat. Biotechnol.* 2007;25(7):778–785.

98. Cade L, Reyon D, Hwang WY, et al. Highly efficient generation of heritable zebrafish gene mutations using homo- and heterodimeric TALENs. *Nucleic Acids Res.* 2012;40(16):8001–8010.

99. Hwang WY, Fu Y, Reyon D, et al. Efficient genome editing in zebrafish using a CRISPR-Cas system. *Nat. Biotechnol.* 2013;31(3):227–229.

100. Jao L-E, Wente SR, Chen W. Efficient multiplex biallelic zebrafish genome editing using a CRISPR nuclease system. *Proc. Natl. Acad. Sci. U. S. A.* 2013;110(34):13904–13909.

101. Gjini E, Mansour MR, Sander JD, et al. A zebrafish model of myelodysplastic syndrome produced through tet2 genomic editing. *Mol. Cell. Biol.* 2015;35(5):789–804.

102. Huang P, Xiao A, Zhou M, et al. Heritable gene targeting in zebrafish using customized TALENs. *Nat. Biotechnol.* 2011;29(8):699–700.

103. Xiangguo S, Bai-Liang H, Ma ACH, et al. Functions of idh1 and its mutation in the regulation of developmental hematopoiesis in zebrafish. *Blood*. 2015;125(19):2974–2984.

104. Auer TO, Duroure K, De Cian A, Concordet JP, Del Bene F. Highly efficient CRISPR/Cas9-mediated knock-in in zebrafish by homology-independent DNA repair. *Genome Res.* 2014;24(1):142–153.

105. Chavez A, Scheiman J, Vora S, et al. Highly efficient Cas9-mediated transcriptional programming. *Nat. Methods*. 2015;12(4):326–328.

106. Wu RS, Lam II, Clay H, et al. A Rapid Method for Directed Gene Knockout for Screening in G0 Zebrafish. *Dev. Cell*. 2018;46(1):112-125.e4.

107. Bill BR, Petzold AM, Clark KJ, Schimmenti LA, Ekker SC. A primer for morpholino use in zebrafish. *Zebrafish*. 2009;6(1):69–77.

108. He B-L, Shi X, Man CH, et al. Functions of flt3 in zebrafish hematopoiesis and its relevance to human acute myeloid leukemia. *Blood*. 2014;123(16):2518–2529.

109. Tan J, Zhao L, Wang G, et al. Human MLL-AF9 Overexpression Induces Aberrant Hematopoietic Expansion in Zebrafish. *Biomed Res. Int.* 2018;2018:6705842.

110. Corkery DP, Dellaire G, Berman JN. Leukaemia xenotransplantation in zebrafish--chemotherapy response assay in vivo. *Br. J. Haematol.* 2011;153(6):786–789.

111. Bentley VL, Veinotte CJ, Corkery DP, et al. Focused chemical genomics using zebrafish xenotransplantation as a pre-clinical therapeutic platform for T-cell acute lymphoblastic leukemia. *Haematologica*. 2015;100(1):70–76.

112. Traver D, Winzeler A, Stern HM, et al. Effects of lethal irradiation in zebrafish

and rescue by hematopoietic cell transplantation. *Blood*. 2004;104(5):1298–1305.

113. Pruvot B, Jacquel A, Droin N, et al. Leukemic cell xenograft in zebrafish embryo for investigating drug efficacy. *Haematologica*. 2011;96(4):612–616.

114. He C, Klionsky DJ. Analyzing autophagy in zebrafish. *Autophagy*. 2010;6(5):642–644.

115. Khuansuwan S, Barnhill LM, Cheng S, Bronstein JM. A novel transgenic zebrafish line allows for in vivo quantification of autophagic activity in neurons. *Autophagy*. 2019;15(8):1322–1332.

116. Lee E, Koo Y, Ng A, et al. Autophagy is essential for cardiac morphogenesis during vertebrate development. *Autophagy*. 2014;10(4):572–587.

117. Chen X-K, Kwan JS-K, Chang RC-C, Ma AC-H. 1-phenyl 2-thiourea (PTU) activates autophagy in zebrafish embryos. *Autophagy*. 2021;17(5):1222–1231.

118. Klionsky DJ, Abdel-Aziz AK, Abdelfatah S, et al. Guidelines for the use and interpretation of assays for monitoring autophagy (4th edition)(1). *Autophagy*. 2021;17(1):1–382.

119. Hu Z, Zhang J, Zhang Q. Expression pattern and functions of autophagy-related gene atg5 in zebrafish organogenesis. *Autophagy*. 2011;7(12):1514–1527.

120. Meng X-H, Chen B, Zhang J-P. Intracellular Insulin and Impaired Autophagy in a Zebrafish model and a Cell Model of Type 2 diabetes. *Int. J. Biol. Sci.* 2017;13(8):985–995.

121. Khor E-S, Noor SM, Wong P-F. Understanding the Role of ztor in Aging-related Diseases Using the Zebrafish Model. *In Vivo*. 2019;33(6):1713–1720.

122. Schulte-Merker S, Stainier DYR. Out with the old, in with the new: reassessing

morpholino knockdowns in light of genome editing technology. *Development*. 2014;141(16):3103–3104.

123. Stainier DYR, Raz E, Lawson ND, et al. Guidelines for morpholino use in zebrafish. *PLoS Genet.* 2017;13(10):e1007000.

124. Lai JKH, Gagalova KK, Kuenne C, El-Brolosy MA, Stainier DYR. Induction of interferon-stimulated genes and cellular stress pathways by morpholinos in zebrafish. *Dev. Biol.* 2019;454(1):21–28.

125. Mastrodonato V, Beznoussenko G, Mironov A, et al. A genetic model of CEDNIK syndrome in zebrafish highlights the role of the SNARE protein Snap29 in neuromotor and epidermal development. *Sci. Rep.* 2019;9(1):1211.

126. Zhang R, Varela M, Vallentgoed W, et al. The selective autophagy receptors Optineurin and p62 are both required for zebrafish host resistance to mycobacterial infection. *PLoS Pathog.* 2019;15(2):e1007329.

127. Chen X-K, Yi Z-N, Lau JJ-Y, Ma AC-H. Distinct roles of core autophagy-related genes (ATGs) in zebrafish definitive hematopoiesis. 2022;

128. Kimmel CB, Ballard WW, Kimmel SR, Ullmann B, Schilling TF. Stages of embryonic development of the zebrafish. *Dev. Dyn. an Off. Publ. Am. Assoc. Anat.* 1995;203(3):253–310.

129. Picot S, Morga B, Faury N, et al. A study of autophagy in hemocytes of the Pacific oyster, Crassostrea gigas. *Autophagy*. 2019;15(10):1801–1809.

130. Kabeya Y, Mizushima N, Ueno T, et al. LC3, a mammalian homologue of yeast Apg8p, is localized in autophagosome membranes after processing. *EMBO J.* 2000;19(21):5720–5728.

131. Matsuo Y, MacLeod RA, Uphoff CC, et al. Two acute monocytic leukemia (AML-M5a) cell lines (MOLM-13 and MOLM-14) with interclonal

phenotypic heterogeneity showing MLL-AF9 fusion resulting from an occult chromosome insertion, ins(11;9)(q23;p22p23). *Leukemia*. 1997;11(9):1469–1477.

132. Chen CS, Hilden JM, Frestedt J, et al. The chromosome 4q21 gene (AF-4/FEL) is widely expressed in normal tissues and shows breakpoint diversity in t(4;11)(q21;q23) acute leukemia. *Blood*. 1993;82(4):1080–1085.

133. Xu F, Taki T, Eguchi M, et al. Tandem duplication of the FLT3 gene is infrequent in infant acute leukemia. Japan Infant Leukemia Study Group. *Leukemia*. 2000;14(5):945–947.

134. Konopka JB, Watanabe SM, Singer JW, Collins SJ, Witte ON. Cell lines and clinical isolates derived from Ph1-positive chronic myelogenous leukemia patients express c-abl proteins with a common structural alteration. *Proc. Natl. Acad. Sci. U. S. A.* 1985;82(6):1810–1814.

135. Tsuchiya S, Yamabe M, Yamaguchi Y, et al. Establishment and characterization of a human acute monocytic leukemia cell line (THP-1). *Int. J. cancer*. 1980;26(2):171–176.

136. Wang C, Curtis JE, Minden MD, McCulloch EA. Expression of a retinoic acid receptor gene in myeloid leukemia cells. *Leukemia*. 1989;3(4):264–269.

137. Koeffler HP, Golde DW. Acute myelogenous leukemia: a human cell line responsive to colony-stimulating activity. *Science*. 1978;200(4346):1153–1154.

138. Towatari M, Ito Y, Morishita Y, et al. Enhanced expression of DNA topoisomerase II by recombinant human granulocyte colony-stimulating factor in human leukemia cells. *Cancer Res.* 1990;50(22):7198–7202.

139. Palumbo A, Minowada J, Erikson J, Croce CM, Rovera G. Lineage infidelity

of a human myelogenous leukemia cell line. *Blood*. 1984;64(5):1059–1063.

140. Fukui Y, Hashimoto O, Sanui T, et al. Haematopoietic cell-specific CDM family protein DOCK2 is essential for lymphocyte migration. *Nature*. 2001;412(6849):826–831.

141. Wu J, Liu S, Liu G, et al. Identification and functional analysis of 9p24 amplified genes in human breast cancer. *Oncogene*. 2012;31(3):333–341.

142. Dobbs K, Conde CD, Zhang SY, et al. Inherited DOCK2 deficiency in patients with early-onset invasive infections. *N. Engl. J. Med.* 2015;372(25):2409–2422.

143. Garcia-Rudaz C, Luna F, Tapia V, et al. Fxna, a novel gene differentially expressed in the rat ovary at the time of folliculogenesis, is required for normal ovarian histogenesis. *Development*. 2007;134(5):945–957.

144. Lee T-HD, Streb JW, Georger MA, Miano JM. Tissue expression of the novel serine carboxypeptidase Scpep1. *J. Histochem. Cytochem. Off. J. Histochem. Soc.* 2006;54(6):701–711.

145. Daver N, Schlenk RF, Russell NH, Levis MJ. Targeting FLT3 mutations in AML: review of current knowledge and evidence. *Leukemia*. 2019;33(2):299–312.

146. Tapia C, Kutzner H, Mentzel T, et al. Two mitosis-specific antibodies, MPM-2 and phospho-histone H3 (Ser28), allow rapid and precise determination of mitotic activity. *Am. J. Surg. Pathol.* 2006;30(1):83–89.

147. Zhang N, Chen Y, Shen Y, Lou S, Deng J. Comprehensive analysis the potential biomarkers for the high-risk of childhood acute myeloid leukemia based on a competing endogenous RNA network. *Blood Cells, Mol. Dis.* 2019;79(July):102352.

148. Grandi A, Santi A, Campagnoli S, et al. ERMP1, a novel potential oncogene involved in UPR and oxidative stress defense, is highly expressed in human cancer. *Oncotarget*. 2016;7(39):63596–63610.

149. Pan X, Grigoryeva L, Seyrantepe V, et al. Serine Carboxypeptidase SCPEP1 and Cathepsin A Play Complementary Roles in Regulation of Vasoconstriction via Inactivation of Endothelin-1. *PLoS Genet.* 2014;10(2):.

150. Park J, Lee SB, Lee S, et al. Mitochondrial dysfunction in Drosophila PINK1 mutants is complemented by parkin. *Nature*. 2006;441(7097):1157–1161.

151. Yang Y, Gehrke S, Imai Y, et al. Mitochondrial pathology and muscle and dopaminergic neuron degeneration caused by inactivation of Drosophila Pink1 is rescued by Parkin. *Proc. Natl. Acad. Sci. U. S. A.* 2006;103(28):10793–10798.

152. Michiorri S, Gelmetti V, Giarda E, et al. The Parkinson-associated protein PINK1 interacts with Beclin1 and promotes autophagy. *Cell Death Differ.* 2010;17(6):962–974.

153. Pietschmann K, Bolck HA, Buchwald M, et al. Breakdown of the FLT3-ITD/STAT5 axis and synergistic apoptosis induction by the histone deacetylase inhibitor panobinostat and FLT3-specific inhibitors. *Mol. Cancer Ther.* 2012;11(11):2373–2383.

154. Cooper TM, Cassar J, Eckroth E, et al. A Phase I Study of Quizartinib Combined with Chemotherapy in Relapsed Childhood Leukemia: A Therapeutic Advances in Childhood Leukemia & Lymphoma (TACL) Study. *Clin. cancer Res. an Off. J. Am. Assoc. Cancer Res.* 2016;22(16):4014–4022.

155. Weisberg E, Liu Q, Nelson E, et al. Using combination therapy to override stromal-mediated chemoresistance in mutant FLT3-positive AML: synergism

between FLT3 inhibitors, dasatinib/multi-targeted inhibitors and JAK inhibitors. *Leukemia*. 2012;26(10):2233–2244.

156. Heydt Q, Larrue C, Saland E, et al. Oncogenic FLT3-ITD supports autophagy via ATF4 in acute myeloid leukemia. *Oncogene*. 2018;37(6):787–797.

157. Hwang DY, Eom J-I, Jang JE, et al. ULK1 inhibition as a targeted therapeutic strategy for FLT3-ITD-mutated acute myeloid leukemia. *J. Exp. Clin. Cancer Res.* 2020;39(1):85.

158. Varga M, Sass M, Papp D, et al. Autophagy is required for zebrafish caudal fin regeneration. *Cell Death Differ.* 2014;21(4):547–556.

159. Koschade SE, Klann K, Shaid S, et al. Translatome proteomics identifies autophagy as a resistance mechanism to on-target FLT3 inhibitors in acute myeloid leukemia. *Leukemia*. 2022;36(10):2396–2407.

160. Nishihara H, Kobayashi S, Hashimoto Y, et al. Non-adherent cell-specific expression of DOCK2, a member of the human CDM-family proteins. *Biochim. Biophys. Acta - Mol. Cell Res.* 1999;1452(2):179–187.

161. Geng J, Klionsky DJ. The Atg8 and Atg12 ubiquitin-like conjugation systems in macroautophagy. “Protein modifications: beyond the usual suspects” review series. *EMBO Rep.* 2008;9(9):859–864.

162. Min Wu1, Max Hamaker1, Li Li2, Donald Small2 and ASD. DOCK2 Interacts with FLT3 and Modulates the Survival of FLT3- Expressing Leukemia Cells Min. *Leukemia*. 2017;176(1):139–148.

163. Hasan K, Yu J, Widhopf GF, et al. Wnt5a induces ROR1 to recruit DOCK2 to activate Rac1/2 in chronic lymphocytic leukemia. *Blood*. 2018;132(2):170–178.

164. Kikuchi T, Kubonishi S, Shibakura M, et al. Dock2 participates in bone

marrow lympho-hematopoiesis. *Biochem. Biophys. Res. Commun.* 2008;367(1):90–96.

165. Yu L, Chen Y, Tooze SA. Autophagy pathway: Cellular and molecular mechanisms. *Autophagy*. 2018;14(2):207–215.

166. Chen J, Streb JW, Maltby KM, Kitchen CM, Miano JM. Cloning of a novel retinoid-inducible serine carboxypeptidase from vascular smooth muscle cells. *J. Biol. Chem.* 2001;276(36):34175–34181.

167. Kollmann K, Damme M, Deuschl F, et al. Molecular characterization and gene disruption of mouse lysosomal putative serine carboxypeptidase 1. *FEBS J.* 2009;276(5):1356–1369.

168. Lőrincz P, Juhász G. Autophagosome-Lysosome Fusion. *J. Mol. Biol.* 2020;432(8):2462–2482.

169. Ito K, Turcotte R, Cui J, et al. Self-renewal of a purified Tie2+ hematopoietic stem cell population relies on mitochondrial clearance. *Science*. 2016;354(6316):1156–1160.

170. Fan S, Price T, Huang W, et al. PINK1-Dependent Mitophagy Regulates the Migration and Homing of Multiple Myeloma Cells via the MOB1B-Mediated Hippo-YAP/TAZ Pathway. *Adv. Sci. (Weinheim, Baden-Wurttemberg, Ger.* 2020;7(5):1900860.

171. Liang XH, Jackson S, Seaman M, et al. Induction of autophagy and inhibition of tumorigenesis by beclin 1. *Nature*. 1999;402(6762):672–676.